REPUBLIC OF TURKEY
FIRAT UNIVERSITY
THE GRADUATE SCHOOL OF NATURAL AND APPLIED SCIENCES

RESERVOIR CHARACTERIZATIONS OF THE UPPER CRETACEOUS DEEP MARINE TURBIDITES TO THE CLOSE SOUTHERN PART OF SULAIMANIYAH (NORTHERN IRAQ)

Master Thesis

Tavan Mohammed HAMA SALIH
Department: Geological Engineering
Program: General Geology (Sedimentology)
Supervisor: Assoc. Prof. Dr. Hasan ÇELİK

JULY-2017

REPUBLIC OF TURKEY
FIRAT UNIVERSITY
THE GRADUATE SCHOOL OF NATURAL AND APPLIED SCIENCES

RESERVOIR CHARACTERIZATIONS OF THE UPPER CRETACEOUS DEEP MARINE TURBIDITES TO THE CLOSE SOUTHERN PART OF SULAIMANIYAH (NORTHERN IRAQ)

MASTER THESIS

Tavan Mohammed HAMA SALIH
142116117

Supervisor: Assoc. Prof. Dr. Hasan ÇELİK (Fırat U.)
Committee: Prof. Dr. Ercan AKSOY (Fırat U.)
Committee: Assoc. Prof. Dr. Orhan KAVAK (Dicle U.)

ACKNOWLEDGEMENTS

First of all, I wish to express my great gratitude and appreciation to my supervisor, Assoc. Prof. Hasan ÇELİK for this continuous supervisions, encouragement, kindness, friendly behavior and valuable help during my study.

I would like to express my gratitude to my brother Mr. Hemin Muhammad Hama Salih, who is student in University of Fırat, for his assistance during field work and laboratory work. I will never forget.

My best thanks and appreciation for Professor Dr. Polla Azad Khanaqa head of the Institute we work with (KISSR) for using their laboratory during my laboratory work for drilling core of the samples, cutting, grinding and examine porosity tests.

My thanks also Dr. Musher M. Baziany he gave me some information.

I would also like to thank all those who contributed to help me, in one way or another, and participated in the completion of this thesis.

Finally, I would like to express my special appreciation to my lovely family during the preparation of this research, their continuous support and encouragement, this work can never be accomplished, for their helping throughout all stage of this research.

TAVAN MOHAMMED HAMA SALIH

SUMMARY

RESERVOIR CHARACTERIZATIONS OF THE UPPER CRETACEOUS DEEP MARINE TURBIDITES TO THE CLOSE SOUTHERN PART OF SULAIMANIYAH (NORTHERN IRAQ)

In this study reservoir characterization of the low density turbidite sandstones of Upper Cretaceous Tanjero Formation cropping out next to the Arbat town in the southeastern part of Sulaimaniyah city, Northern Iraq was analyzed. The sandstone portion of the unit has been examined by measuring six sections through field and laboratory based studies which their thicknesses are about 40-50 meter, and taking samples from the outcrop. The sections are located on the southern limb of an anticline in the high folded zone which is characterized by intense folding and orogenic uplift with closely packed narrow anticlines and synclines. The outcrops of the formation are characterized by a sequence of sandstones, siltstones and shale.

The base of the logs are not clear to see which formation is underlying the logs as they were taken from an outcrop that was brought surface by a small river next to the Arbat road and on an anticline limb. Possibly it was Shranish Formation which is generally comformably underlying the unit around the city.

The analysis of lithofacies and architectural elements of the sandstones in the studied area, leads to recognition of three main lithofacies and forty-nine total subfacies of the turbidites in the location. The main facies represent the grain size from fine to coarse grain sandstone. The subfacies are consisting of many types of combinations of the complete Bouma sequence associated with turbidites. These facies point out that the environment of the turbidites is in the transition area between middle fan and outer fan. In the meaning of lobe hierarchy, the turbidite beds in thin and medium thicknesses represent lobe fringe. Only one architectural element recognized in the section is small sandy channel fills in about ten meters length and a few meters thick representing beginning of outer fan or in lobe fringe.

For porosity and permeability tests 35 rock samples were taken from the logs for laboratory analyses. Porosity of the studied sandstones range from 4.56% to 16.56% which is poor to

beginning of fair with an average value of 9.2%. The obtained permeability varies between 36.388-623.328 md and their mean value is 426.68 md representing very good permeability.

Petrographic works based on modal analysis of the clastic rock fragments and the other components such as cement, opaque minerals ect. show that these turbidites are mainly composed of sedimentary rock fragments such as carbonate, microcrystalline and cryptocrystalline quartz bearing siliceous sedimentary cherts, radiolaria fossil bearing cherts, and released radiolaria from the cherts during a short distance transportation. Quartz and feldspar ratios in the whole thin sections are below two percent. The modal analysis of the sandstones shows calclithite (litharenite) indicating sedimentary source rocks mainly consisting of carbonate rocks and radiolarian and chert rich limestone.

The composition of the sandstones suggests a recycled sedimentary sources. Likewise, the Qm,F,L ternary diagram suggests that the sediments are derived lithic recycled provenance which may be the Lower Cretaceous Qulqula Formation.

Keywords: Tanjero Formation, turbidite sandstone, reservoir characterization, Arbat southeastern Sulaimaniyah, Northern Iraq.

ÖZET

SÜLEYMANİYE YAKIN GÜNEYİNDEKİ ÜST KRETASE YAŞLI DERİN DENİZ TÜRBİDİTLERİNİN HAZNE KAYA ÖZELLİKLERİ (KUZEY IRAK)

Bu çalışmada Süleymaniye ilinin (Kuzey Irak) güneydoğusunda Arbat kasabası yakınlarında yüzeyleme veren Üst Kretase yaşlı Tanjero Formasyonu'na ait türbidit kumtaşlarının rezervuar özellikleri incelenmiştir. Bu kapsamda kalınlıkları 40-50 m arasında değişen altı adet ayrıntılı ölçülü stratigrafik kesit (log) alınmıştır. Bu kesitlerin alındığı bölge tektonizmadan oldukça yoğun bir şekilde etkilenmiş olan ve yüksek kıvrımlarla temsil edilen "yüksek kıvrımlı zon" içerisinde ve bir kıvrımın güney kanadında bulunmaktadır. Formasyonun buradaki yüzeylemesi kumtaşı, silttaşı ve şeyl ardalanmalarından oluşmaktadır.

Ölçülü kesitler bir antiklinalin kanadından alındığı için ve yüzeylemenin küçük bir derenin aşındırması sonucu ortaya çıkmış olmasından dolayı birimin tabanı görülememiştir. Genellikle bu bölgede birimin altında uyumlu olarak bulunan Şiraniş Formasyonu'nun burada da tabanda mevcut olduğu düşünülmektedir.

İnceleme alanındaki kumtaşlarının litofasiyes analizleri ve yapısal özellikleri, 3 adet ana ve litofasiyes ve 49 adet alt fasiyesin mevcut olduğunu ortaya koymuştur. Ana fasiyesler ince taneliden iri taneliye kadar değişen kumtaşlarıyla temsil edilmektedir. Alt fasiyesler ise türbiditlerle ilişkili olan tam Bouma istifinin farklı bölümlerinin kombinasyonlarından meydana gelmektedir. Bu fasiyesler, turbiditlerin orta yelpaze ile dış yelpaze arasındaki bir alanda çökelmiş olduklarını göstermektedir. Lob hiyerarşisi bakımından ise tane boyu ve tabaka kalınlıklarına göre depolanma ortamının lob eksen bitişiği ve lob kenarı olduğu belirlenmiştir. İnceleme alanında yapısal özellik olarak sadece 10 m genişliğinde ve birkaç m kalınlığında kumlu kanal dolgusu yapısı görülmüştür. Bu yapı dış fanın başlangıcını ve lob kenarını temsil etmektedir.

Porozite ve permeabilite deneyleri için ölçülü kesitlerden alınan 35 kayaç örneği incelenmiştir. İncelenen kumtaşlarının porozitesi %4,56 ile %16,56 arasında değişmekte olup ortalaması %9,2'dir. Bu ortalama "düşük- orta" değerler arasındadır. Permeabilite değerleri ise

36,388 ile 623,328 milidarcy arasında ve 426,68 milidarcy ortalamaya sahiptir. Bu ortalama ise “çok iyi” sınıfına girmektedir.

Bileşenlerin tayini ve modal analizlerine dayalı olan petrografik incelemeler, bu turbiditlerin, karbonatlı, kırıntılı, mikrokristalen ve kriptokristalen çört, radyolaryalı çört gibi sedimanter kayaç parçaları ile yakın mesafeden taşınma esnasında serbest kalmış radyolarya fosillerinden meydana geldiğini göstermiştir. Kuvars ve feldspat oranı tüm kayaç örneklerinde % 2’ nin altındadır ve feldspatlar çok ender olarak görülmektedir. Modal analizler bu kumtaşlarının kalklitit olduğunu ortaya koymuştur. Buna göre kaynak alanın karbonat kayaçlarca zengin olduğu sonucuna varılır. İnceleme alındaki kumtaşlarının bileşimi ve Qm,F,KP üçgen diyagramı “litik döngü kategorisi”ni temsil etmektedir. Eski akıntı yönü analizi ve petrografik incelemelerden hareketle bu litik döngü içerisindeki birimin, türbiditlere kaynak alan (provenans) olan ve tamamen sedimanter kayaçlardan meydana gelmiş Erken Kretase yaşlı Kulkula Formasyonu olduğunu göstermektedir.

Anahtar kelimeler: Tanjero Formasyonu, türbidit kumtaşları, rezervuar özellikleri, Arbat, güneydoğu Süleymaniye, Kuzey Irak

TABLE OF CONTENTS

LIST OF FIGURES

LIST OF TABLES

LIST OF PLATES

1. INTRODUCTION

This study was done as an MSc thesis at the Geological Engineering Department of Engineering Faculty in Firat University on the turbidite outcrop of Upper Cretaceous Tanjero Formation cropping out southeastern part of Sulaimaniyah city in Northern Iraq.

Tanjero Formation is the one of the best known formation in the Northern Iraq region since there are several geological studies were done on the formation for different goals as seen in the previous works (e.g: Kassab, 1975; Al-Mehaidi, 1975; Al-Rawi, 1981; Saadallah and Hassan, 1987; Al-Rawi Al-Rawi, 2002; Karim, 2004, 2005, 2007 and 2012 2014) part of the thesis not including any reservoir characterization study on the formation.

As (Qadir, 2008) mentioned that "Northern Iraq is one of the world's petroleum-rich countries in close future it might developed one of the central producers, as it is endowed with multiple petroleum systems that contain Paleozoic, Mesozoic and Cenozoic rocks and the common of Iraq's oil fields are positioned in the Zagros-Mesopotamian Cretaceous-Tertiary petroleum carbonates system" mainly the reservoir systems are composed of carbonates.

This study is sharing to be the first examine of the reservoir characterization on the clastic turbidite succession of Tanjero Formation which is one of the main unit cropped out in the area. The location of the study is situated southeast of Sulaimaniyah city close to the Arbat road. The other contemporaneous study is being held by Hemin Muhammad Hama Salih, in the same department supervised by Prof. Hasan Çelik, located to the northwest of the city. Further works in the future on the different parts of the unit will present the whole reservoir characteristics of the formation.

With this thesis important results for depositional environment of the unit according to lobe architecture in hierarchy, facies types and changes, petrographic analysis for provenance and architectural elements of the turbidites had been presented besides porosity and permeability for geoscientist.

This study opened a new window and pointed out that if the turbidites are suitable for oil and gas productions or not for the geologists and geophysicist working for oil companies in Iraq.

2. AIM OF THE STUDY

The aims of this research are to study the character of reservoir from the Upper Cretaceous deep marine turbidites of Tanjero Formation to the close southern Part of Sulaimaniyah (Northern Iraq) close the Arbat town. With this thesis it is planned to do:

a. Estimation of total porosity, permeability, and determination of effective porosity.

b. Examination the relationship between effective porosity and permeability with reservoir.

c. Facies identification of the unit by logging six measured sections.

d. Studying sedimentary structures and interpreting them for inferring palaeocurrent orientation with petrographic examine to analysis provenance.

e. The thesis additionally aims to establish depositional environment of the unit in the meaning of lobe architecture in hierarchy using lithofacies types.

F. Examination thin section for petrography for modal analysis and provenance.

3. METHODS

The study can be divided into three stages:

3.1. Office work

1. Collecting literature review.
2. Interpretation of logs and using distinct computer programs for drawing all measured sections from the field work and separating lithofacies, editing photos, rose diagrams for palaeoflow directions and bedding attitudes.
3. Finally writing thesis.

3.2. Field work

During field work six detail measured sections were logged by measuring bed by bed thickness, recognizing rock types, bed contact, marker bed, sedimentary structures along with orientation of local palaeocurrent. Rock samples were collected along the six sections in which the selection of lithology and grain sizes observed.

From the logs 35 rock samples for porosity, more than 20 samples for permeability and 25 for thin section analysis were collected. Labelled such as TL1-1, TL2-4 etc.

3.3. Laboratory works including

1. Taking core in all samples for porosity, permeability and preparing thin sections for petrography.
2. Identification of reservoir properties and measurement of effective porosity, and permeability: 35 rock sample were tested for porosity, 20 sample tested for permeability by using "BLP-530 Gas Porosimeter" and "Reservoir Permeability Tester" devices by using (Helium or Nitrogen), for all of them.
3. Testing variables such as effective porosity, mean grain volume, and Bulk volume contents to estimate the reservoir quality.
4. More than 25 thin sections were studied in the laboratory under polarizer microscopes for analyzing and identifying the petrographic constituents and taking photo of the most petrographic characteristics, 25 of them were added in the petrography table in this thesis.

4. LOCATION

The studied area is located at 15 km southeast of Sulaimaniyah city, which located in northeast of Iraq close to Iranian border (Figure 4.1). The area is called as Arbat road it extends to a narrow strip from Halabja town.

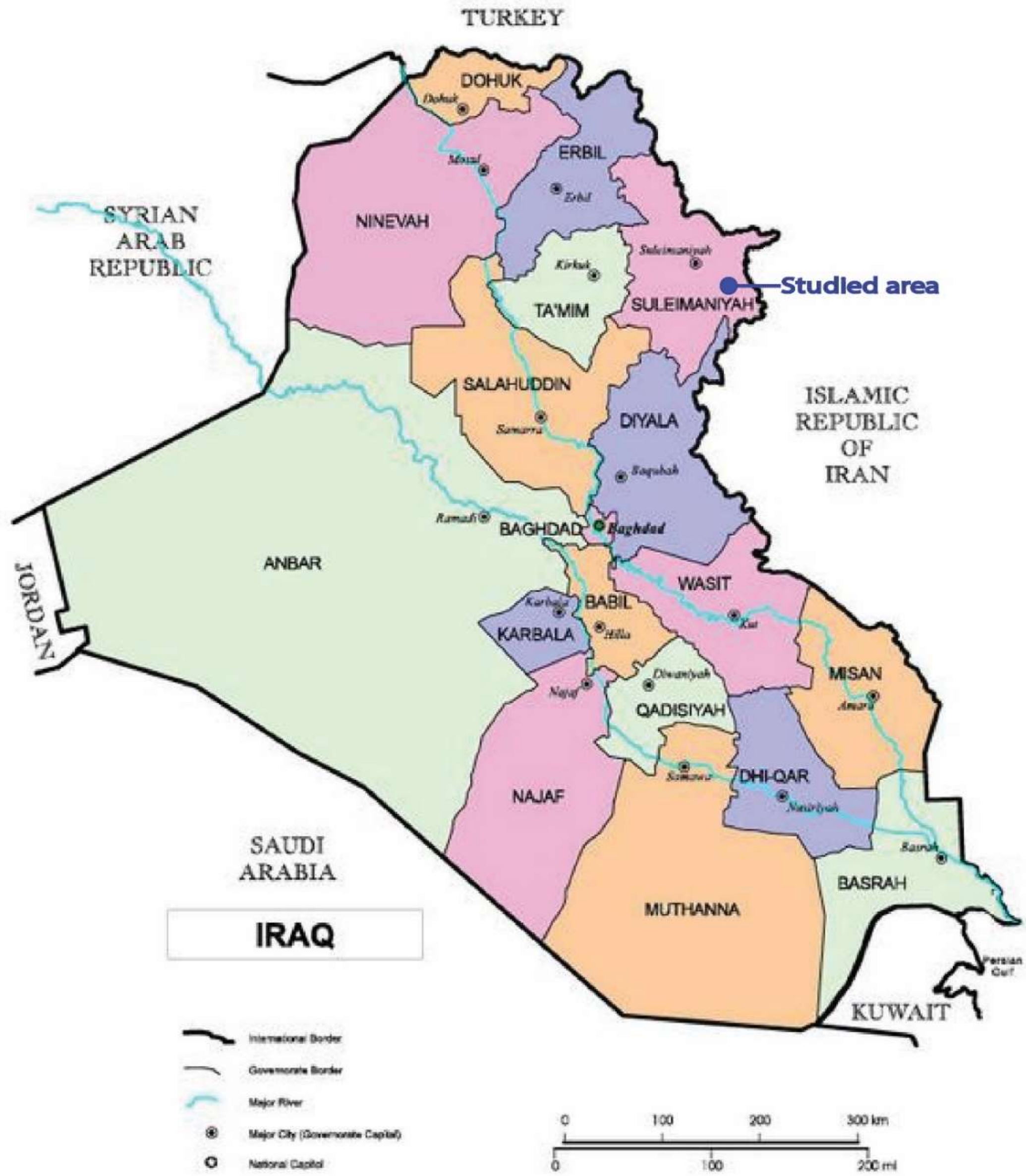

Figure 4.1. Location map of Iraq (http://iraqpictures.org/map-of-iraq/)

Figure 4.2. Google Earth image indicating the study area.

5. PREVIOUS WORKS

Since the Tanjero Formation is one of the main unit of the area composed of many oil bearing formations, several geological studies were done in the area. The most known studies are given in the following paragraphs.

Bellen et al. (1959), in their work stated that Tanjero Formation is first defined and known as Tanjero Clastic Formation by Dunnington in 1952. They mentioned that the type section of the unitlocated in Sirwan Valley, 1km to the south of Kani Karweshkan village, close to Halabja Town and at the right side of Sirwan River (upstream of Dialla River). They defined briefly the distribution, age, lithology, fossil content, stratigraphy of the formation, and surface distribution at different localities in northeastern Iraq.

Kassab (1972) Kassab (1975) studied the biostratigraphy of this formation and indicated its age as late Campanian -Maastrichtian.

Al-Mehaidi (1975) briefly discussed the tectonic plates and stratigraphy of the formation in Chuarta area, and revealed the occurrence of the Aqra formation in the upper part of the formation of Tanjero.

Al-Rawi (1981) studied the sedimentology and petrology of the formation in selected sections (Sulaimaniyah, Dukan and Rawandoz Sections). He said that the lower part of Sulaimaniyah has a shallow environment of deposition and concluded that the paleocurrent towards the northwest and the parallel flow of Tanjero trough axis. He studied in detail the clay minerals and sandstone formation. He also classified sandstones by Pettijohn (1975) and plotted them on triangles.

Abdel-Kireem (1986a) studied the formation within stratigraphy of Upper Cretaceous and Lower Tertiary of Sulaimaniyah- Dokan Region. He suggested to take out the word clastic from the formation’s name also to place the lower part of the formation with Shiranish Formation.

Abdel-Kireem (1986b) studied planktonic forams and stratigraphy of Tanjero Formation. He gave the chronological age of Middle-Late Maastrichtian for this formation in Dokan area.

Saadallah and Hassan (1987) analyzed the sedimentological composition deposits in selected sections of Dokan and Sulaimaniyah regions. They determined that the paleocurrent directed to the west and southwest.

Jaza (1992) which deals with the analysis of sedimentary facies for the formation in selected sections of Sulaimaniyah and Dokan regions. He documented the turbidite and the submarine fan (as the deposition feature of the basin) in the formation.

Minas (1997) studied sequence stratigraphy of Tanjero Formation and put it in deeper environment as compared with Shiranish Formation and considered the formation as a transgressive part of the cycle.

Lawa et al. (1998) studied carbonate layers in the upper part of Tanjero Formation at Chuarta-Mawat area and conclude that these beds belong to Aqra Formation, which interfingered with Tanjero Formation.

Al-Rawi and Al-Rawi (2002) studied the formation as turbidite illustration of flysch type in northeast and north of Iraq. They determined that the formation deposited in deep environment without the limestone beds that are deposited in shallow environment.

Karim (2004) studied basin analysis of Tanjero Formation in Sulaimaniyah area, NE-Iraq. He found and detailed many sedimentary structures for the first time and discussed them in more detail He changed the previous two parts (lower and upper) of this formation into three parts (lower, middle and upper). He detected that the lithology for the formation is almost a reflection of that of Qulqula Radiolarian Formation.

Karim (2004), Karim and Surdashy (2005a) they studied tectonic and depositional history of Upper Cretaceous Tanjero Formation in Sulaimaniyah Area, NE Iraq. Indicated the palaeocurrent direction by sedimentary structures and direction of the channels and incised valleys, they proved that the direction toward southern and southwestern direction.

Karim (2004), Karim and Surdashy (2005b) they found that the basin of Tanjero Formation is consider as early foreland basin while in the older studies it considered as trench or miogeosyncline. They found the basin of the formation connected tectonically with that of underlying Shiranish Formation in one single basin, which is sometimes called initial Zagros Foreland Basin.

Karim (2005c) studied source of ball and pillow-like structures in Tanjero Formation in Sulaimaniyah area, NE-Iraq.

Karim and Surdashy (2006a) they studied Sequence Stratigraphy of Upper Cretaceous Tanjero Formation in Sulaimaniyah Area, NE-Iraq, They studied the complete rock body for the formation and divided into two main depositional sequences and correlated in eight sections that are named lower and upper Sequences. The writers stated that about 80% of this formation is deposited into the upper sequence although the rest is deposited into the lower sequence.

Karim (2006b) studied the environment of Tanjero Formation, he found the sedimentation rate of the formation (high and in some cases more than 30cm in a day). He concluded that the depositional environment of upper and lower part of Tanjero Fn. is shallow marine while the middle part has deposited in deep basin.

Karim (2006c) studied comparison involving the Khabour and Tanjero Formations from North Iraq. The writer discovered that Tanjero Formation is just one of the best studied stratigraphic units and recently been shown to be deposited in foreland basin in various shallow and deep environments, and he found many sedimentary structure.

Karim (2007) studied possible affectation of storm on Sediments of Upper Cretaceous Foreland Basin: The author had a research study for tempestite in Tanjero Formation, Sulaimaniyah Area, NE-Iraq and found many sedimentary structures in lower and upper part of Tanjero Formation those shows shallow environment. These sedimentary structures revealed that during deposition of those parts the sea level is really lowered that the sediments are affected repeatedly by storms surges. The writer mentioned that these storms reworked sediments to form storm deposits (tempestite) or to be transported to deeper water and deposited as turbidite.

Sharbazheri (2007) studied age of unconformity in the Tanjero Formation in Chwarta Area Northeast of Iraq and then concluded that the chronological age of the thick succession of 500m conglomerate and red clay stone layers within the incised valleys during the lower part of Tanjero Formation at Chwarta area is estimated as (1.23 m. y) duration. The age determination is attained by Planktonic Foraminiferal.

Sharbazheri (2010) studied planktonic foraminiferal biostratigraphy for the Upper Cretaceous Reddish to Pale brown transitional succession in Smaquli Area, Northeast and found that the interval time of the reddish to pale brown succession (Shiranish-Tanjero transition unit) of the studied section in the Smaquli area is appreciated to be more than (2.150 my). In his work planktonic foraminifer's bio zones of this studied section displays continuous sedimentary succession.

Karim et al. (2012) studied relations between cretaceous stratigraphic units he discovered that the relations are organized in simple graphical style of temporal and special relations between Cretaceous Tanjero Formations designated as lateral correspondent facies of Aqra Formation.

Karim et al. (2014) studied origin of fossiliferrous limestone beds inside the upper part of Tanjero Formation during the Northwest of Sulaimaniyah Area, The Aqra Formation involve fossiliferrous and biogenic detrital limestone with Omphalocyclus, Loftusia, solitary coral and *Orbitoides* fossils. They pointed out that the limestone is transported by submarine mass wasting from neritic environment in Chwarta-Mawat area to deep environment at the current position. In the Thrust and High Folded Zones, Tanjero and Aqra formations were sharing same basin and tectonic setting during Late Cretaceous in large foreland basin without paleo ridge between them.

6. GEOLOGICAL SETTING

Northern Iraq is located in the northern Arabian Platform and Northern of Iraq contains the northwestern extension of the Zagros Mountain range (the Zagros Fold and Thrust belt) and the northern part of the stable Arabian Platform (Figure 6.1 and Figure 6.2). The convergent boundary between the Eurasian and Arabian plates forms the Zagros folds and belt (Ahmed, 2013).

The Zagros fold and thrust belt is positioned along the NE margin of the Arabian Plate. It has developed as a cause of the oblique collision between the sub ducting NE Arabian margin and the Eurasian margin (Homke et al. 2004), reflecting gradual closure of the Neotethys Ocean, generally through Late Cretaceous-Cenozoic times (Talbot and Alavi 1996) after (Awdal et al., 2013).

Closure of the oceanic basin and related ophiolite obduction is considered to be Campanian-early Maastrichtian (Jassim and Goff 2006; Aqrawi et al. 2010), when ophiolitic thrust sheets affected regional loading and crustal flexing, setting up an originally narrow fore deep basin. This fore deep to wedge top basin is now wide and deep (Fared et al. 2006), and extends along the NE margin of the Arabian Plate (Aqrawi et al. 2010). Toward the hinterland, the ophiolite thrust sheets and associated sedimentary rocks, accretionary subduction complexes and island arc plutons have been uplifted above sea level (Jassim and Goff2006; Aqrawi et al. 2010), then eroded and redeposited in the foreland basin system as flysch-type deposits (Aqrawi et al. 2010) after (Awdal et al., 2013).

The current configuration of the Zagros orogenic belt can be divided into distinct structural zones, all trending NW-SE, parallel with the fold and thrust belt. These zones are, from the NE hinterland to the SW-verging thrusts are found in the imbricate and high folded zones, whereas major folds above blind thrusts characterize the Foothill Zone. There is transitional boundary of very gentle to subhorizontal detachment folding further SW towards the Mesopotamian foreland basin (e.g. Fared et al.2006) in the foothills, syntectonic deposit are mainly found as narrow and folded lenticular wedges between ridges of upfolded deeper sedimentary units, gradually forming a continuous blanket of gently folded, undisturbed sedimentary units in the direction of the foreland. The foothill to foreland zones of Kurdistan have anticlines that are characterized by high surface topography and very good exposures, whereas synclines from low terrains that are generally covered by soil and river deposits (Awdal et al., 2013).

The basin of Tanjero Formation is affected by the Campanian-Maastrichtian orogenic movements in the adjacent basin to the east (Zagros) in northeastern Iraq and (western and southwestern Iran). The depositional environment was separated by a ridge from the area of the unstable shelf (Bellen et al., 1959, Buday, 1980, Al-Rawi, 1981).

Based on the type locality The Tanjero Formation is exposed along a belt extending NW-SE through Sulaimaniyah (Al-Rawi, 1981). This long narrow area by which the Tanjero Formation is exposed lies mostly with into the imbricated zone and partly with into the high fold zone (Buday and Jassim, 1987) the studied sections located in high fold zone (Figure 6.2).

Although in the Imbricated Zone, according to (Lawa et al., 1998), Red Bed Series overlie the formation by conformable. The type section of the formation is found at Sirwan valley near Halabja town about 50 km to the southeast of Sulaimaniyah City (Bellen et al., 1959).

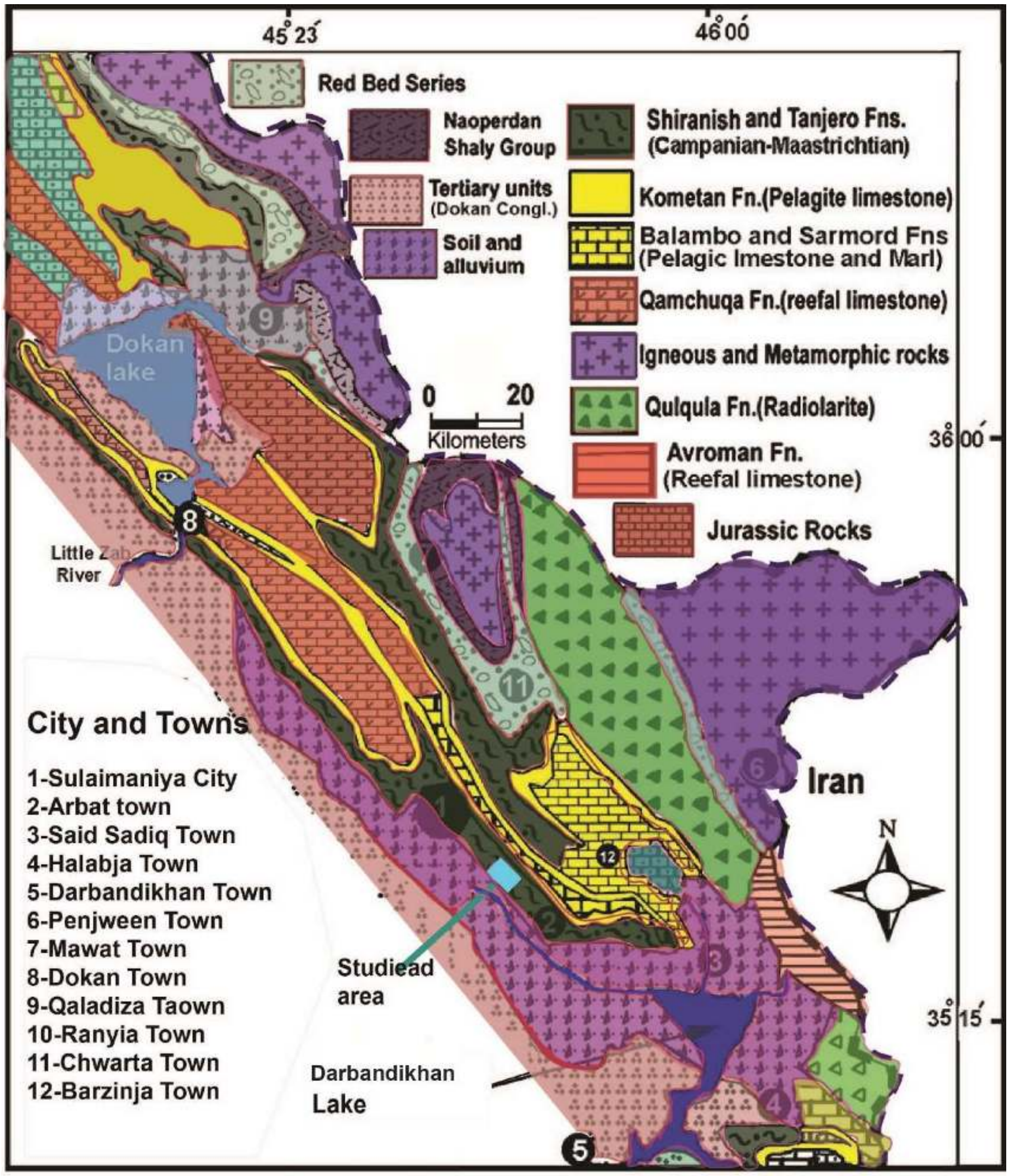

Figure 6.1. Geological map of Sulaimaniyah area including study area located between Arbat (2) and the city center of Sulaimaniyah (1), modified after (Karim and Khanaqa, 2016).

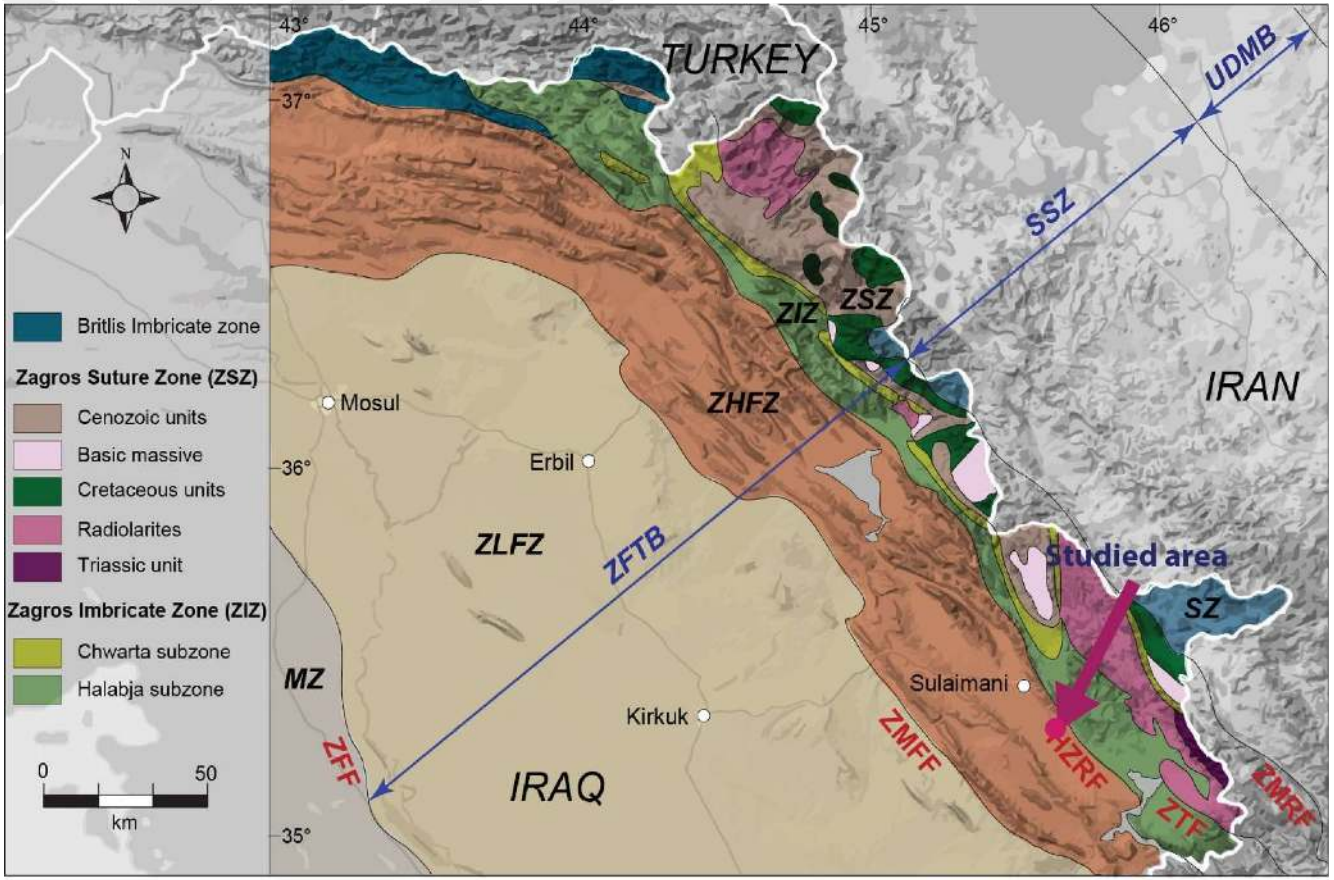

Figure 6.2. Tectonic map of northeast Iraq showing regional tectonic divisions and the location of the study area within the Zagros Orogenic . (Z¬FTB: Zagros Fold–Thrust Belt; ZLFZ: Zagros Low Folded Zone; ZHFZ: Zagros High Folded Zone; ZIZ: Zagros Imbricate Zone; ZSZ: Zagros Suture Zone; SZ: Shalair Zone; SSZ: Sanandaj-Sirjan Zone; UDMB: Urumieh Dokhtar Magmatic Belt; MZ: Mesopotamian Zone; ZFF: Zagros Foredeep Fault; ZMFF: Zagros Mountain Front Fault; HZRF: High Zagros Reverse Fault; ZTF: Zagros Thrust Front; ZMRF: Zagros Main Reverse Fault) (Baziany, 2014).

7. TANJERO FORMATION

7.1. Definition

The Tanjero clastic formation was first defined by Dunnington in 1952. The type section is located southeast of Darbandikhan near the Halabja town (Bellen, 1959). The name Tanjero Formation was used many other investigator as mentioned in the previous works section of the thesis

7.2. Outcrop distribution and stratigraphic contacts

Tanjero Formation is widely cropping out along and lying parallel to the Iranian border (Figure 6.1). It is distributed in the Imbricated zone in northern Iraq and High Folded zone southeast of the Greater Zab River (Figure 6.2).

A lot of formations were defined in the Northern Iraq region (Figure 7.1). Some of them have lateral and vertical stratigraphic relation with the Tanjero Formation. These relations can be find in many previous works. Some important explanations for the stratigraphic relations are in the following paragraphs and related stratigraphic columnar section in the (Figure 7.1).

Tanjero Formation from upper contact with Kolosh Formation is unconformable contact and marked by a total faunal change (Bellen et al., 1959, Buday, 1980). Also some place in it overlies the Shiranish Formation or the Upper Cretaceous limestones unconformably (Jassim and Goff, 2006). Recently, from a biostratigraphic study, (Sharbazheri, 2008) conclude that in several places of the High Folded zone in Northern Iraq continuous sedimentation without interruption or any gaps marks the Kolosh/Tanjero boundary as shown in (Figure 7.1).

The Kolosh Formation and Red bed Series overlay the Tanjero Formation (Figure 7.1). The contact with the Red Bed Series is gradational contact like in the Chwarta area (Lawa et al., 1998), or gradational and unconformable in different localities in Chwarta and Qandil areas (Karim, 2004).

The upper contact of the Tanjero Formation with the Paleogene Kolosh Formation is a disconformity (Bellen et al., 1959, Buday, 1980, Jassim and Goff, 2006). Though more recently (Sharbazheri et al., 2009) through the study associated with the Foraminifera bio-zonation, found a conformable contact (Ahmed, 2013).

The lower contact is conformable with Balambo Formation (Figure 7.1) in the far northeast of non-continuous shallow water reefal carbonate deposition occurred during Maastrichtian inside the foreland basin (Figure 7.2). The shallow water reefal carbonates known as Aqra lenses are intercalated in the Tanjero flysch(Al-Rawi, 1981).

In the studied area (near Arbat town) the lower and upper contacts of the Tanjero Formation are covered and not visible. However, the outcrop is the only turbidite exposure composed of mainly fine to coarse grained excellent thick sandstone beds (Figure 7.3 and Figure 7.4) and small sandy channel fills of Tanjero Formation in the southern part of Sulaimaniyah for as MSc thesis.

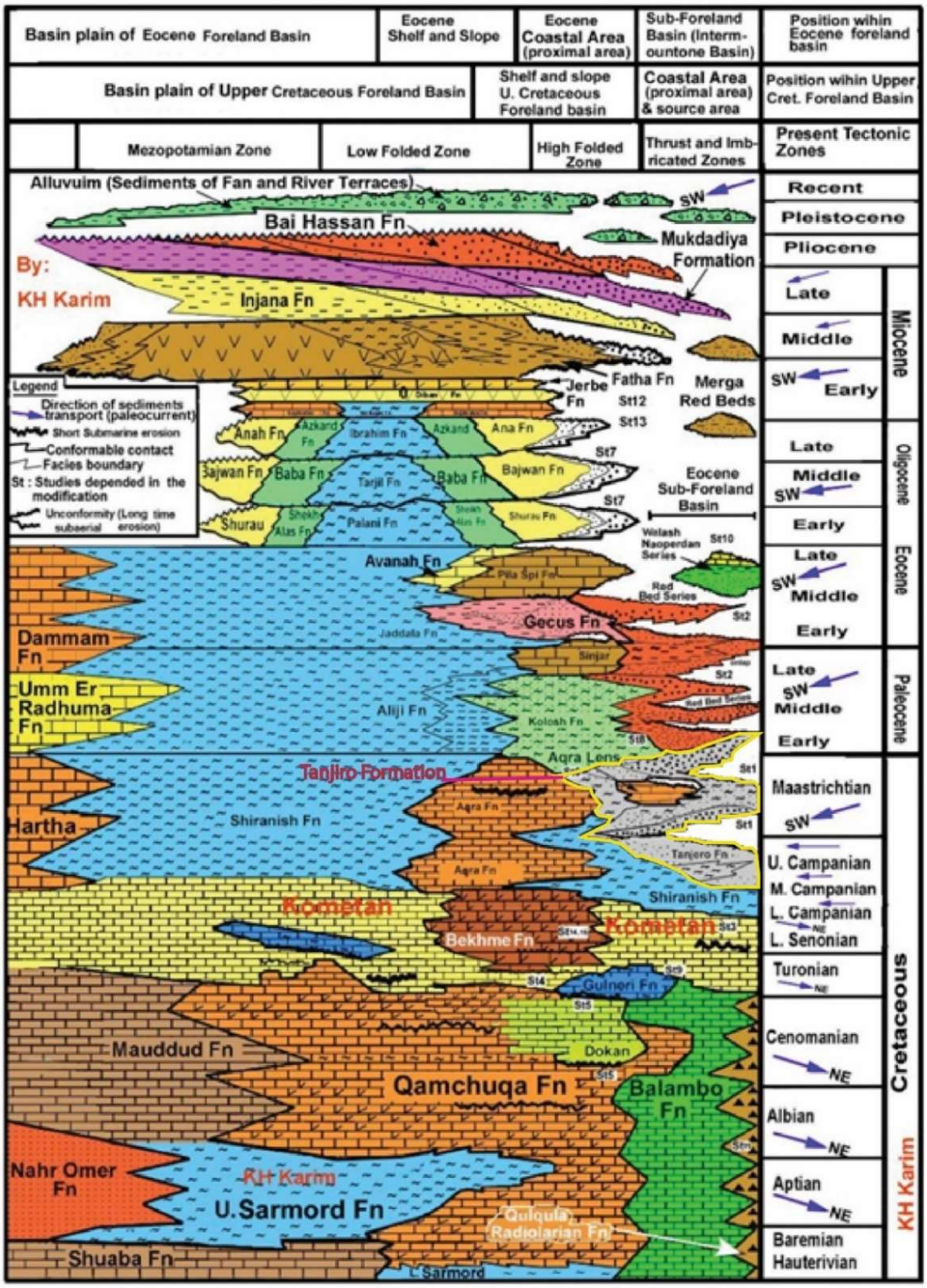

Figure 7.1. New chronostratigraphic Column of Northeast Iraq in which the stratigraphy of the Imbricated and Thrust Zones are shown and most of the previous unconformities in the High and Low Folded Zone are rejected (modified from Bellen et al, 1959 and Omeri and Sadiq, 1977). After (Karim, 2010).

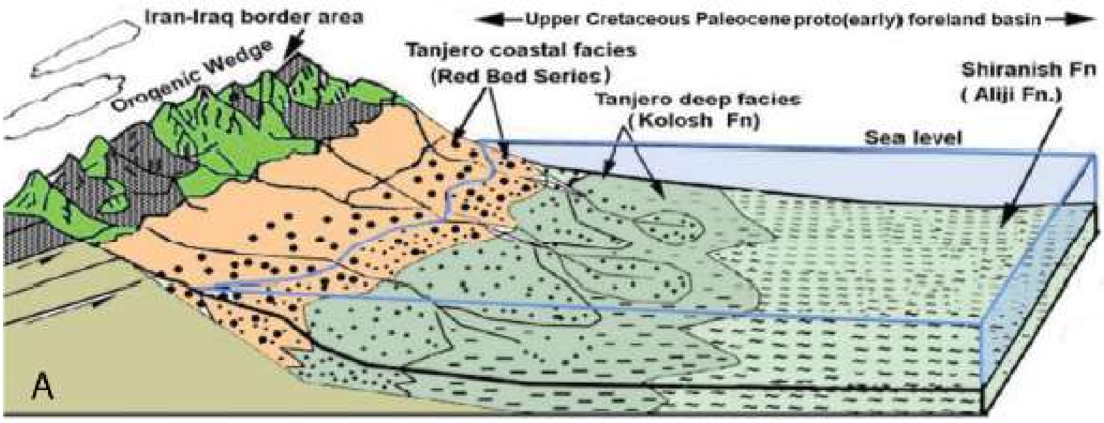

Figure 7.2. Maastrichtian to Lower Eocene basin evolution of Northern Iraq (Karim et al., 2008).

7.3. Lithology

The formation was separated by Dunnington, (1952), (Bellen et al. (1959) on the basis of lithology, in the type section, into two parts; lower and upper parts. The investigator explained that, the lower part thickness is 484 meters and composed of the alternation of pelagic marl with some siltstone and rare marly limestone. According to him the upper part consists of silty marls, siltstone, sandstone, conglomerate and sandy biogenic detrital limestone; the thickness of this part is 1532 meters.

Karim (2004) divided the Tanjero Formation into three parts, lower, middle and upper, according to its lithological differences. The investigator explained the three parts as the followings:

Lithology of the lower part is composed of a thick succession of conglomerate in the areas near to the source areas in the north (such as the Qandil Mountain, and the Chwarta and Mawat areas), and alternation of sand and calcareous shales in the area far from the source (such as Dokan area). The thickness of this part varies from 50 to 1000 m.

The lithology of this part has highly variable lateral grain size distribution. The thick succession of conglomerate is dominant at areas such as to the Qandil Mountain, Chuarta and Mawat areas. These areas are called proximal area (part of the basin that is near to source area). It changes to sand and calcareous shale at Sharazoor and Piramagroon plains in addition to Dokan area. These areas are called distal area (part of the basin that is far from the source area).

The middle part includes thick beds of dark green calcareous marls with thin layers of sandstone and conglomerate. In Chwarta and Mawat areas the middle part is 300 m thick, while in Dokan area it is 130 m thick. This part is simply distinguished from lower and upper parts except at the type locality, which is differentiated by very thick beds of dark green calcareous shale (marl) with less content of conglomerate and sandstone as compared to the other two parts.

Lithology of the upper part is composed of a succession of thick fossiliferrous limestones alternating with black silty calcareous shales or marl (about 50-200 m thick).

Abdel-Kireem (1986a) divided the Tanjero Formation in the Dokan area into three units. The upper unit is 124m thick, composed of sandy bioclastic limestones, silty shales and graded sandstones. The middle unit is 209 m thick and composed of chalky marls with abundant planktonic foraminifera. The lower unit is made of 460 m of green marls and siltstones interbedded with fine-grained sandstones.

In studied area the lithology of the formation is alternation of sandstones, shales, highly variable grain size distribution, and thick beds of sandstone (Figure 7.4 and Figure 7.5) alternated with thin beds of shale and some thin bedded turbidites (tbt). The color of the sandstone generally greenish and gray represent lithological variation and weathering, and some part of shale is light greenish in color. The thickness of the measured sections in the studied area reach 50 m. The lithology of the Tanjero Formation for the studied area was given in detail in the measured sections and lithofacies parts (7.3.1 and 7.3.2) of the thesis.

Figure 7.3. Medium to thick beds of the Tanjero Formation mainly consisting of fine to coarse grained deep marine low density turbidite sandstone. Arbat road view to NW.

Figure 7.4. Widely continuous medium to thick beds interbedded with shales of the Tanjero Formation mainly consisting of fine to coarse grained deep marine low density

Turbidite sandstone on the Arbat road view to SE. Ta and Tb divisions of Bouma sequence were illustrated on the sandstone bed in the lower middle part of the photo.

Figure 7.5. Thick shale interval between sandstone representing lobe intervals during non-deposition time of turbidites. Arbat road section view to the West.

7.3.1. Measured Sections

Six measured sections were taken for the facies analysis, taking rock samples, palaeoflow directions in the Arbat road section (Figure 7.6). The thickness of the logs are ranging between 45-50 m and labelled as TL1 to TL6. From these measured sections 49 facies types were recognized. The explanations for the symbols and patterns are in the (Figure 7.7).

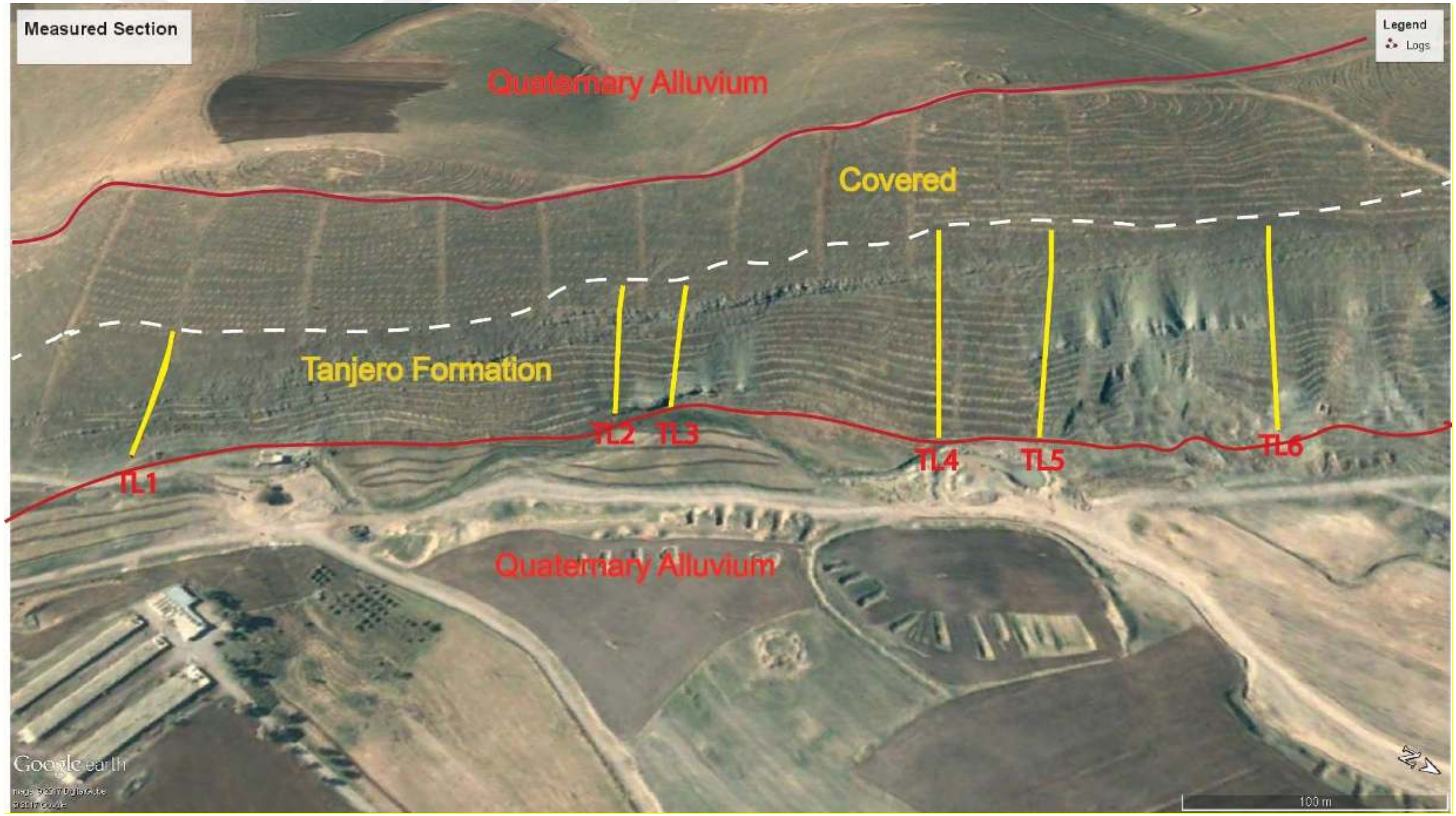

Figure 7.6. Google Earth image indicating the locations of the measured sections. From left to right the logs traces, red lines in the image, are numbered 1 to 6. Arbat road section, about 15 km SE of Sulaimaniyah city center.

1. TL1 this section is located between latitudes 35°26′ 39.92″ north and longitudes 45˚33′32.68″ east.

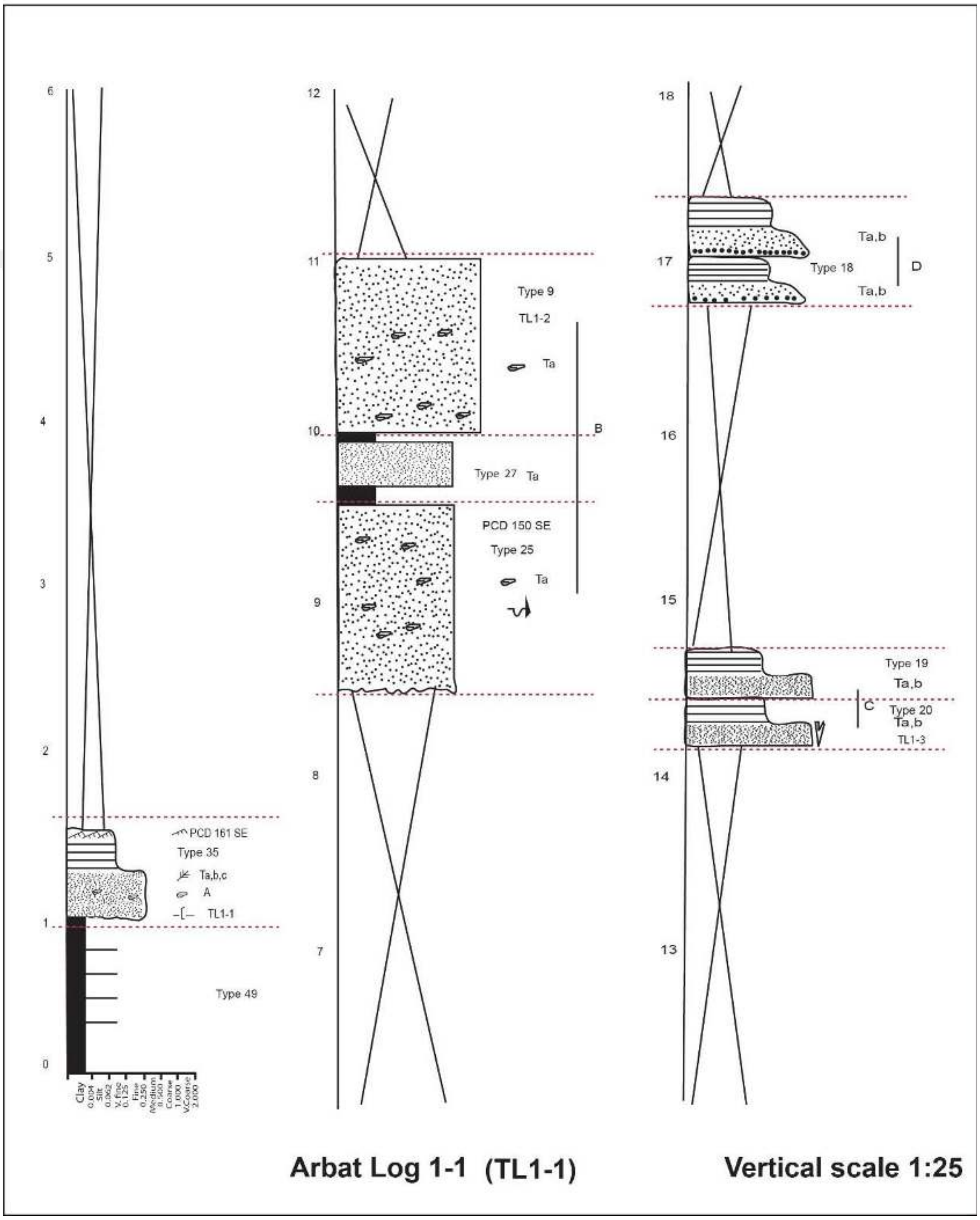

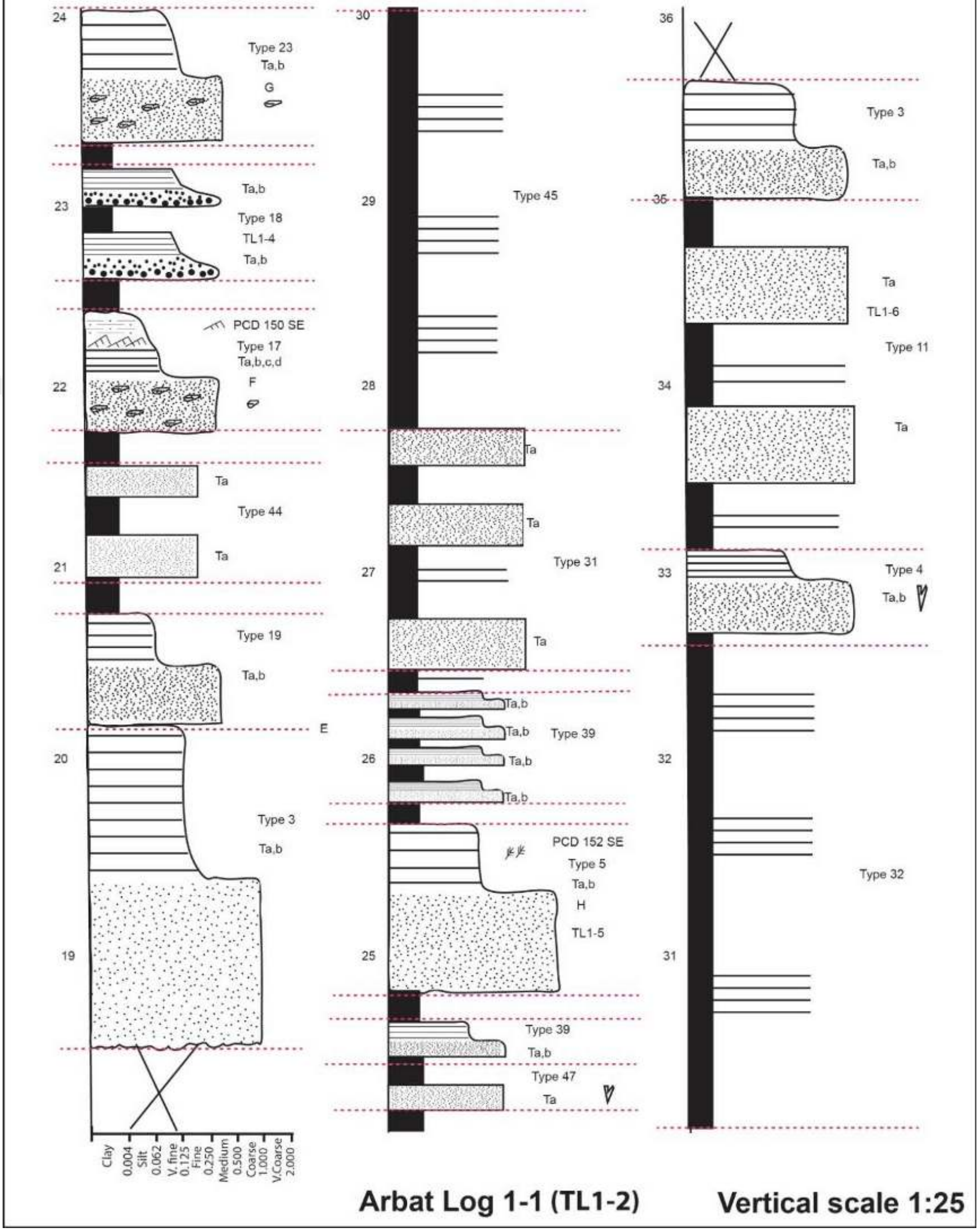

24
Type 23
Ta,b
G
23
Ta,b
Type 18
TL1-4
Ta,b
PCD 150 SE
Type 17
Ta,b,c,d
22
F
Ta
Type 44
21
Ta
Type 19
Ta,b
E
20
Type 3
Ta,b
19
Clay
0.004
Silt
0.062
V.fine
0.125
Fine
0.250
Medium
0.500
Coarse
1.000
V.Coarse
2.000
30
29
Type 45
28
Ta
Ta
27
Type 31
Ta
Ta,b
Ta,b
Type 39
26
Ta,b
Ta,b
PCD 152 SE
Type 5
Ta,b
H
TL1-5
25
Type 39
Ta,b
Type 47
Ta
36
Type 3
Ta,b
35
Ta
TL1-6
Type 11
34
Ta
33
Type 4
Ta,b
32
Type 32
31
Arbat Log 1-1 (TL1-2)
Vertical scale 1:25

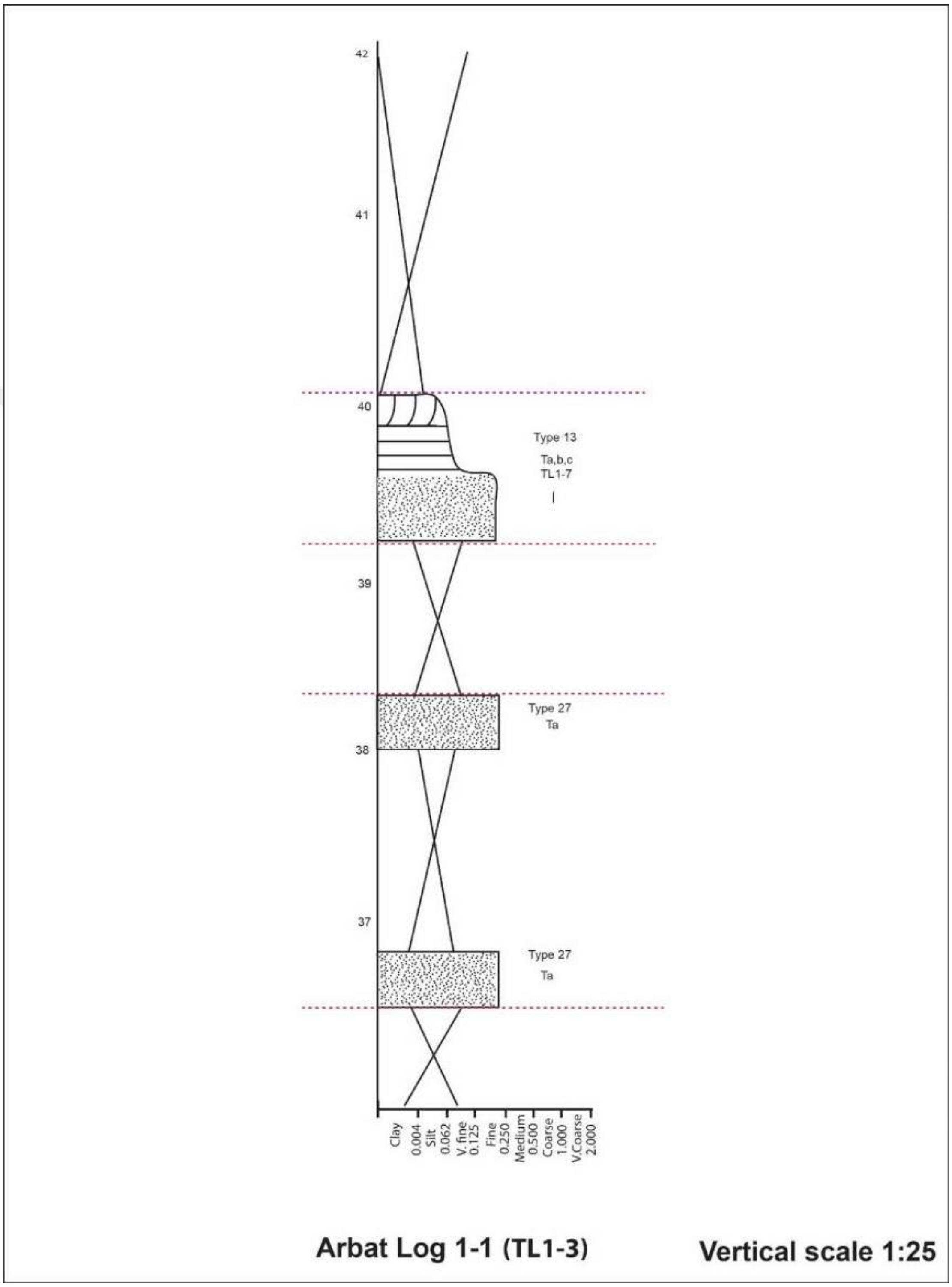
42
41
40
Type 13
Ta,b,c
TL1-7
39
Type 27
Ta
38
37
Type 27
Ta
Clay
0.004
Silt
0.062
V. fine
0.125
Fine
0.250
Medium
0.500
Coarse
1.000
V.Coarse
2.000
Arbat Log 1-1 (TL1-3)
Vertical scale 1:25

2. TL2 this section is located between latitudes 35˚26′47.69″ north and longitudes 45˚33′ 26.32″east.

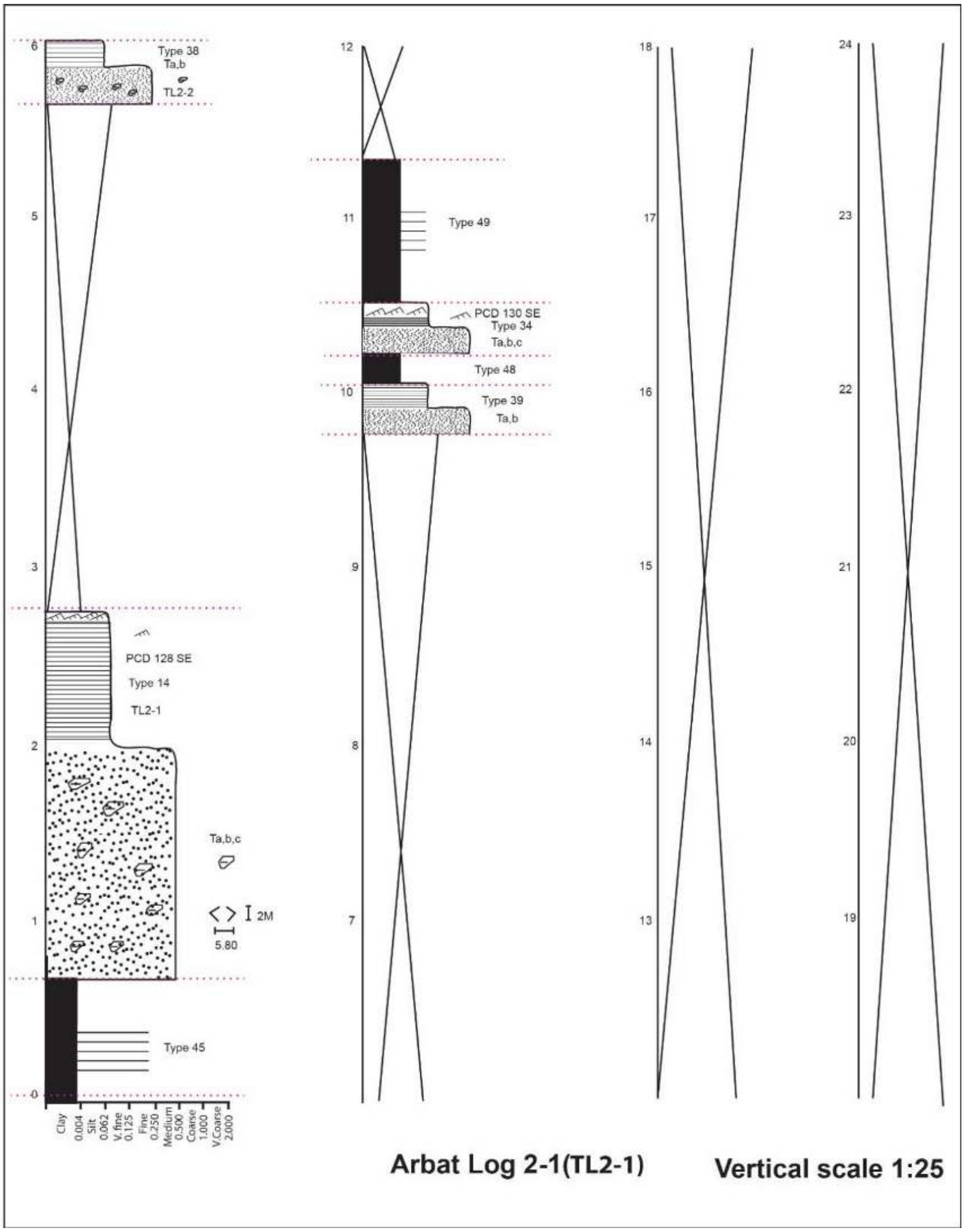

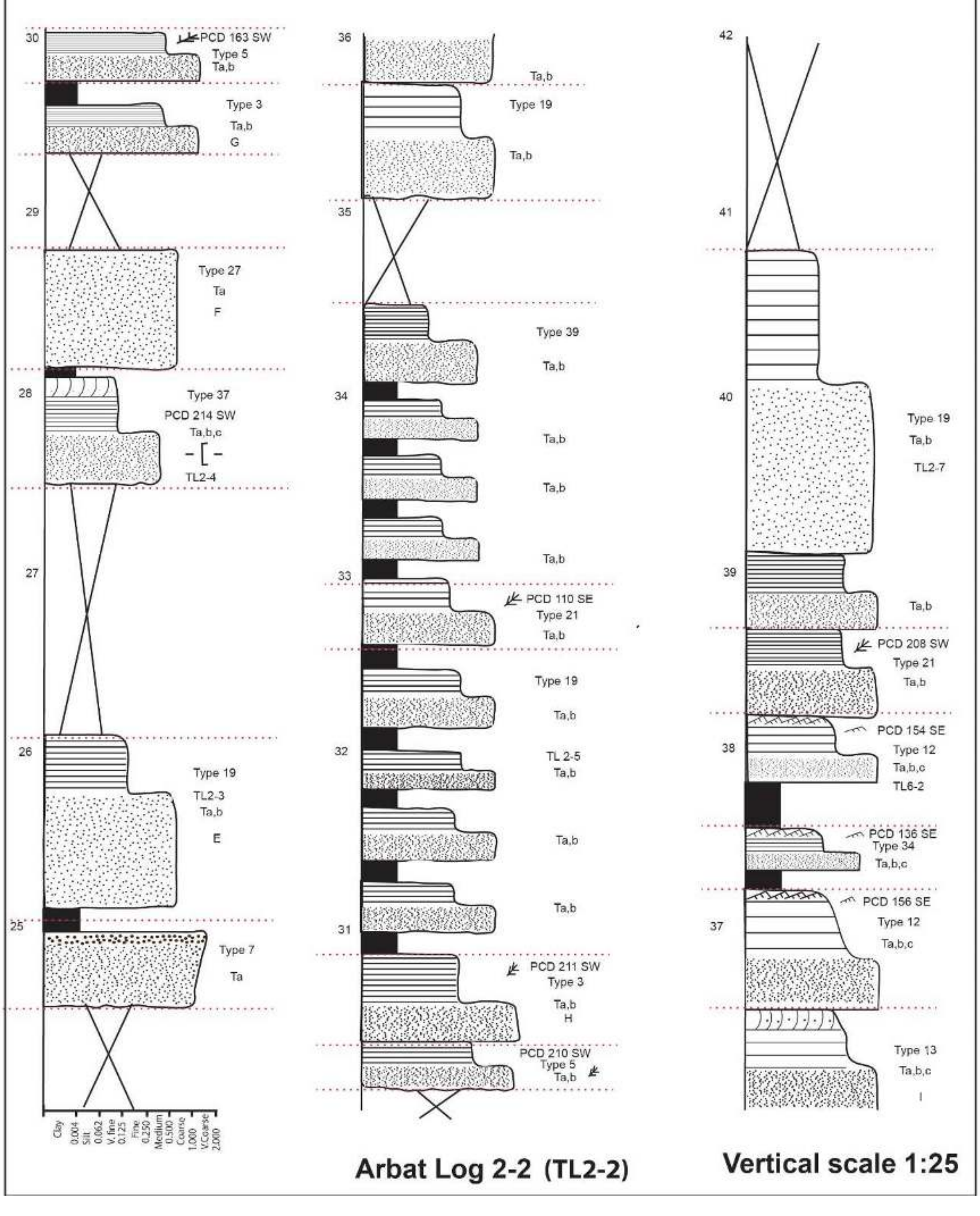
PCD 163 SW
Type 5
Ta,b
Type 3
Ta,b
G
Type 27
Ta
F
Type 37
PCD 214 SW
Ta,b,c
TL2-4
Type 19
TL2-3
Ta,b
E
Type 7
Ta
Clay
0.004
Silt
0.062
V. fine
0.125
Fine
0.250
Medium
0.500
Coarse
1.000
V.Coarse
2.000
Type 19
Type 39
PCD 110 SE
Type 21
TL 2-5
PCD 211 SW
Type 3
H
PCD 210 SW
Type 5
Type 19
TL2-7
PCD 208 SW
Type 21
PCD 154 SE
Type 12
Ta,b,c
TL6-2
PCD 136 SE
Type 34
PCD 156 SE
Type 12
Type 13
I
Arbat Log 2-2 (TL2-2)
Vertical scale 1:25

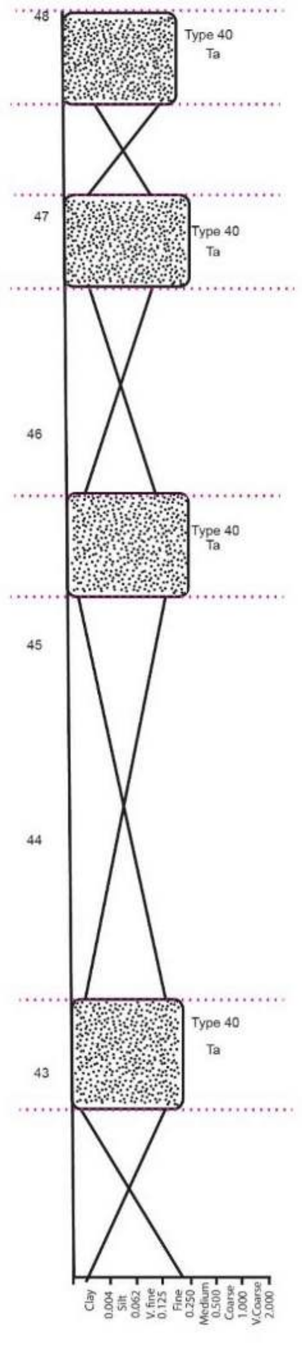

Arbat Log 2-3 (TL2-3) **Vertical scale 1:25**

3. TL3, this section is located between latitudes 35˚26′ 48.48″ north and longitudes 45°33′25.69″ east.

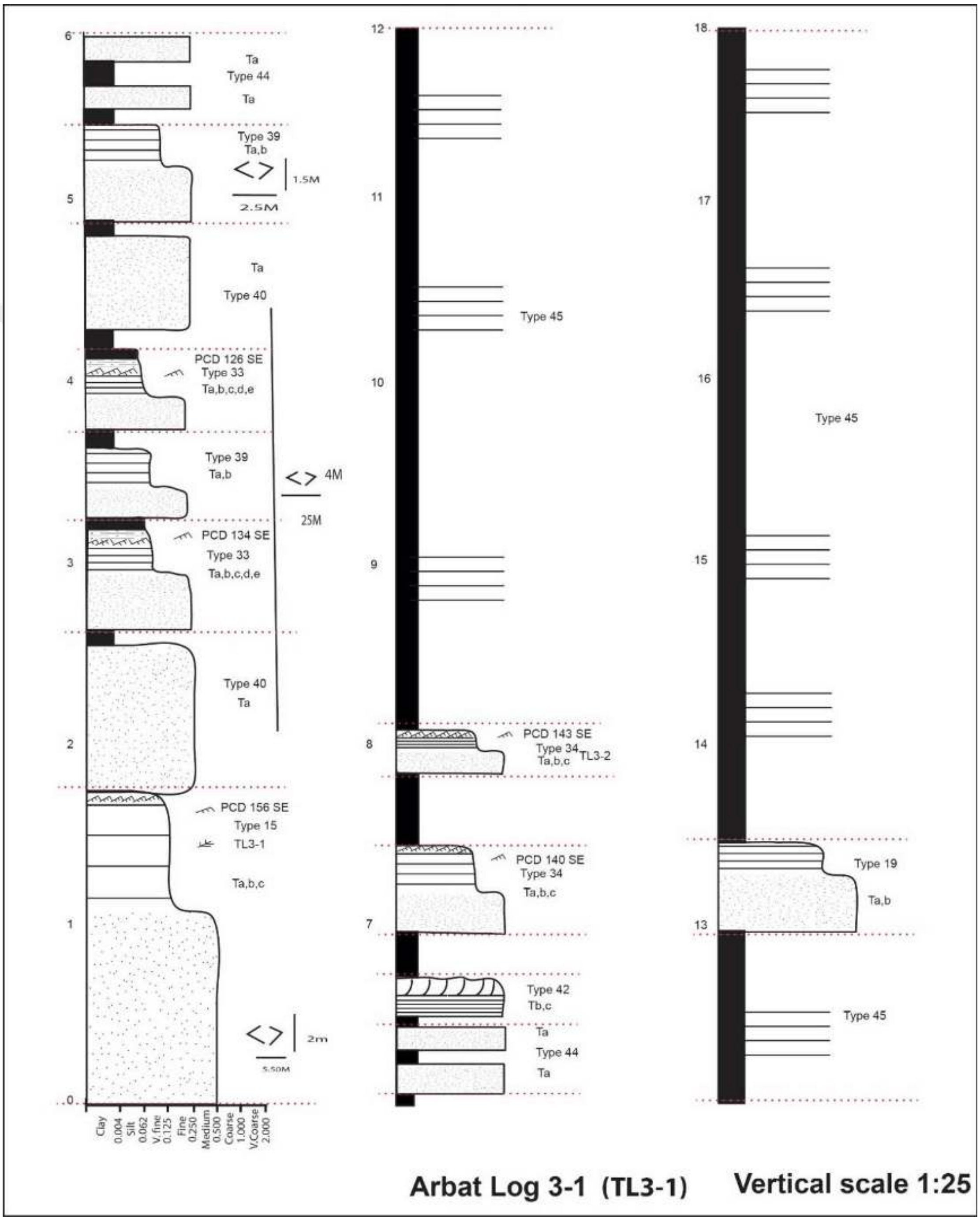

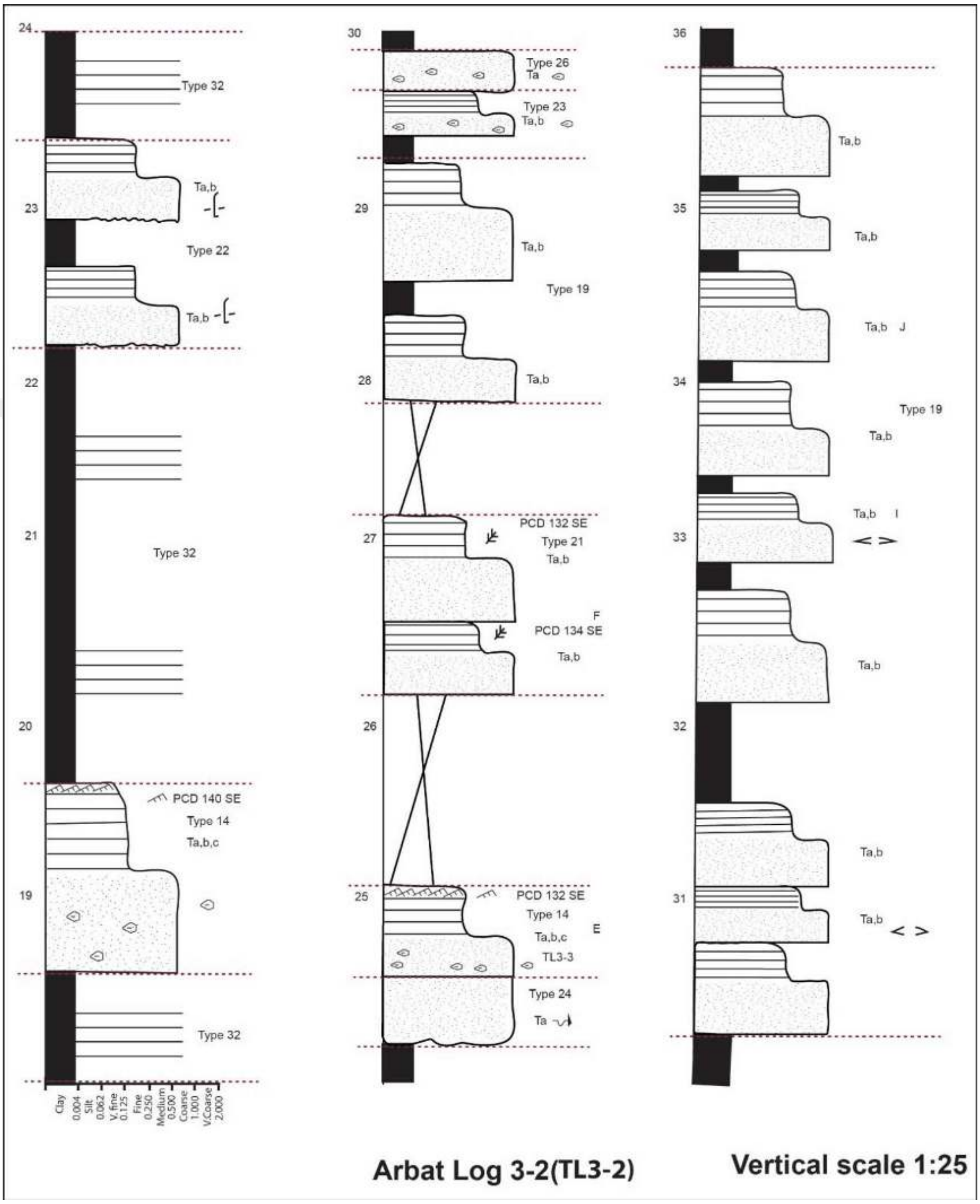

24
Type 32
23
Ta,b
Type 22
Ta,b
22
21
Type 32
20
PCD 140 SE
Type 14
Ta,b,c
19
Type 32
Clay
0.004
Silt
0.062
V. fine
0.125
Fine
0.250
Medium
0.500
Coarse
1.000
V.Coarse
2.000
30
Type 26
Ta
Type 23
Ta,b
29
Ta,b
Type 19
28
Ta,b
27
PCD 132 SE
Type 21
Ta,b
F
PCD 134 SE
Ta,b
26
25
PCD 132 SE
Type 14
Ta,b,c
E
TL3-3
Type 24
Ta
36
Ta,b
35
Ta,b
Ta,b J
34
Type 19
Ta,b
Ta,b I
33
Ta,b
32
Ta,b
31
Ta,b
Arbat Log 3-2(TL3-2)
Vertical scale 1:25

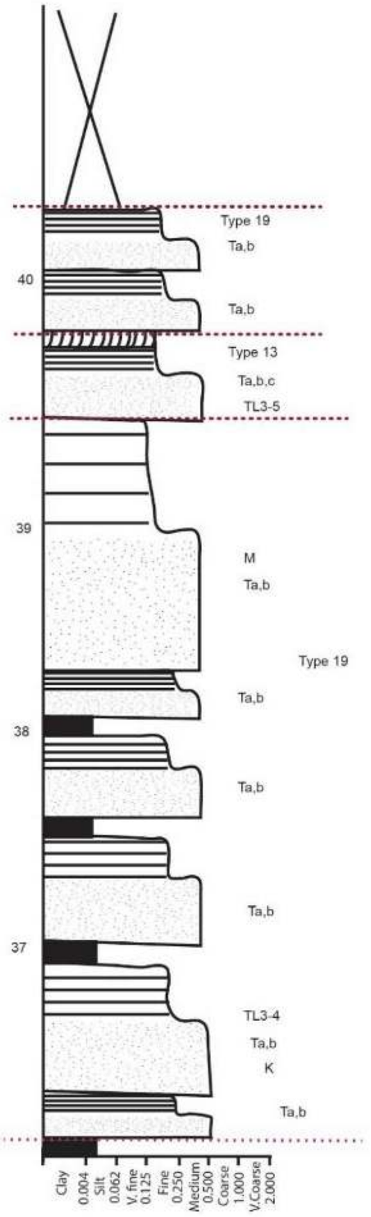

Arbat Log 3-3 (TL3-3) Vertical scale 1:25

4. TL4, this section is located between latitudes 35˚26′ 52.48″ north and longitudes 45˚33′23.76″east.

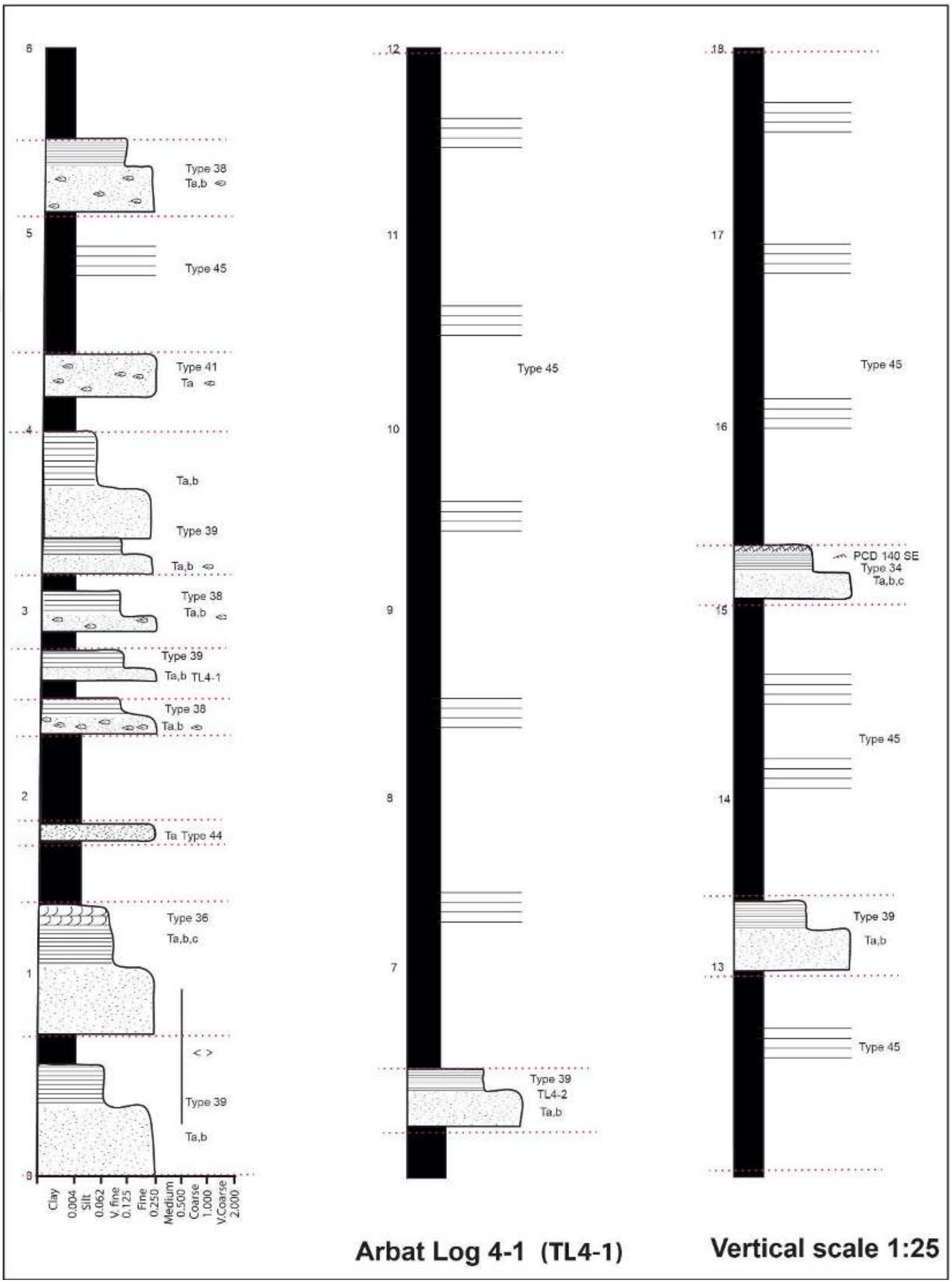

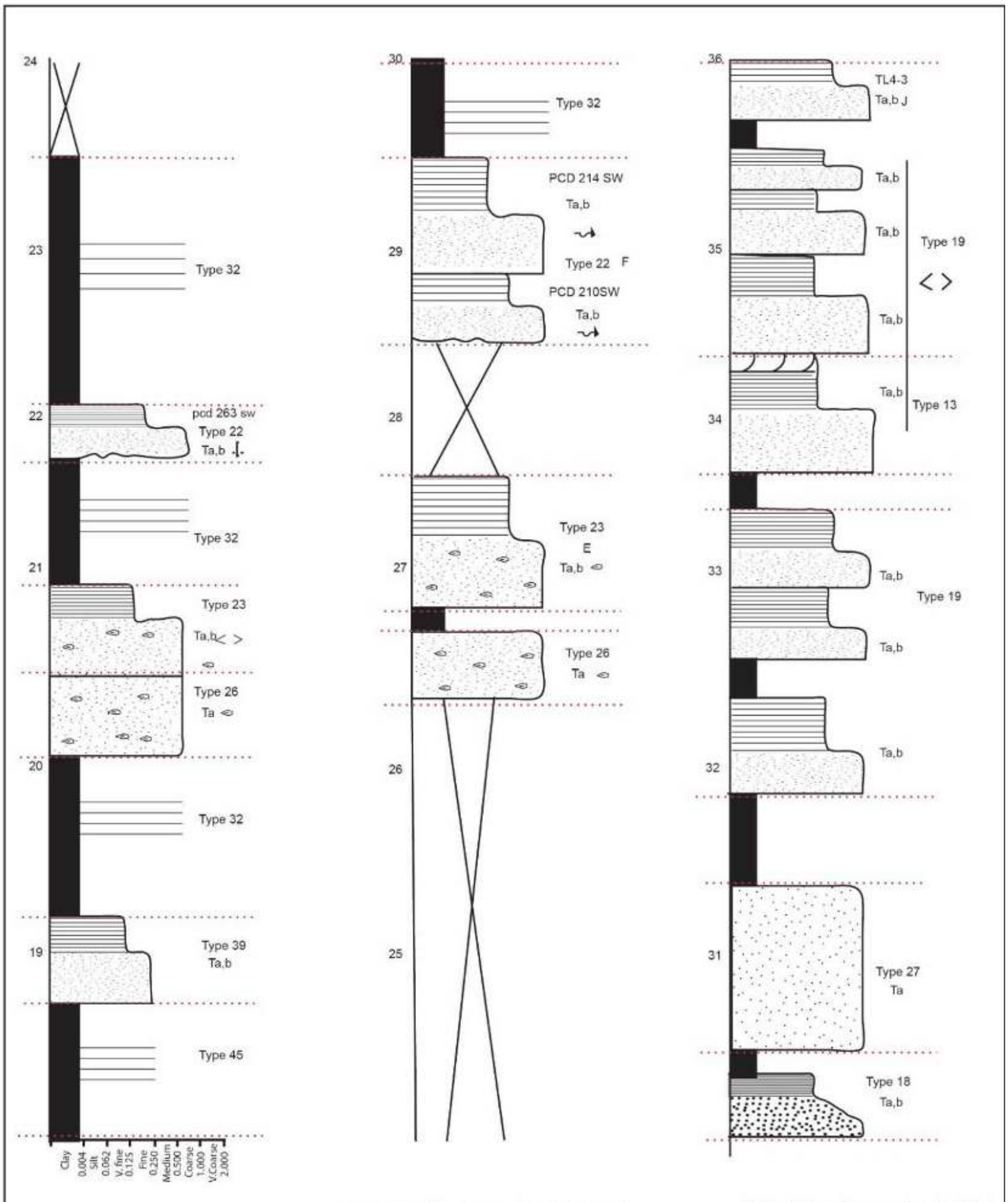

Arbat Log 4-2 (TL4-2) Vertical scale 1:25

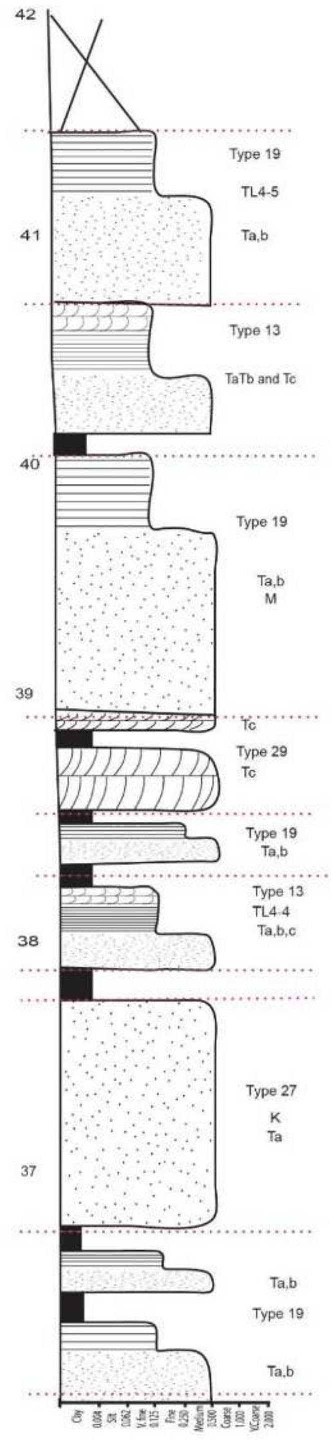

Arbat Log 4-3 (TL4-3) Vertical scale 1:25

5. TL5 this section is located between latitudes 35˚26′ 53.92″ north and longitudes 45˚33′23.05″east.

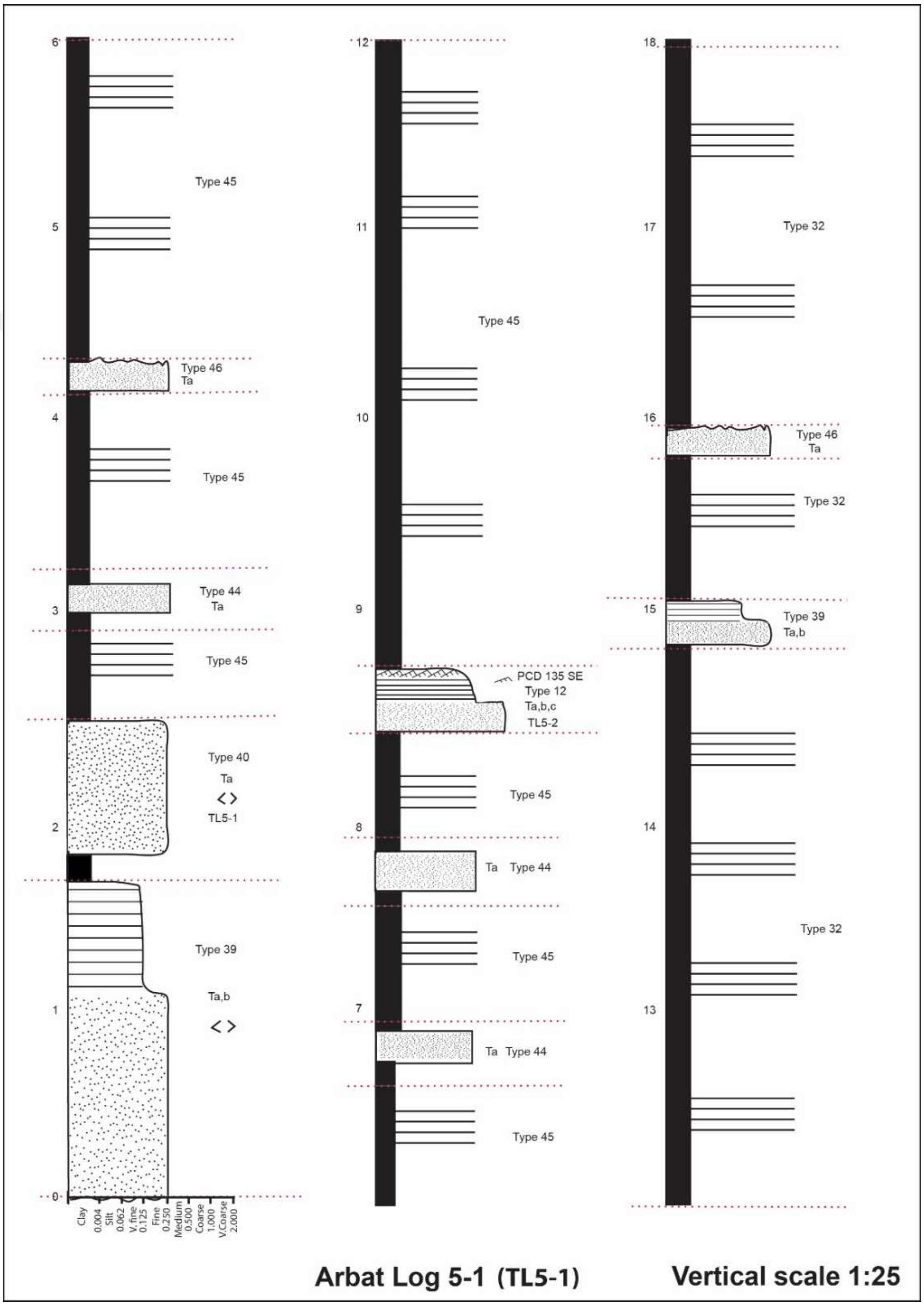

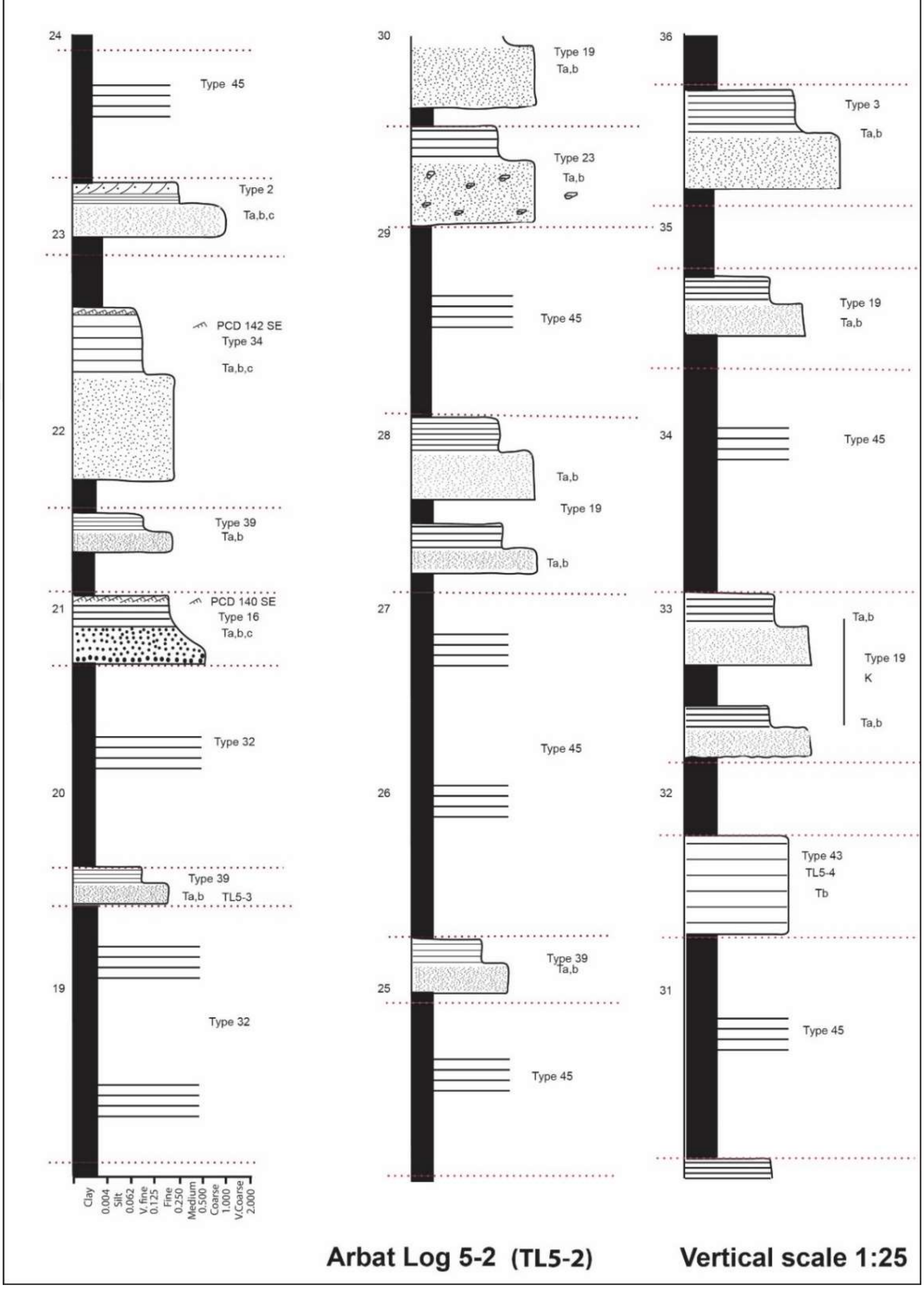

24
Type 45
Type 2
Ta,b,c
23
PCD 142 SE
Type 34
Ta,b,c
22
Type 39
Ta,b
21
PCD 140 SE
Type 16
Ta,b,c
Type 32
20
Type 39
Ta,b
TL5-3
19
Type 32
Clay
0.004
Silt
0.062
V.fine
0.125
Fine
0.250
Medium
0.500
Coarse
1.000
V.Coarse
2.000
30
Type 19
Ta,b
Type 23
Ta,b
29
Type 45
28
Ta,b
Type 19
Ta,b
27
Type 45
26
Type 39
Ta,b
25
Type 45
36
Type 3
Ta,b
35
Type 19
Ta,b
34
Type 45
33
Ta,b
Type 19
K
Ta,b
32
Type 43
TL5-4
Tb
31
Type 45
Arbat Log 5-2 (TL5-2)
Vertical scale 1:25

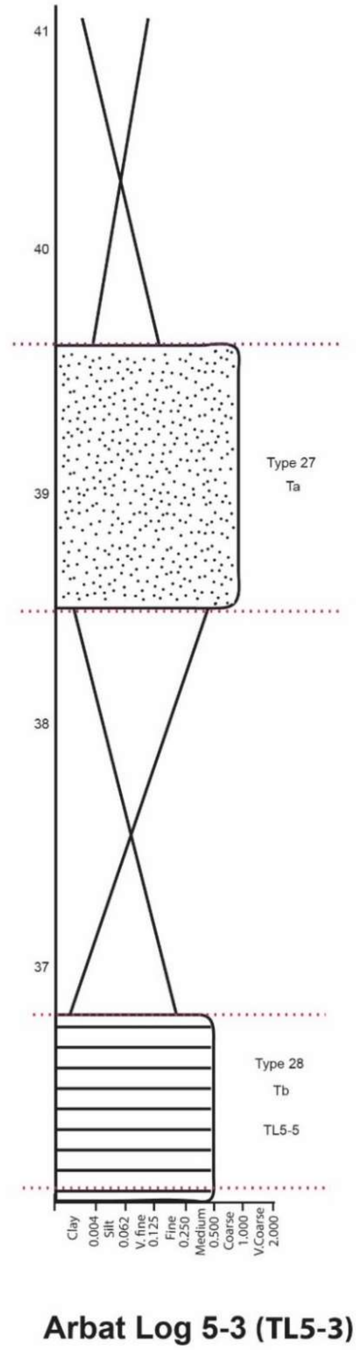

Arbat Log 5-3 (TL5-3) **Vertical scale 1:25**

6. TL6 this section is located between latitudes 35˚26′ 57.14″ north and longitudes 45˚33′21.12″east.

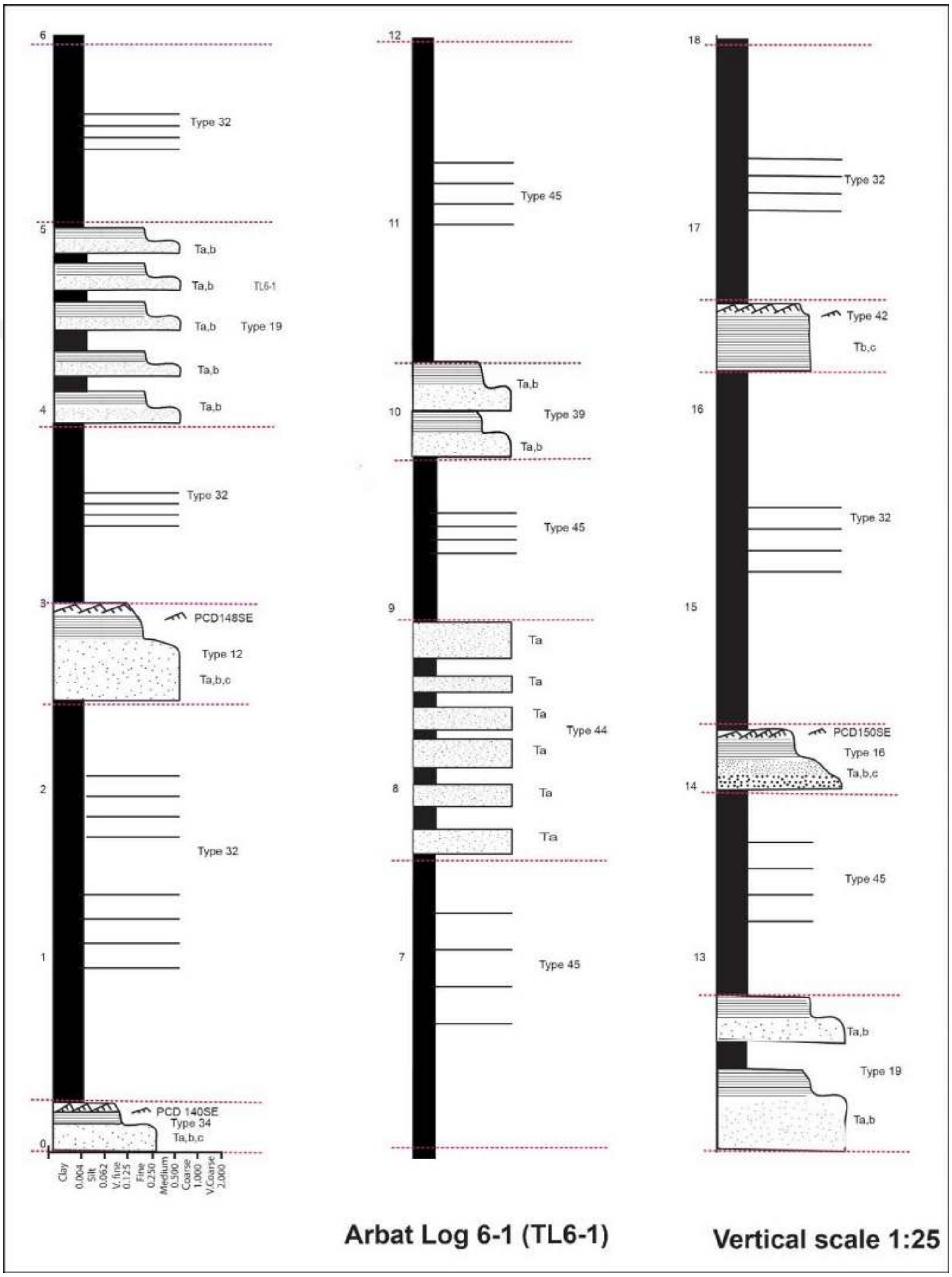

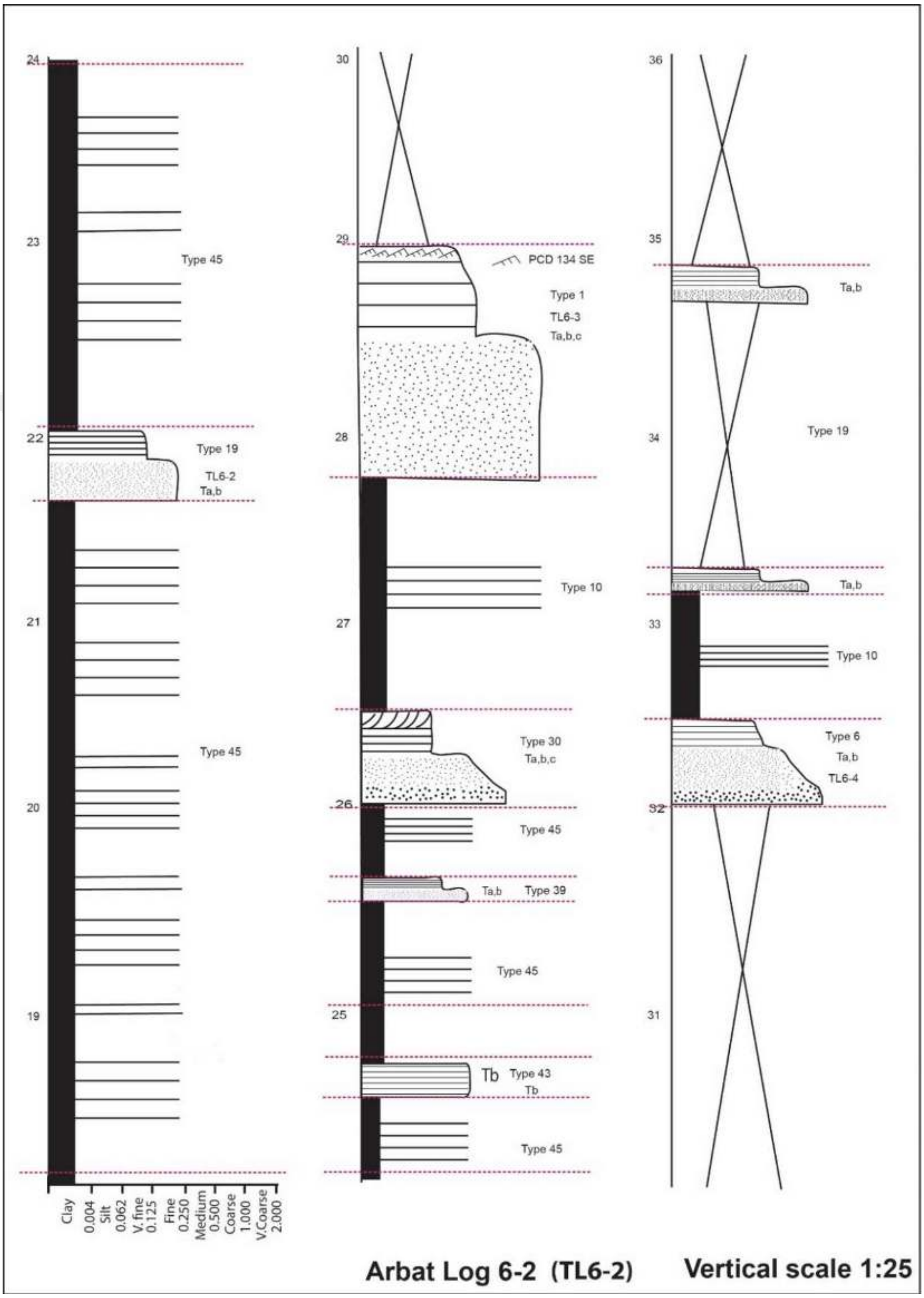
Type 45
Type 19
TL6-2
Ta,b
Type 45
PCD 134 SE
Type 1
TL6-3
Ta,b,c
Type 10
Type 30
Ta,b,c
Type 45
Ta,b
Type 39
Type 45
Tb
Type 43
Tb
Type 45
Ta,b
Type 19
Ta,b
Type 10
Type 6
Ta,b
TL6-4
Clay
0.004
Silt
0.062
V.fine
0.125
Fine
0.250
Medium
0.500
Coarse
1.000
V.Coarse
2.000
Arbat Log 6-2 (TL6-2)
Vertical scale 1:25

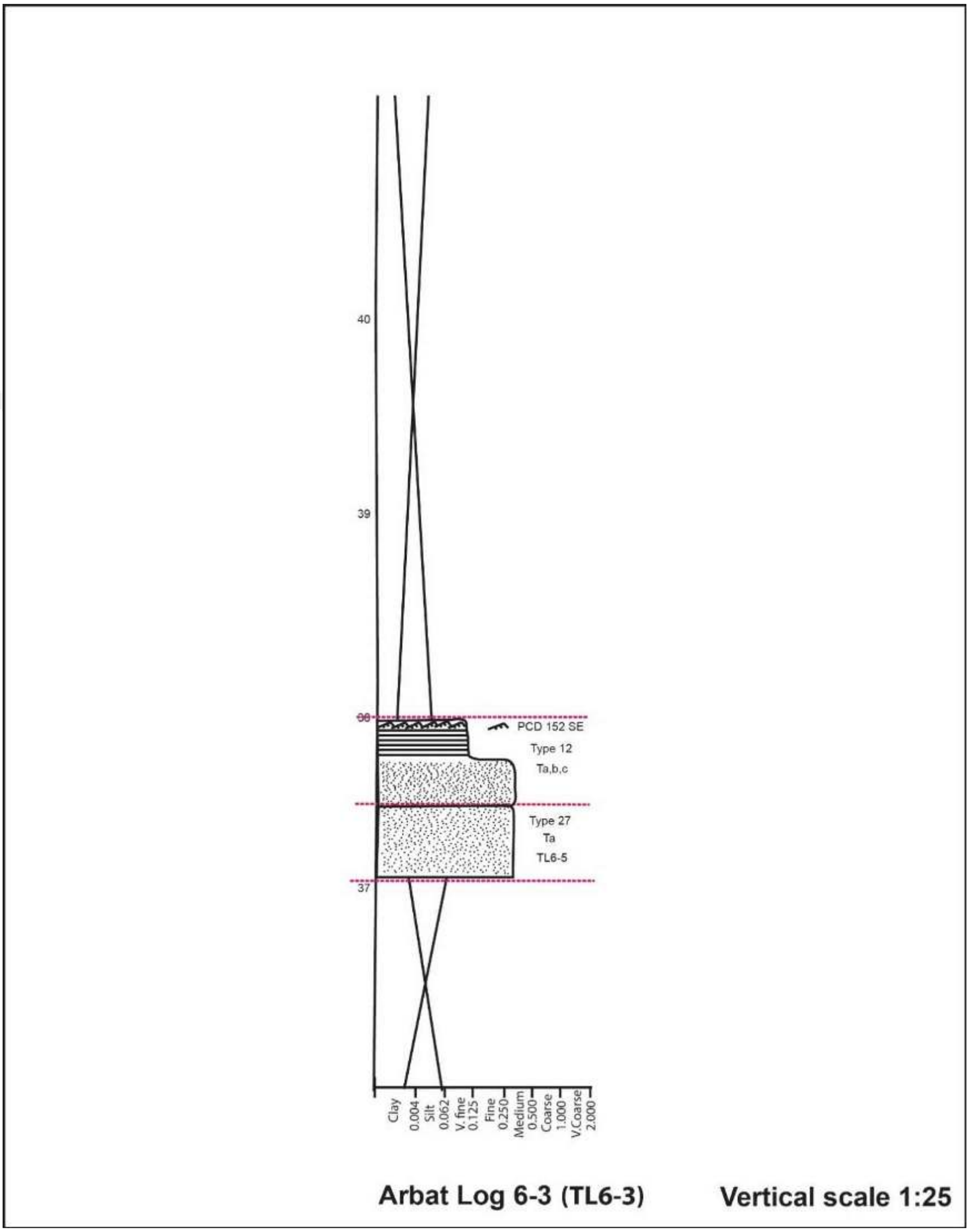
40
39
38
37
PCD 152 SE
Type 12
Ta,b,c
Type 27
Ta
TL6-5
Clay
0.004
Silt
0.062
V. fine
0.125
Fine
0.250
Medium
0.500
Coarse
1.000
V.Coarse
2.000
Arbat Log 6-3 (TL6-3)
Vertical scale 1:25

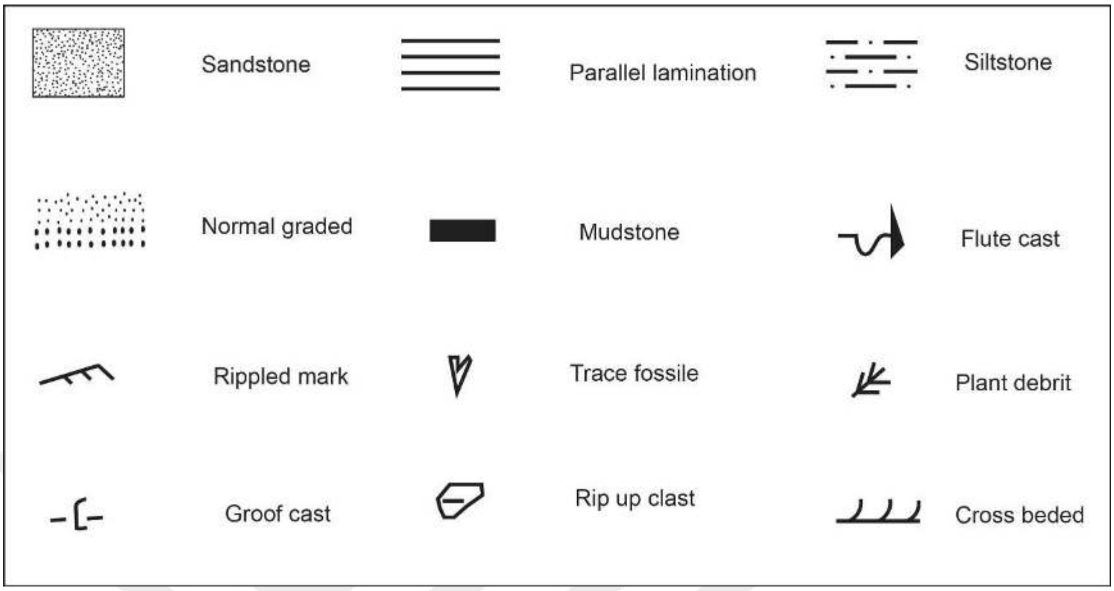

Figure 7.7. Symbols used in the measured sections and facies types.

7.3.2. Facies types

In order to interpret the sedimentary environment of the turbidite cropping out around Arbat six detail measured sections taken from eastern side of a hill oriented about NW-SE direction have been studied. The thickness of the measured sections ranges from 40-50 m.

The analysis of lithofacies and architectural elements, leads to recognition of three main lithofacies and forty-nine. Total subfacies of the turbidites in the location. The main facieses represent the grain size from fine to coarse grain sandstone. The subfacieses are consisting of many types of combinations of complete Bouma sequence associated with thin bedded turbidites were illustrated in the following pages. Some of the facies types are shown in the (Figure 7.8, Figure 7.9, Figure 7.10, Figure 7.11 and Figure 7.12).

All the facies types show the character of low density turbidites. The facies types were used to interpret depositional environment of the turbidite sandstone of Tanjero Formation outcrops around the Arbat area in the depositional environment section (7.4).

1-Coarse grained sandstone turbidite facies model

No	No. of facies	Facies type	Explanation
1	Type 1	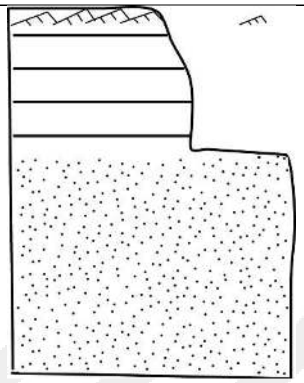	Coarse grain sandstone Ta massive Tb laminated and Tc rippled in the top
2	Type 2	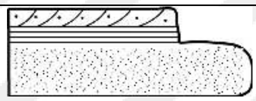	Coarse grain sandstone Ta massive Tb laminated and Tc cross bedded in the top
3	Type 3	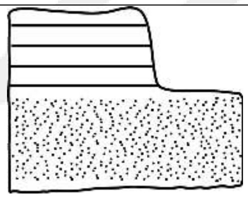	Coarse grain sandstone Ta massive and Tb laminated
4	Type 4	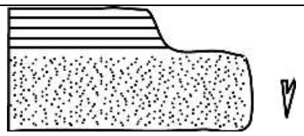	Coarse grain sandstone Ta massive (trace fossil) and Tb laminated
5	Type 5	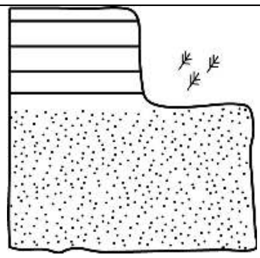	Coarse grain sandstone Ta massive and plant material rich sandstone more laminated towards the top
6	Type 6	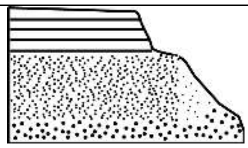	Coarse grain sandstone Ta normally graded and Tb laminated

7	Type 7	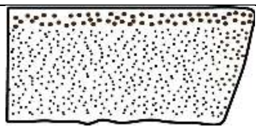	Coarse grain sandstone Reversely graded
8	Type 8	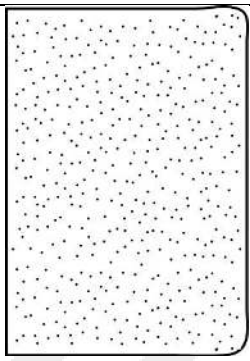	Coarse grain sandstone Ta massive sandstone
9	Type 9	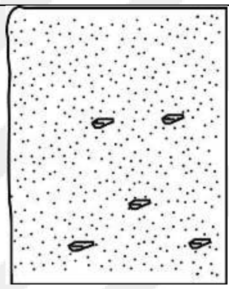	Coarse grain sandstone Ta massive sandstone with rip-up clasts common
10	Type 10	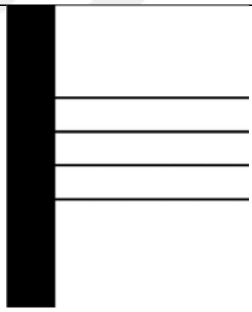	Coarse grain sandstone (inter bedded sandstone and shale). Sandstone ratio =% 6 and shale ratio = %94
11	Type 11		Inter bedded sandstone and mudstone with Ta massive (Coarse grain sandstone). Sandstone ratio =57.6 ,shale ratio=43.4

		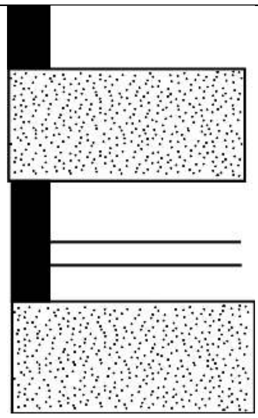	

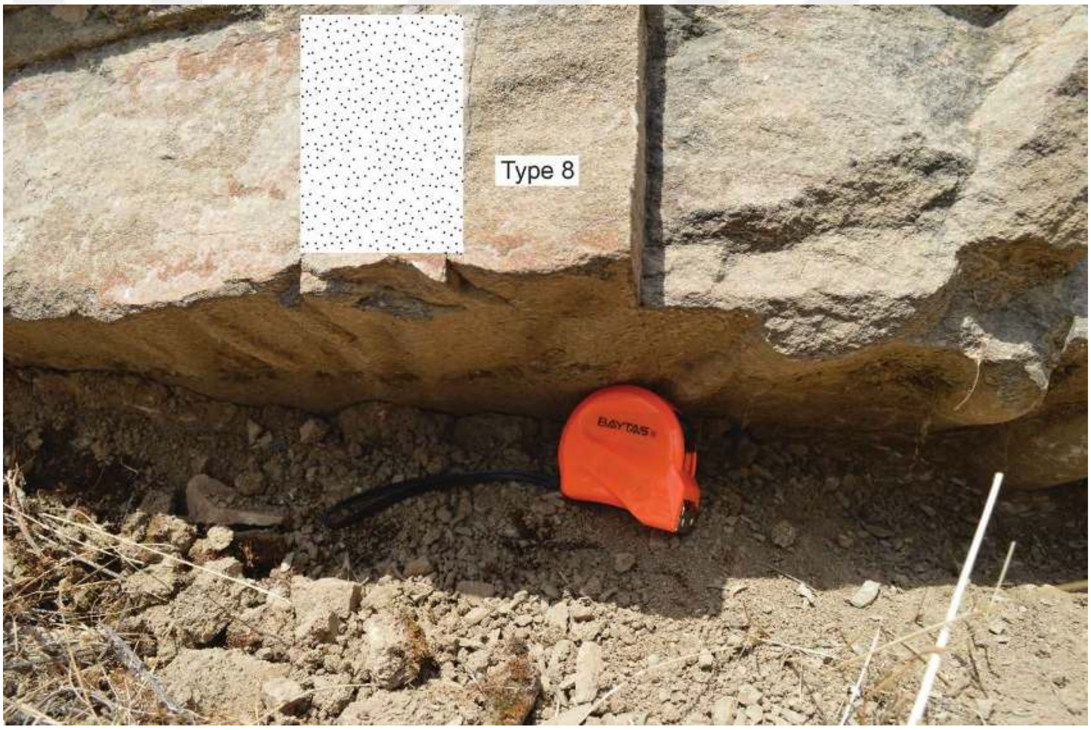

Figure 7.8. Photo showing Facies Type 8, coarse grain sandstone Ta massive sandstone

2-Medium-grained sandstone turbidite facies model

No	Number of facies	Facies type	Explanation
12	Type 12	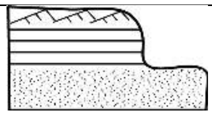	Medium grain sandstone three Bouma subdivision Ta massive flat base, Tb laminated and Tc rippled in the top
13	Type 13	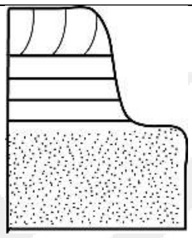	Medium grain sandstone Ta massive Tb laminated or Tc planar cross bed in the top
14	Type 14	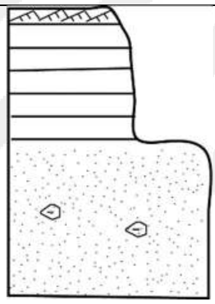	Medium grain sandstone Ta massive with rip-up clasts Tb laminated or Tc rippled in the top
15	Type 15	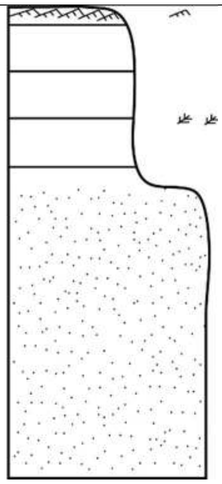	Medium grain sandstone Ta massive, plant material rich sandstone in Tb laminated and Tc rippled in the top
16	Type 16	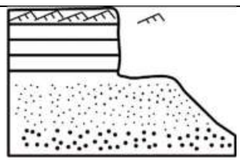	Medium grain sandstone Ta Normally graded, Tb laminated and Tc rippled in the top

17	Type 17	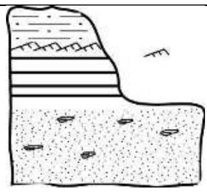	Medium grain sandstone three or more subdivision Ta massive with rip-up clasts, Tb laminated, Tc rippled and Td siltstone in the top
18	Type 18	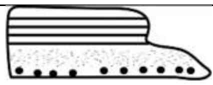	Medium grain sandstone Ta normal graded and Tb more laminated in the top
19	Type 19	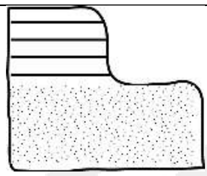	Medium grain sandstone Ta massive and Tb laminated in the top
20	Type 20	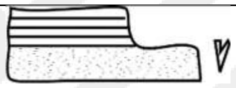	Medium grain sandstone Ta massive, trace fossil and Tb laminated
21	Type 21	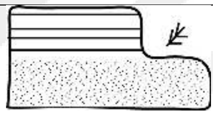	Medium grain sandstone Ta massive, plant material rich sandstone, and Tb more laminated
22	Type 22	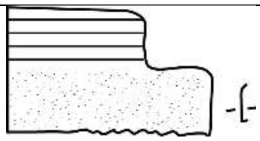	Medium grain sandstone Erosional base, groove cast, Ta massive and Tb laminated
23	Type 23	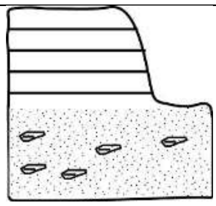	Medium grain sandstone Ta massive common rip-up clasts and Tb laminated in the top
24	Type 24	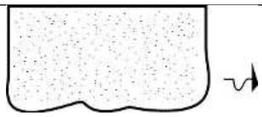	Medium grain sandstone, Erosional bas, Flute casts, Ta massive

25	Type 25	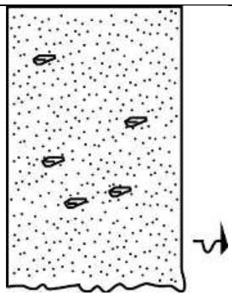	Erosional base, Ta massive, Flute casts, with common rip-up clasts
26	Type 26	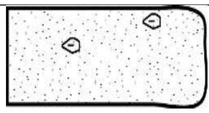	Medium grain sandstone Ta massive and rip-up clasts
27	Type 27	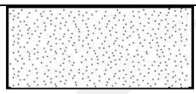	Medium grain sandstone Ta massive
28	Type 28	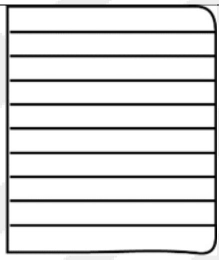	Medium grain sandstone Tb more laminated
29	Type 29	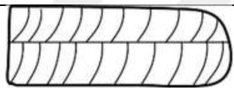	Medium grain sandstone Tc planar cross bed
30	Type 30	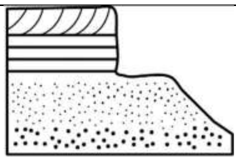	Medium grain sandstone two or three subdivisions Ta normal graded, Tb laminated and Tc planar cross bed in the top
31	Type 31	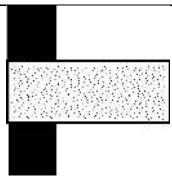	Inter bedded sandstone and mudstone, Sandstone ratio =37% with Shale ratio=63 % (Medium grain sandstone)

32	Type 32	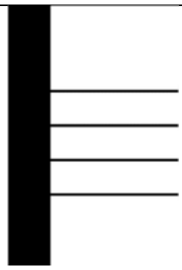	Medium grain sandstone thin bedded the ratio of sandstone=5% and shale ratio =95%

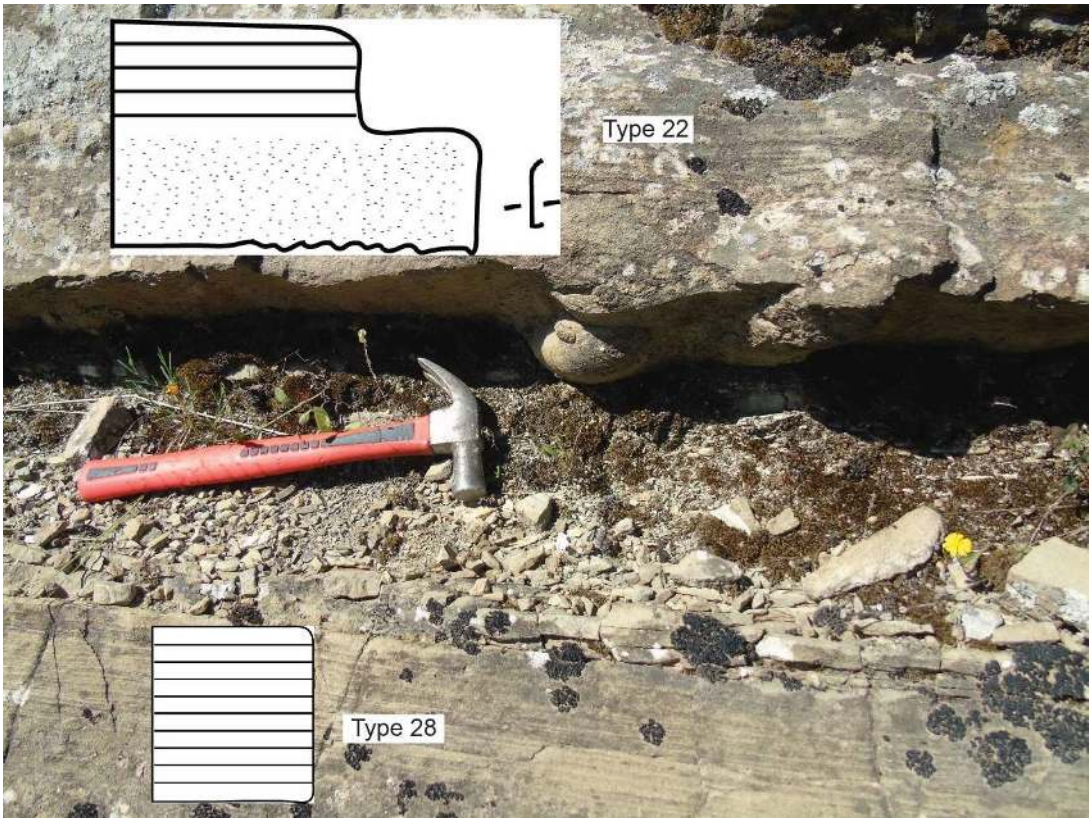

Figure 7.9. Photo showing Facies Type 22, medium grain sandstone erosional base, groove cast, Ta massive and Tb laminated and Facies Type 28, medium grain sandstone Tb more laminated.

3-Fine-grained sandstone turbidite Facies model:

No	Number of facies	Facies type	Explanation
33	Type 33	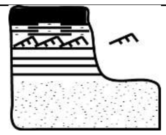	Fine grain sandstone Ta, b, c, d, e Low density turbidities three or more subdivisions Rippled tops
34	Type 34	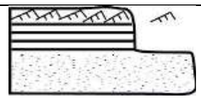	Fine grain sandstone Ta, b, c, Massive Ta planar laminated or rippled in the top
35	Type 35	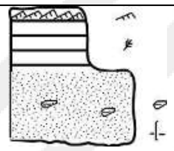	Fine grain sandstone, Erosional bas, Ta massive, rip-up clasts and plant material rich sandstone, Tb laminated with Tc ripple in the top, (groove cast) in the bas
36	Type 36	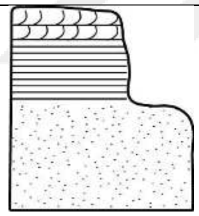	Fine grain sandstone Ta Massive, Tb planar or cross laminations in the top
37	Type 37	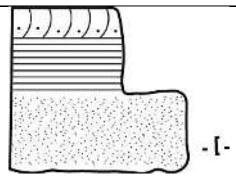	Fine grain sandstone, Erosional bas, Ta Massive, Tb planar more laminated or Tc cross laminations in the top, (Groove cast)
38	Type 38	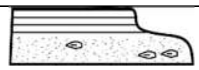	Fine grain sandstone Ta massive with rip-up clasts Tb laminated in the top
39	Type 39	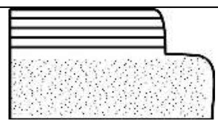	Fine grain sandstone Ta massive or Tb laminated in the top

40	Type 40	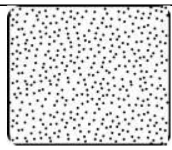	Fine grain sandstone Ta massive
41	Type 41	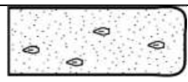	Fine grain sandstone Ta Massive with rip –up clasts
42	Type 42	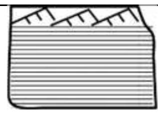	Fine grain sandstone Tb laminated and Tc rippled in the top
43	Type 43		Fine grain sand, Tb laminated
44	Type 44	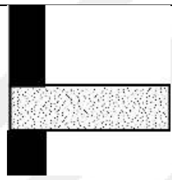	Fine grain sandstone Mixed, sandstone ratio the ratio = 25% and shale ratio =75%
45	Type 45	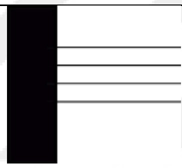	Fine grain sandstone, Inter bedded sandstone and mudstone, Thin bedded sandstone ratio=7%and shale ratio=93%
46	Type 46	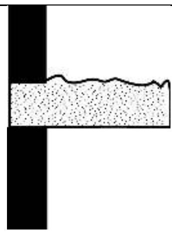	Fine grain sandstone, Ta erosional in the top sand stone ratio=24%and shale ratio=76%
47	Type 47	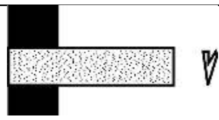	Fine grain sandstone, Ta massive, trace fossil, sandstone ratio =28% shale ratio=72%
48	Type 48		Shale
49	Type 49		Shale ratio=88% and silt ratio=12% thin bedded

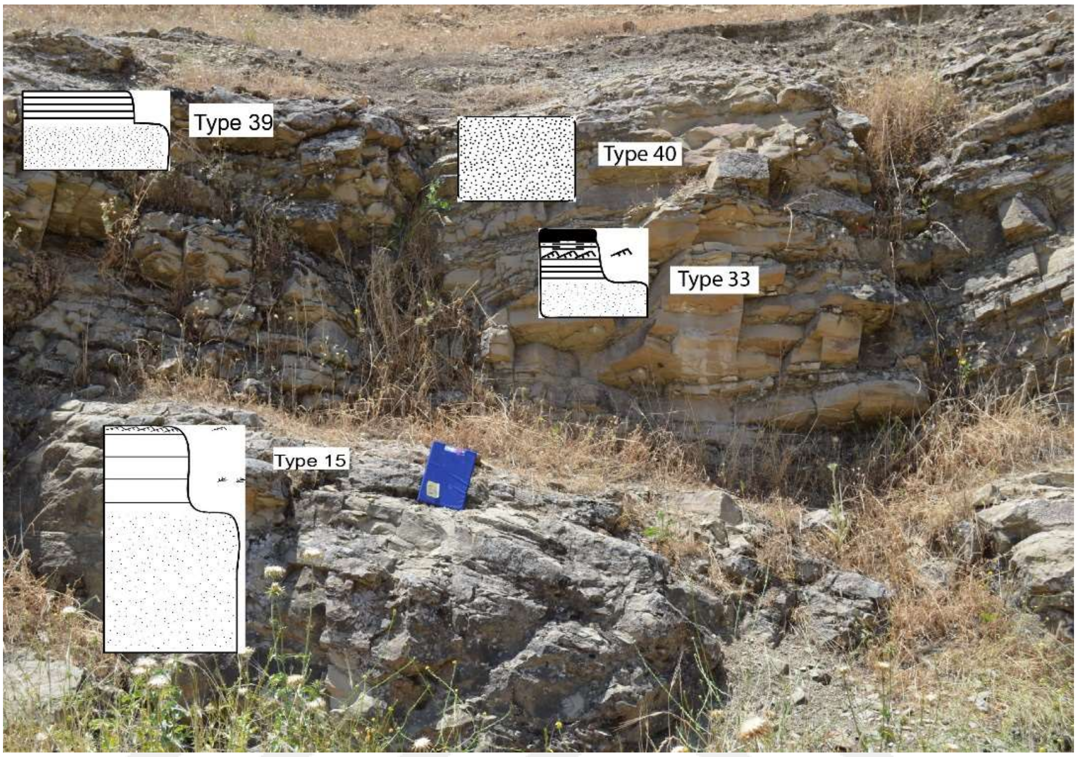

Figure 7.10. Photo showing Facies Type 39, fine grain sandstone Ta massive or Tb laminated in the top, Facies Type 40, fine grain sandstone Ta massive or Tb laminated in the top, Facies Type 33, fine grain sandstone Ta, b, c, d, e, Facies Type 15, medium grain sandstone Ta massive, plant material rich sandstone in Tb laminated and Tc rippled in the top.

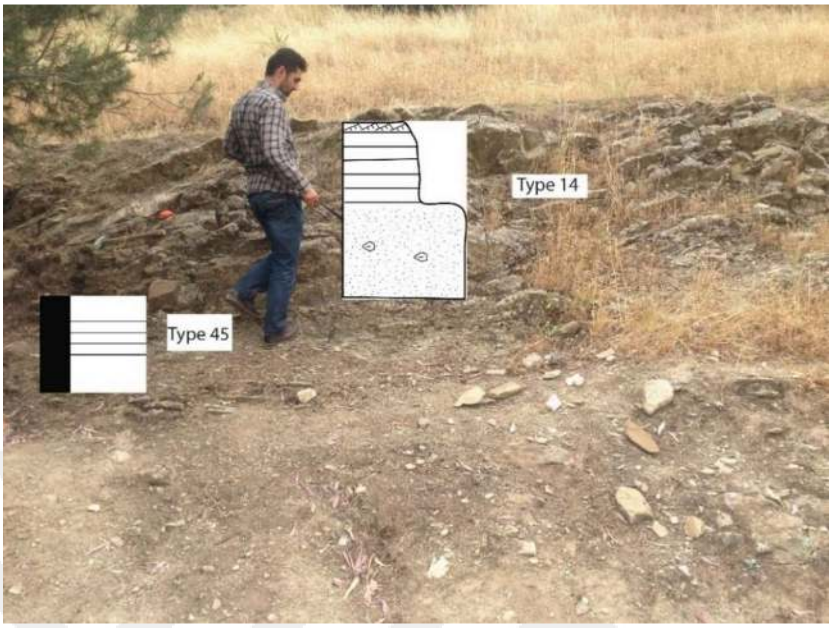

Figure 7.11. Photo showing Facies Type 45, fine grain sandstone, interbedded sandstone and mudstone, thin bedded sandstone ratio=7% and shale ratio=93% and Facies Type 14, medium grain sandstone Ta massive with rip-up clasts Tb laminated or Tc rippled in the top.

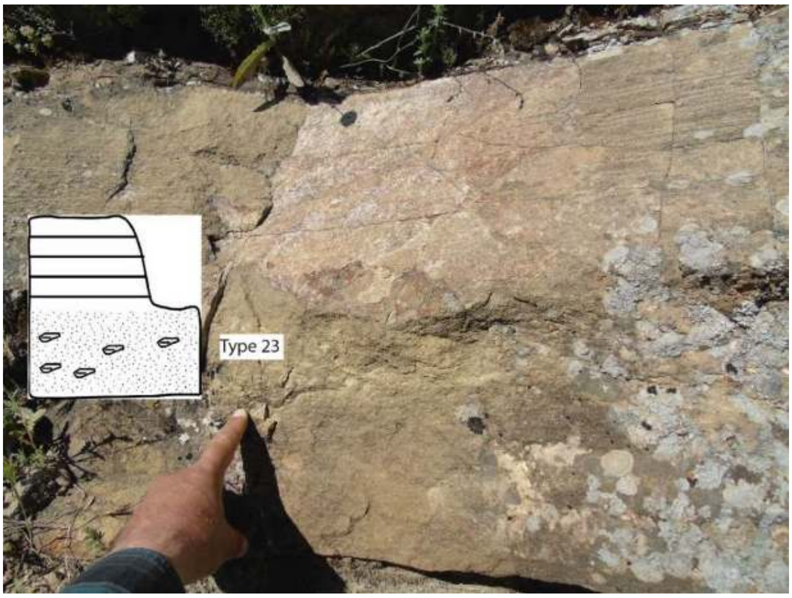

Figure 7.12. Poto showing Facies Type 23, medium grain sandstone Ta massive common rip-up clasts and Tb laminated in the top.

7.4. Depositional Environment of Tanjero Formation in Arbat Area

Some previous studies discussing the environment of the sandstones were summarized below.

Initial geological researches on the formation used old concepts to explain its environment like Jaza (1992) mentioned in his study that, (Dzulinski and Walton, 1965), Van Bellen (1959), Al-Rawi (1981) and Saadaallah and Hassan (1987) described the sandstone as a flysch deposits.

(Jaza, 1992), by using interpretation of general facies and facies models, stated that it really is determined that the Tanjero trough is much more like an elongate-submarine fan with NW-SE axis. The author says that the proximal turbidite part (inner fan-middle fan) of the elongate sub-marine fan is positioned in Sulaimaniyah area and migrate northwest toward Dokan area which mainly become the distal part (outer fan and basin plain). The proximal part is indicated by the abundance of conglomerate facies, thinning upward cycles and thin turbidite beds the later one represents the levee deposits. The distal part is described as the absence of conglomerates and also the inter bedding of sandstones that is an indication of basin plain environment.

Karim (2004) gave some information for the environment of the unit based on sedimentary structures, facies analysis, and sequence stratigraphy and pointed out that depositional environment of Tanjero Formation is shallower than Shiranish Formation for the deep marine part of the unit (middle part in his divisions).

None of the previous studies aimed to express depositional environment of Tanjero Formation is based on detailed facies types in the turbidite succession. In this study 49 facies types were used to find out the depositional environment by using lobe hierarchy concepts and deep marine fan models.

In the following paragraphs some useful information obtained from elsewhere were given to correlate this study according to the result of the previous lobe hierarchy works on turbidites.

Depending on the predominant lithology, sandstone bed thickness, and proportion of mudstone and grain size (Figure 7.13a), four facies associations identified and comparable to four subsets (Figure 7.13 b) of lobe deposits in deep-water fan system are: lobe axis, lobe off-axis, lobe fringe and lobe distal fringe (Prelat et al., 2009, Prélat and Hodgson, 2013).

Lobe off-axis consists of facies massive or normally graded sandstone, lamination sandstone and shale, predominated by medium-grained sandstone beds that are commonly 0.1–0.6 m thick and occupy more than 60% of total measured thickness of this facies association (Figure 7.13 c). The FA2 is bounded by a flat top and lower planar or scour surface with deformed structures and sole marks (Figure 7.13 a, b, c, and m). Geometry of each bed is tabular or sheet-like. Intercalation of thin- to medium-bedded, planar- to wavy-laminated and fine- to medium-grained sandstone beds and shale beds might have been formed in lobe off-axis sub-environment (Meyer and Ross, 2007, Prelat et al., 2009, Prélat and Hodgson, 2013).

Lobe fringe comprises facies massive or normally graded sandstone, fine-grained sandstone and shale. In this facies association, shale beds are predominant (60–80%). The FA3 commonly comprises couplets of thin-bedded, climbing-ripple laminated, very fine sandstone facies and shale facies beds. The sandstone and shale beds are generally range in thickness from several cm to decimeters (Figure 7.13 c). Lobe fringe is supported by a high proportion of shale, thin-bedded sandstone, alternation of very fine-grained Sandstone and shale beds, sheet-like geometry, and good lateral continuity (Prélat and Hodgson, 2013).

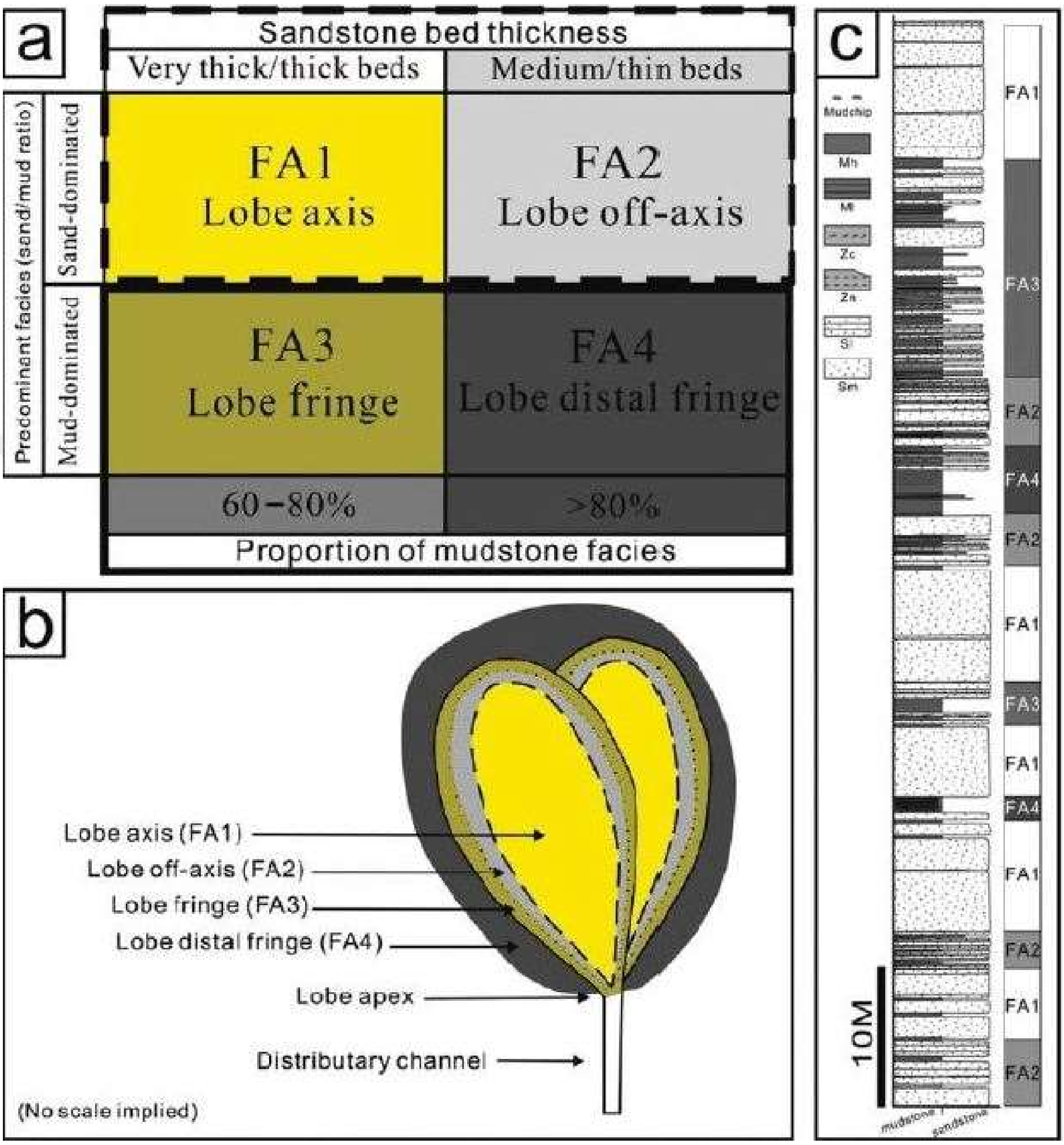

Figure 7.13. (a) Facies associations are classified on the basis of predominant lithology (sand or mud), sandstone bed thickness (very thick/thick beds or medium/thin beds: dashed line box) and proportion of mudstone facies (60–80% or >80%: bold line box). FA: facies association. (b) Schematic model for the facies associations of the Taean Formation. Individual facies associations represent different components of distributive lobe deposits (after Prelat et al., 2009). (c) The application of the facies associations using a sedimentary log in the Gomseom section. Sm: massive sandstone, SL: laminated sandstone, Zn: normally graded, silty fine-grained sandstone, Zc: silty fine-grained sandstone and siltstone with climbing ripple, Ml: laminated mudstone, Mh: homogeneous mudstone. (So et al., 2013).

As deep marine fan model:

Seven basic facies, namely A, B, C, D, E, F, and G, were proposed (Figure 7.14) (Mutti and Ricci Lucchi, 1978) these letters shouldn't be mistaken for divisions of this Bouma sequence (Shanmugam and Moiola, 1988). As a whole, a channelized sequence (inner and middle fan) along with its thinning-upward cycles consists of facies A and B, whereas a non-channelized sequence (outer fan) along with its thickening-upward lobe cycles is represented by facies C and D. Although facies F and G take place in all environments, facies F is characteristic of every slope (including levee) and facies G is common into the basin plain, inter channel, and slope environments (Shanmugam and Moiola, 1988).

Submarine-fan channels can be recognized by their sedimentological and geophysical Characteristics (Figure 7.14). Thinning- and fining-upward cycles (Mutti and Ricci Lucchi, 1972, Mutti and Ricci Lucchi, 1975) are used commonly to recognize channel deposition because an Upward-widening channel section results in the emplacement of successively thinner beds (Shanmugam and Moiola, 1988).

In this study sandstone ratio ranges from 26% to 78% and the shale ratio 22% to 69% the average net to gross is 49.8 to 50.2 for the all sections (Table 7.1).

Table 7.1. Sandstone ratio and shale ratio in the studied area.

Log No.	Sandstone Ratio %	Shale Ratio %
Log 1	62	38
Log 2	78	22
Log 3	53	47
Log 4	49	51
Log 5	31	69
Log 6	26	74
Average	49.8	50.2

Depending on the 49 facies and the ratio of sandstone (49.8) and shale (50.2), it was pointed out that in this study “lob off-axis (FA2) and lobe fringe (FA3)” (Figure 7.13) are the depositional environments for the turbidite sandstone of Tanjero Formation depending on lobe hierarchy.

In studied area only one architectural element recognized in the section is small sandy channel fills in about ten meters length and a few meters thick representing beginning of outer fan. Also grain size, bed thicknesses and combinations of Bouma turbidite divisions show that the sandstones in the studied area are indicate a transition between middle fan and outer fan in the fan model of (Mutti and Ricci Lucchi, 1972), (Figure 7.14).

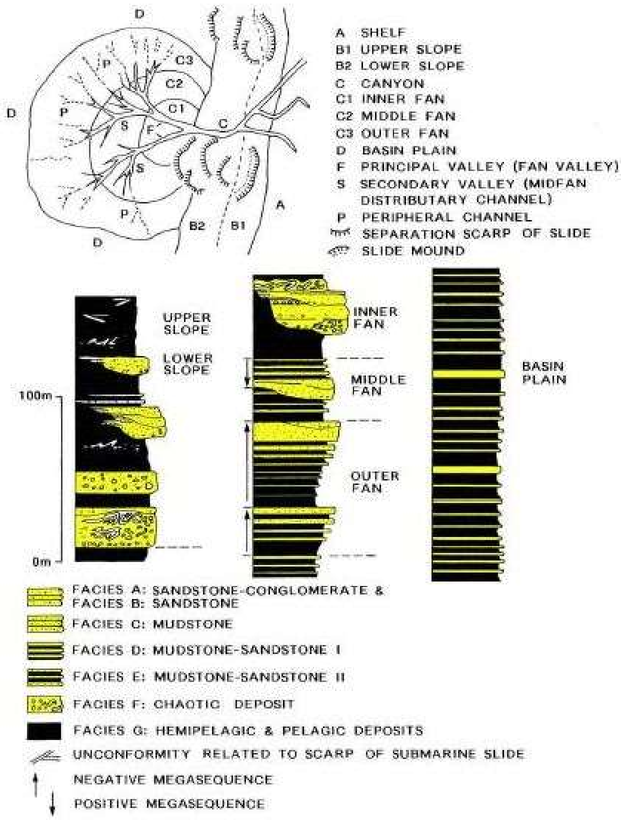

Figure 7.14. General fan model for ancient submarine fans; drawn after Mutti and Ricci Lucchi (1972), (Mattern, 2002).

7.5. Palaeoflow Analysis

Many authors explained paleoflow direction in Tanjero Formation by using sedimentary structures. Some of them were mentioned below:

Al-Rawi (1981) studied paleoflow direction of Tanjero Formation in various places, by using sedimentary structures such as flute casts, groove casts, ripple marks and cross bedding for indicating palaeoflow. He discovered that N45W in Rawandoz area, N45W and N85W in Dokan area and N45W in Sulaimaniyah area. And he determined that the source area is through the east and also the main direction of transportation from Northwest –West.

(Karim, 2004)) studied palaeoflow on the turbidites by measuring ripple marks, elongate fossils, cross bedding, plant fragment, and imbricate pebbles in addition to direction of channel and incised valleys around Sulaimaniyah area Azmar-bchkola valley, Darbandikhan and Chwarta area. All proved the palaeoflow direction is toward south and southwest.

In the studied area two types of sedimentary structures were measured while taking measured sections (Table 7.2). These are:

1-Unidirectional sedimentary structures:

They are indicating one direction of flow. The types of unidirectional sedimentary structures in Tanjero Formation consist of cross bedding, ripple marks and flute casts. The main direction is toward southeast (Figure 7.15).

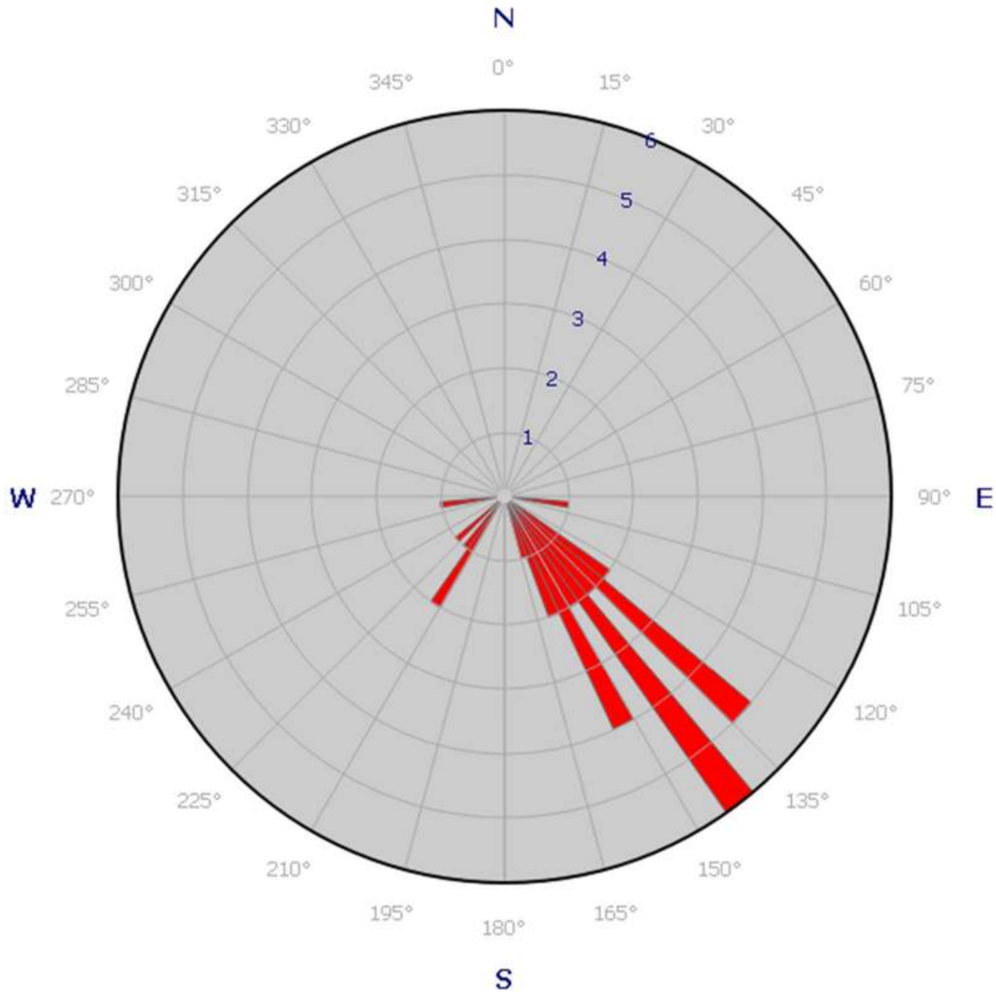

Figure 7.15. Rose Diagram showing unidirectional paleoflow of Tanjero Formation around Arbat Northern Iraq.

2-Bidirectional sedimentary structures:

They are those structures, which indicate two direction of flow, the type of bidirectional sedimentary structures in Tanjero Formation consist of plant material and groove cast. The main direction is toward north west and south east (Figure 7.16).

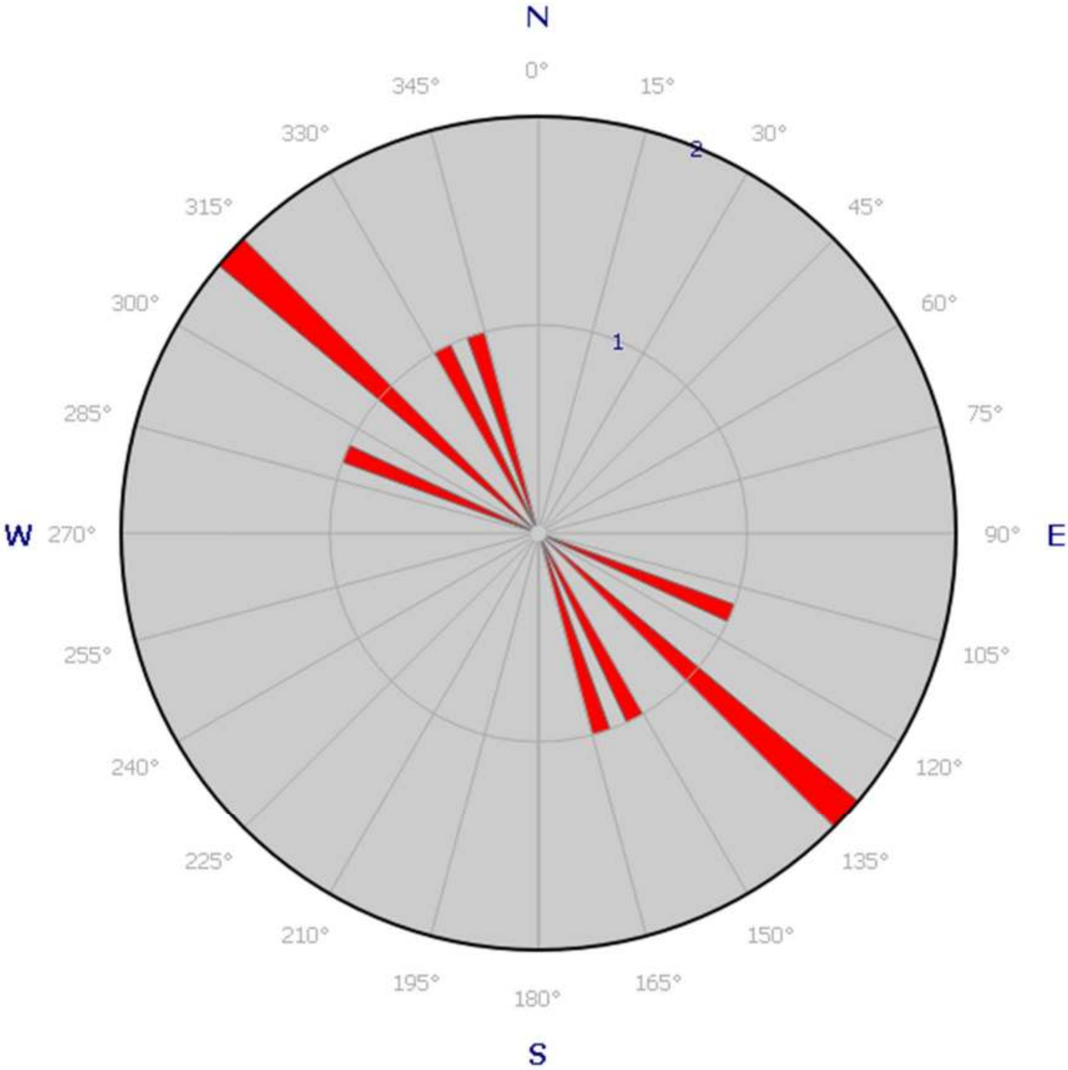

Figure 7.16. Rose Diagram showing bidirectional paleoflow of Tanjero Formation in around Arbat Northern Iraq.

7.6. Rose-diagram plotting

In the studied area plotting data consist of bi-directional and unidirectional sedimentary structures based on Geo Rose program was used as bellow:

1- The original dip direction data of the compass readings are taken in the field as compass quadrant readings, but for entering the PC they were converted to their equivalent azimuthal readings.

2- According to Potter and Petti john (1977), Tucker (1988) there is a limit for tilt correction and they revealed that tilt, below 30 degrees needs no correction and more than 30 degrees needs correction. In the studied area dip angle of beds generally less than 30 degrees (Figure 7.17) because of that no needs to correction.

3-The azimuths of these structures are plotted on the rose diagram using Geo Rose program. The option of "full rose" and "bi-directional" are given to the program when the bidirectional sedimentary structures are entered while for unidirectional ones "half rose" and "unidirectional" option is activated.

Table 7.2. Palaeoflow direction, sedimentary structure, dip angle and dip direction.

No.	Paleoflow direction (X^0) Unidirectional	Bidirectional	Sedimentary Structure	Dip angle	Dip direction (Azimuth)
1	161		Ripple mark	25	225
2	150		Ripple mark	24	221
3	152	332	plant material	25	221
4	128		Ripple mark	23	223
5	130		Ripple mark	23.5	224
6	214		Sole mark		
7	163	343	plant material	23.2	221
8	210	30	plant material	23	220
9	211		Sole mark	21	221
10	110	290	plant material	20	222
11	156		Ripple mark	25	225
12	136		Ripple mark	22	224
13	154		Ripple mark	24	223
14	208	28	Plant material		
15	156		Ripple mark	21	227
16	134		Ripple mark	29	222
17	126		Ripple mark	21	224
18	140		Ripple mark	25	225
19	132		Ripple mark		
20	140		Ripple mark		

-**Table 7.2.** continues-

No.	Paleoflow direction (X^0) Unidirectional	Bidirectional	Sedimentary Structure	Dip angle	Dip direction (Azimuth)
21	98		Sole mark		
22	216		Sole mark		
23	228		Sole mark		
24	132		Ripple mark		
25	134	314	Plant material		
26	132	312	Plant material		
27	140		Ripple mark	20	222
28	236	56	Grove cast	25	226
29					
30	241	61	Grove cast		
31	260		Sole mark		
32	258	78	Grove cast		
33	135		Ripple mark	26	225
34	140		Ripple mark	21	199
35	142		Ripple mark		
36	140		Ripple mark	29	209
37	148		Ripple mark	21	213
38	150		Ripple mark	23	214
39	146		Ripple mark	25	215
40	134		Ripple mark	23	197
41	152		Ripple mark	27	196

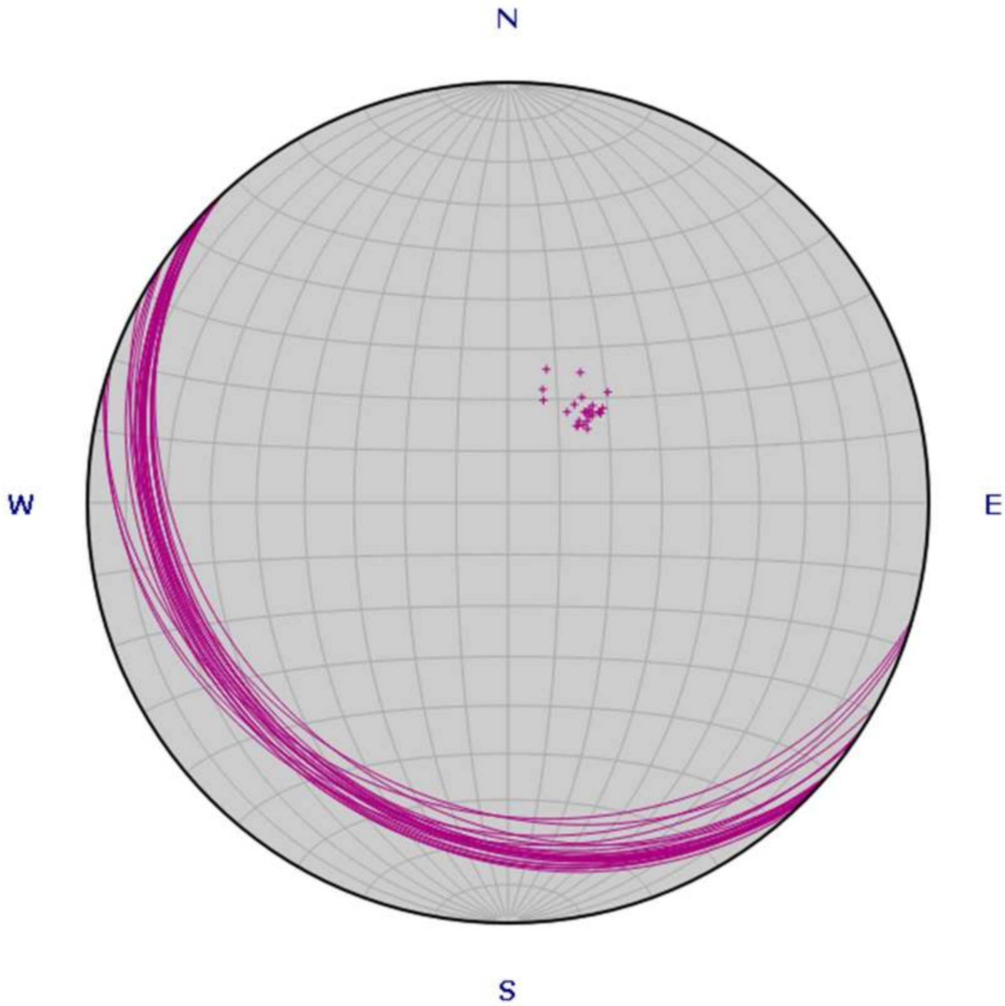

Figure 7.17. Bedding planes of sandstone beds in the studied area plotted on Streonet by Geo Rose software showing of dip angle less than 30 degrees.

8. RESERVOIR CHARACTERIZATION

For reservoir characterization of the sandstone besides facies analysis and depositional environment; porosity, permeability and petrographic constituents of the rock samples taken from the sandstones were also analyzed. These are the first porosity and permeability tests have been done so far on the Tanjero Formation to find the reservoir quality of the sandstone.

8.1. Porosity

Porosity test for 35 cored rock samples of the studied outcrop of sandstone measured by helium BLP-530 Gas Porosimeter. The porosity of the sandstone ranges from poor to fair as porosimeter ranges from 4.56% to 16.56% (with an average value of 9.2%, Table 8.3), according to “Range of Porosity Values” (North, 1985, Table 8.1).

Table 8.1. Range of porosity values (North, 1985).

Porosity %	Qualitative evaluation
0-5	Negligible
5-10	Poor
10-15	Fair
15-20	Good
20-25	Very good

Beard and Weyl (1973), proposed a correlation table of permeability-porosity-grain size and sorting to interpret initial porosity for sandstones (Figure 8.1). According to the figure the sandstone in this study characterized by very fine to coarse grain size, poorly to moderately sorting (Table 8.4) indicate an initial porosity of about 33 % on average using the table (ranging from 30% to 36%, blue transparent area indicated by red arrow in the (Figure 8.1).

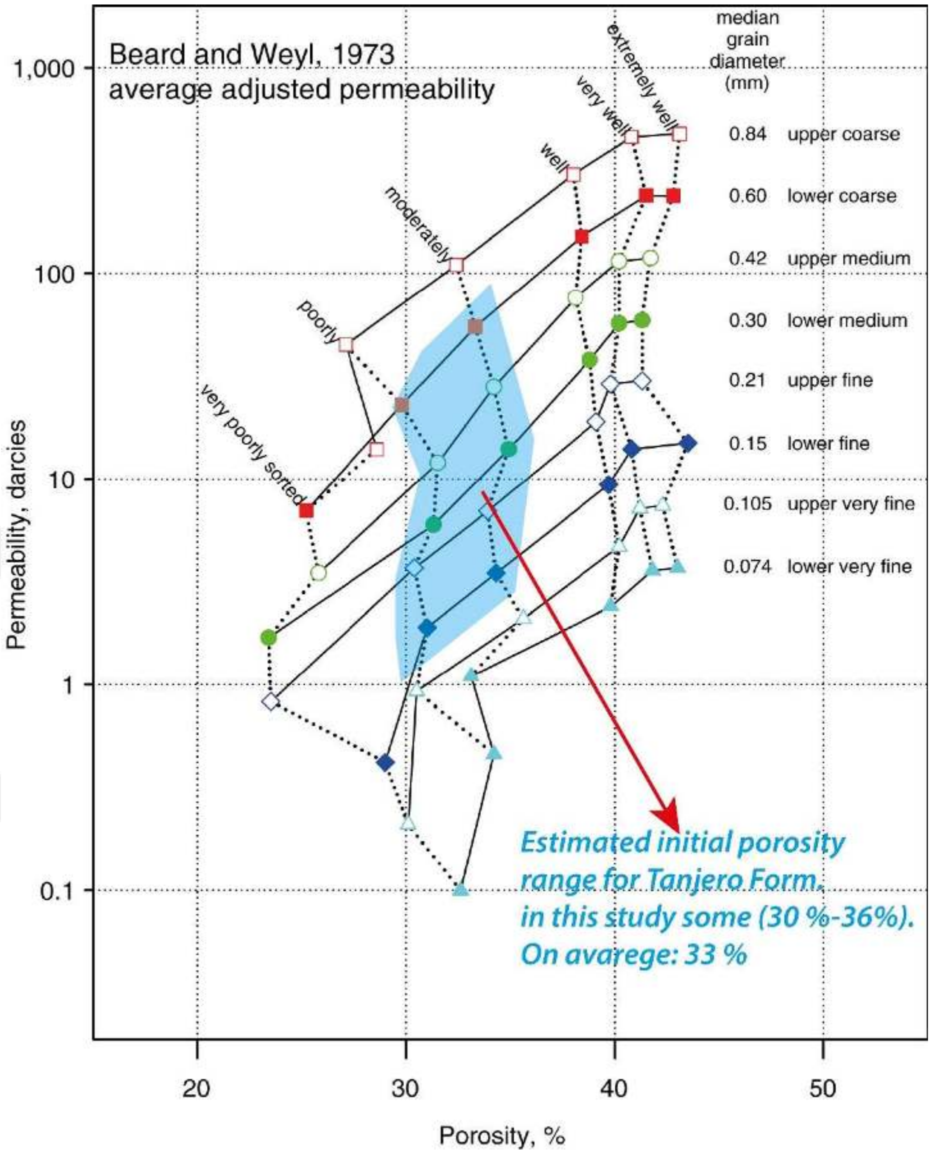

Figure 8.1. Permeability/porosity data from unconsolidated artificial sand packs by(Beard and Weyl, 1973). Symbols linked with solid lines denote size ranges; dotted lines distinguish sorting classes. Pale brownish area shown by the red arrow represents the grain size-sorting and porosity ranges for the sandstone of Tanjero Formation for this study.

Poorly to moderately sorting, tightly packing and moderate compaction and the ratio of the bitumen fillings ranging from 1% to 8% (Table 8.4) obtained from petrographic analysis on the thin sections, are blocking the pores. For these porosity tests indicate poor to fair, with an average value of 9.5%, porosity type (

Table 8.3) for the sandstones.

Solid bitumen fillings ranging from 1 % and 8 % (Table 8.4) is blocking the pores (Plate 8.3, Plate 8.4, Plate 8.5, Plate 8.9 and Plate 8.10, for amount of the bitumen fillings) indicate that before the fillings many sandstones had an initial "good" porosity (Table 8.1) value of (9.5% + 8 %) 17.5 % before the bitumen fillings.

8.2. Permeability

The studied sandstones from the Tanjero Formation (30 samples were tested) reflect a wide range of permeability values, between 36.388-623.328 millidarcy, with an average value of 426.68 md (

Table 8.3). These values can be qualitatively described as "very good" according to (North, 1985).

However, the relationship between porosity and permeability of the samples from the Tanjero Formation shows a negative relation in the (Figure 8.2), this is because of the scale of the graphics which had to be like in the figure. If we reduce the scale for porosity the relationship is becoming random in the area between 6% and 12% on the horizontal axis.

Table 8.2. Range of Permeability values (North, 1985).

Type of permeability	Range of permeability
Poor to fair	**<1.0-15 md**
Moderate	**15-50 md**
Good	**50-250 md**
Very good	**250-1000 md**
Excellent	**>1000 md**

Table 8.3. Porosity (%), permeability (millidarcy: md), Bulk volume and average grain volume of outcrop samples (sandstone) from the Tanjero Formation.

No.	Sample Labels	Core Length (cm)	Core Diameter (cm)	Bulk Volume (cm3)	Grain Volume (cm3)	Effective Porosity %	Permeability (md)
1	TL1-1	4.66	3.79	52.57	48.97	10.66	275.868
2	TL1-2	4.52	3.79	50.99	45.78	10.22	320.823
3	TL1-3	4.55	3.79	51.33	47.21	8.02	545.597
4	TL1-4	4.49	3.79	50.65	44.44	12.27	36.388
5	TL1-5	4.5	3.79	50.77	46.41	8.59	487.36
6	TL1-6	4.54	3.79	51.22	46.47	9.27	417.884
7	TL1-7	4.48	3.79	50.54	44.44	12.7	67.441
8	TL2-1	4.32	3.79	48.74	43.66	10.42	300.389
9	TL2-2	4.54	3.79	51.22	42.74	16.56	
10	TL2-3	4.82	3.79	54.38	50.15	7.77	571.139
11	TL2-4	4.35	3.79	49.07	43.92	10.5	292.215
12	TL2-5	4.26	3.79	46.06	41.59	13.46	
13	TL2-6	4.62	3.79	52.12	47.03	9.77	366.799
14	TL2-7	4.75	3.79	53.59	47.7	10.98	243.173
15	TL2-8	4.41	3.79	49.75	44.57	10.42	300.389
16	TL3-1	4.51	3.79	50.88	44.31	12.91	45.9853
17	TL3-2	4.27	3.79	48.17	44.44	7.75	624.647
18	TL3-3	4.63	3.79	52.23	47.95	8.21	526.184
19	TL3-4	4.63	3.79	52.23	47.46	9.14	431.166
20	TL3-5	4.64	3.79	52.35	48.43	7.48	600.768
21	TL4-1	4.4	3.79	49.64	44.57	10.22	320.823
22	TL4-2	4.36	3.79	49.19	41.15	8.22	525.163
23	TL4-3	4.55	3.79	51.33	44.7	12.92	44.9636
24	TL4-4	4.4	3.79	49.64	45.02	9.31	413.797
25	TL4-5	4.36	3.79	49.19	45.6	7.3	619.159
26	TL5-1	4.615	3.79	52.06	48.68	6.51	699.873

-**Table 8.3.** continues-							
No.	Sample Labels	Core Length (cm)	Core Diameter (cm)	Bulk Volume (cm3)	Grain Volume (cm3)	Effective Porosity %	Permeability (md)
27	TL5-2	4.73	3.79	53.36	50.11	6.1	741.763
28	TL5-3	4.52	3.79	50.99	47.16	7.52	596.682
29	TL5-4	4.385	3.79	49.47	46.47	6.07	623.328
30	TL5-5	4.63	3.79	52.23	48.72	6.72	678.418
31	TL6-1	4.71	3.79	53.14	49.67	6.53	
32	TL6-2	5.05	3.79	56.97	54.38	4.56	
33	TL6-3	4.62	3.79	52.12	49.08	5.83	
34	TL6-4	3.9	3.79	44	40.1	8.87	458.752
35	TL6-5	4.32	3.79	48.74	44.51	8.68	623.328
AVERAGE						9,2	426,68

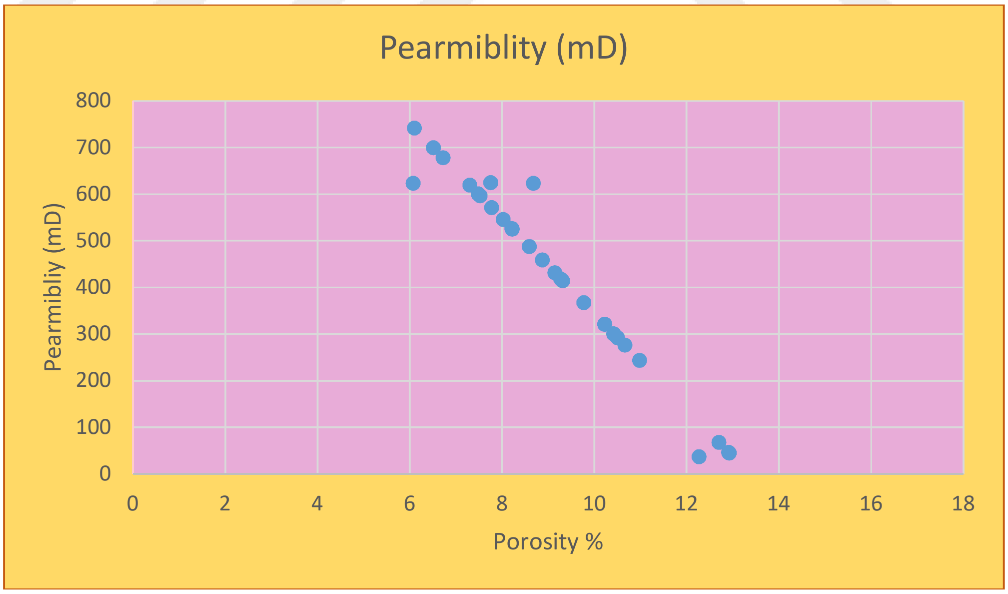

Figure 8.2. Relationship between porosity and permeability of the samples from the Tanjero Formation.

8.3. Petrography

For petrographic analysis a new style of table was created which includes compositional ratios of Q, F and Rf (rock fragments), cement type, alteration/dissolution, fossils content, sedimentary structures, sorting, roundness, modal classification for the ternary diagrams of Pettijohn et al. (1987), the number of photo taken in each thin section and rock name depended on grain size (Table 8.4).

Compositional analysis (Table 8.4) and classical point counting method used to apply the quartz (Q), feldspars (F) and rock fragments (Rf) ternary diagram of Pettijohn et al. (1987). For each thin section 500 points were counted. According to the analysis the low density turbidites sandstones of Upper Cretaceous Tanjero Formation are classified as calclithite subdivision of litharenite (Figure 8.3 and Figure 8.4: Close up of Figure 8.3).

Texturally the turbidites are very fine to coarse grain sandstone (Table 8.4). Sandstone framework consist of subangular to subrounded rock fragments, very angular lithic cherts and quartz fragments (Plate 8.4, Plate 8.6, Plate 8.8, Plate 8.10) with concavo convex, long grain, point and tangential grain contact types (Plate 8.6, Plate 8.7, Plate 8.10). Majority of the contact types are point, tangential and long grain, rare and slightly concavo convex (Plate 8.10 radiolaria-shale contact) and pretty little sutured (between carbonate rock fragments). These contact types reflecting the diagenetic events are implying that compaction degree is low to moderate. The effects of compaction are also manifested in the grain deformation. In the turbidite sandstone studied grains are not deformed, only exhibited evidences of fragile deformation in a few cases, mainly in the grains vertices or within internal grain cracks (Plate 8.1, Plate 8.6, Plate 8.7). The analysis types of contact and contact index (average number of contacts per grain) allows us to establish the characteristics of rock packing. The contact index of the sandstone is 3.6. The contact types of the sandstone in this study point out moderate to tightly packing, however is changing among the samples, and since the prevailing of point and tangential contacts suggest that the grains were already cracked at the moment of deposition or they had already cracks during in the host rock of source area.

Floating grain contact is represented by greywacke calclithites since the cement ratio is more than 15% (Table 8.4, greywackes, TL1-3, TL 1-4, TL 1-6).

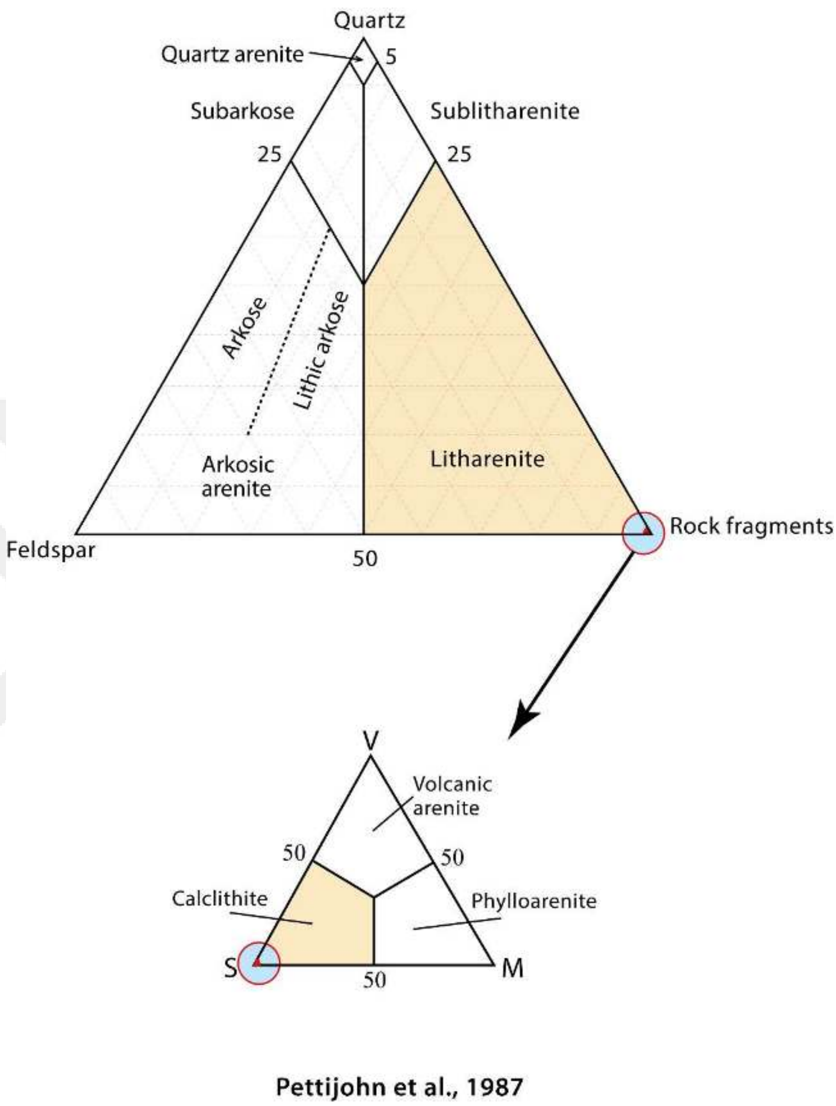

Figure 8.3. Qm-F-Rf and related subdivision V, S,M ternary diagrams illustrating the classification of the Tanjero sandstone in the studied area (after (Pettijohn et al., 1987), redrawn in computer).

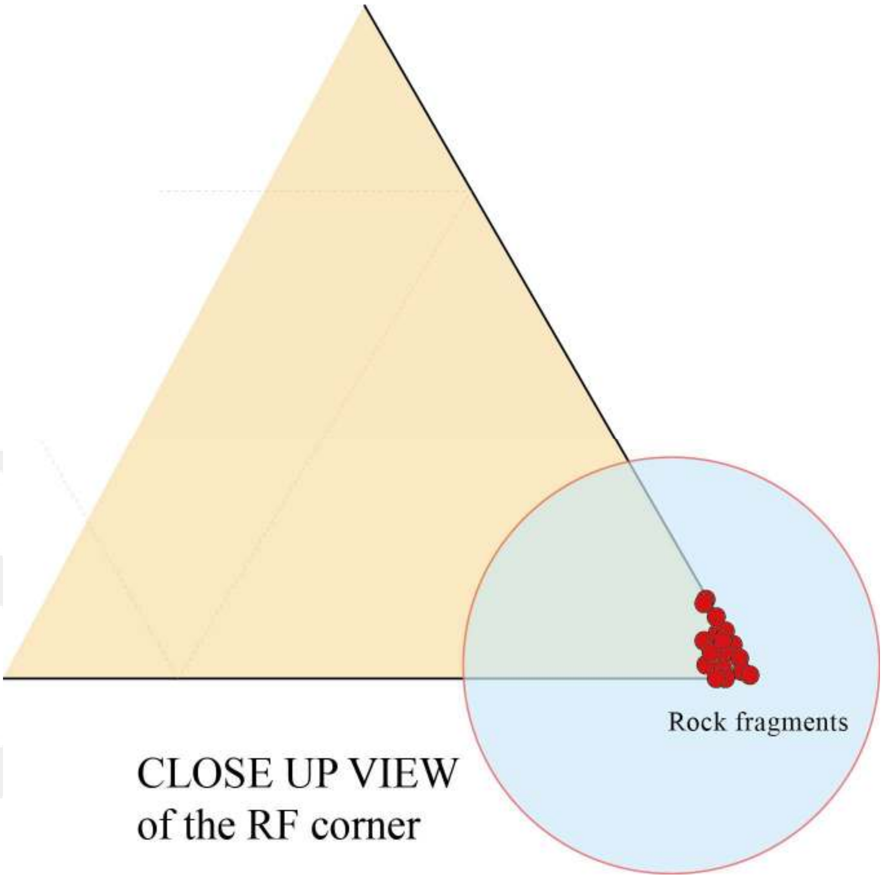

Figure 8.4. Close up view of the Rf corner of the ternary diagram in the Figure 8.3.

Main cement is calcite filling the interstitial pores also replaces the grains, clay and matrix are secondary and in a very low ratio. Solid bitumen fillings are seen in many thin section (in the Table 8.4, Other components column) and it blocks pore spaces and stain the calcite cement to brownish – yellowish in colour (Plate 8.1, Plate 8.3, Plate 8.5, Plate 8.7, Plate 8.9, Plate 8.10).

The turbidites of the Tanjero Formation have monocrystalline, very angular to angular with straight fully extinction common quartz (Table 6 and Table 8). The ratio of the quartz is 0.376 % in average (Table 8.4) for the unit in this study. Only examples of the thin section having polycrystalline quartz are in the photo labelled as TL1-1-0007 and TL5-5-0007. Feldspar ratio is 0.044%, less than quartz. Only one photo could be able to taken to illustrate feldspar in this thesis (Table 10, PPL and XPL images). In this thin section the feldspar with tartan twins hardly can be seen since highly sericitized and altered to clay minerals. Rare heavy mineral presence is notable with low concentration, hematite and pyrite are the most common.

As lithoclasts, carbonate rock fragments are the main constituent of the turbidite sandstone with 64.04 % ratio. Lithic chert has 12.08% and the others are shale, silt, released-reworked radiolaria fossils, benthic fossil shell fragments, radiolarian chert and radiolarian mudstone clast with a ratio of 23.88 % (Table 8.4 and the all Plates). No any metamorphic or magmatic rock clasts were seen in the sandstone thin sections.

All the petrographic examines show that the turbidite sandstone of Upper Cretaceous Tanjero Formation, having less than 5 percentage clay, angular to subangular grains, poorly sorting, dominant tangential and point contact types, are submature (Figure 8.5). This maturity type also indicates a close source area for the sandstones.

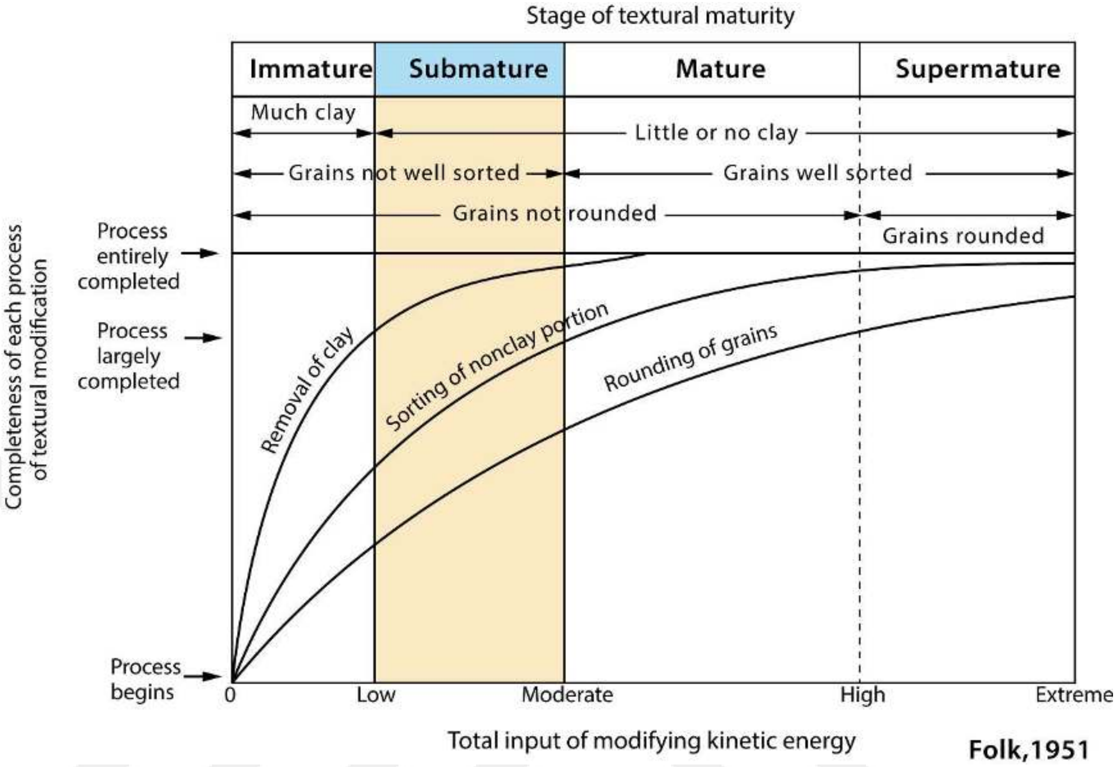

Figure 8.5. Types of maturity. "Submature" is the type for the turbidite sandstones of Tanjero Formation. Clay content is less than 5 %; poorly sorted; grains are angular (Folk, 1951).

Table 8.4. Petrographic content of the thin sections (the numbers for Q, F and RF were rounded to the nearest whole numbers)

NO	Thin Section No:	%Q	%F	%RF	Cement	Matrix	Other components	Alteration/ dissolution	Fossils	Sedimentary structures	Sorting	Roundness	Modal Classification	No. Of photos	Rock name
1	TL 1-1	0.5	0.1	99.4 (chrt:17,Crbnt:52, Mudstone with radiolaria +released radiolaria:31)	Calcite	-	Hematite, tiny rare bitumen fillings	Carbonate rock fragments to calcite, feldspar to clay	Benthic shell fragments, reworked radiolaria	Slightly grain orientation	Poorly	Subangular rock fragments, very angular cherts and quartz	Calclithite	16	Coarse grained sandstone
2	TL 1-3	0.2	0.1	99.7 (chrt:5,Crbnt:75, Mudstone with radiolaria +released radiolaria:20)	Calcite (% 25)	-	Hematite, tiny rare bitumen fillings, subrounded bright green glauconite	Carbonate rock fragments to calcite, feldspar to clay	Benthic shell fragments, reworked radiolaria	-	Poorly	Subangular rock fragments, very angular cherts and quartz	Calclithite (greywacke)	4	Medium grained sandstone
3	TL 1-4	0.1	-	99.9 (chrt:12,Crbnt:75, Mudstone with radiolaria +released radiolaria:20)	Calcite (% 25)	-	Hematite, tiny rare bitumen fillings, subrounded bright green glauconite	Carbonate rock fragments to calcite	Benthic shell fragments, reworked radiolaria	-	Poorly	Subangular rock clasts, very angular cherts and quartz	Calclithite (greywacke)	4	Medium grained sandstone
4	TL 1-6	0.3	-	99.7 (chrt:7,Crbnt:68, Mudstone with radiolaria +released radiolaria:25)	Calcite (% 20)	-	Hematite, subrounded bright green glauconite	Carbonate rock fragments to calcite	Globigerina rare benthic shell fragments+ reworked radiolaria	-	Poorly	Subrounded rock clasts, very angular cherts, hematite and quartz	Calclithite (greywacke)	12	Pebbly fine grained sandstone
5	TL 1-7	0.4	0.1	99.5 (chrt:10,Crbnt:70, Mudstone with and/ released radiolaria:20)	Calcite	-	Hematite, subrounded bright green glauconite, tiny rare bitumen fillings	Carbonate rock fragments to calcite, feldspar to clay	Rare benthic shell fragments+ reworked radiolaria	-	Poorly	Subangular rock clasts, very angular cherts, hematite and quartz	Calclithite	15	Pebbly fine grained sandstone

-**Table 8.4.** Continued-

NO	Thin Section No:	%Q	%F	%RF	Cement	Matrix	Other components	Alteration/ dissolution	Fossils	Sedimentary structures	Sorting	Roundness	Modal Classification	No. Of photos	Rock name
6	TL 2-1	0.5	0.1	99.4 (chrt:12,Crbnt:65, Mudstone with and/ released radiolaria:23)	Calcite (% 20)	-	Hematite, subrounded bright green glauconite, tiny rare bitumen fillings	Carbonate rock fragments to calcite, feldspar to clay	Rare benthic shell fragments+ reworked radiolaria	-	Poorly	Subangular-subrounded rock fragments, very angular cherts, hematite and quartz	Calclithite	2	Very fine grained sandstone
7	TL 2-2	0.5	0.1	99.4 (chrt:8,Crbnt:65, Mudstone with and/ released radiolaria:27)	Calcite	-	Rare black subhedral opaque, hematite, subrounded bright green glauconite	Carbonate rock fragments to calcite, feldspar to clay	Rare benthic shell fragments, reworked radiolaria	Calcite fillings in microfractures	Poorly	Subangular-subrounded rock fragments, very angular cherts and subrounded quartz	Calclithite	8	Pebbly medium grained sandstone
8	TL 2-3	0.3	-	99.7 (chrt:13,Crbnt:58, Mudstone with and/ released radiolaria:29)	Calcite	-	Rare black subhedral opaque, hematite, subrounded bright green glauconite, tiny rare bitumen fillings	Carbonate rock fragments to calcite	Rare benthic shell fragments+ reworked radiolaria	Wavy deformed secondary calcite in fractures	Poorly	Subangular-subrounded rock fragments, very angular cherts and quartz	Calclithite	10	Pebbly medium grained sandstone
9	TL 2-4	0.3	0.1	99.6 (chrt:17,Crbnt:63, Mudstone with radiolaria +released radiolaria:20)	Calcite	-	Hematite, tiny rare bitumen fillings, subrounded bright green glauconite	Carbonate rock fragments to calcite, feldspar to clay	Rare benthic shell fragments+ reworked radiolaria	-	Poorly	Subangular-subrounded rock fragments, very angular cherts and quartz	Calclithite	28	Medium grained sandstone

-**Table 8.4.** Continued-

NO	Thin Section No:	%Q	%F	%RF	Cement	Matrix	Other components	Alteration/ dissolution	Fossils	Sedimentary structures	Sorting	Roundness	Modal Classification	No. Of photos	Rock name
10	TL 2-5	0.2	-	99.8 (chrt:15,Crbnt:60, Mudstone with and/ released radiolaria:25)	Calcite	-	Hematite, tiny rare bitumen fillings, subrounded bright green glauconite	Carbonate rock fragments to calcite	Globigerina + benthic shell fragments+ radiolaria	Secondary calcite occurrences in micro fractures	Moderately	Subangular-rock fragments, very angular cherts, hematite and quartz	Calclithite	10	Very fine grained sandstone
11	TL 2-6	0.3	-	99.7 (chrt:9,Crbnt:78, Siltstone, mudstone with and/ released radiolaria:13)	Calcite	-	Opaque, black euhedral-subhedral heavy minerals, hematite, tiny rare bitumen filling, subrounded bright green glauconite	Carbonate rock fragments to calcite	Globigerina + reworked radiolaria	Secondary calcite occurrences in micro fractures and pebble orientation	Poorly	Subangular-rock fragments, very angular cherts and quartz+ well rounded glauconite	Calclithite	10	Fine grained sandstone
12	TL 2-7	0.5	0.1	99.4 (chrt:10,Crbnt:80, Siltstone, mudstone with and/ released radiolaria:10)	Calcite	-	Opaque, black euhedral-subhedral heavy minerals 1%+ very well rounded green glauconite, carbonized plant fragments, rare tiny bitumen fillings	Carbonate rock fragments to calcite, feldspar to clay	Reworked radiolaria + and foram shell fragments	-	Poorly	Subangular-rock fragments, very angular cherts and subrounded quartz	Calclithite	22	Pebbly fine grained sandstone
13	TL 2-8	0.6	0.1	99.3 (chrt:8,Crbnt:70, Mudstone with and/ released radiolaria:22)	Calcite	-	Opaque, black euhedral-subhedral heavy minerals rare tiny bitumen fillings, hematite	Carbonate rock fragments to calcite, feldspar to clay	Rare benthic shell fragments+ reworked radiolaria	-	Poorly	Subangular-subrounded rock clasts, very angular cherts and quartz	Calclithite	10	Medium grained sandstone

-**Table 8.4.** Continued-

NO	Thin Section No:	%Q	%F	%RF	Cement	Matrix	Other components	Alteration/ dissolution	Fossils	Sedimentary structures	Sorting	Roundness	Modal Classification	No. Of photos	Rock name
14	TL 3-1	0.2	-	99.8 (chrt:5,Crbnt:65 , Mudstone with and/ released radiolaria:30)	Calcite (%30)	-	Opaque, black euhedral-subhedral heavy minerals + very well rounded green glauconite, carbonized plant fragments, tiny bitumen fillings common	Carbonate rock fragments to calcite	Globigerina, reworked radiolaria, benthic shell fragments	Weak pebble long axis orientations	Moderately	Subangular-subrounded rock fragments, very angular cherts and quartz	Calclithite (greywacke)	33	Very fine grained sandstone
15	TL 3-4	0.6	0.1	99.3 (chrt:37,Crbnt:52, Siltstone, mudstone with and/ released radiolaria:11)	Calcite	-	Black euhedral heavy minerals + very well rounded green glauconite +hematite, rare tiny bitumen fillings	Carbonate rock fragments to calcite, feldspar to clay	Reworked radiolaria, benthic shell fragments	Tightly compacted	Poorly	Subangular-rock fragments, very angular cherts and subrounded quartz	Calclithite	21	Medium grained sandstone
16	TL 3-5	0.3	-	98 (chrt:25,Crbnt:30, Mudstone with radiolaria +released radiolaria:45)	Calcite	-	Brown/black euhedral heavy minerals, hematite rare tiny bitumen filling	Carbonate rock fragments to calcite	Reworked radiolaria, benthic shell fragments, globigerina	Tightly compacted	Poorly	Subangular-subrounded rock fragments, very angular cherts and quartz	Calclithite	37	Medium grained sandstone
17	TL 4-4	1	-	99 (chrt:15,Crbnt:70, Siltstone, mudstone with and/ released radiolaria:15)	Calcite	-	Brown/black euhedral heavy minerals, hematite rare tiny bitumen fillings, glauconite	Carbonate rock fragments to calcite	Released radiolaria	-	Moderately	subrounded rock fragments, very angular cherts and quartz	Calclithite	26	Pebbly coarse grained sandstone

-**Table 8.4.** Continued-

NO	Thin Section No:	%Q	%F	%RF	Cement	Matrix	Other components	Alteration/ dissolution	Fossils	Sedimentary structures	Sorting	Roundness	Modal Classification	No. Of photos	Rock name
18	TL 4-5	0.1	-	99.9 (chrt:20,Crbnt:30, Siltstone, mudstone with and/ released radiolaria:50)	Calcite	-	Black subhedral heavy minerals, carbonized plant fragments, subrounded green glauconite, hematite	Carbonate rock fragments to calcite	Rare benthic shell fragments+ reworked radiolaria	-	Very poorly	Subangular- rock fragments, very angular cherts and quartz	Calclithite	25	Pebbly coarse grained sandstone
19	TL 5-1	0.5	-	99.5 (chrt:11,Crbnt:65, Siltstone, mudstone with and/ released radiolaria:24)	calcite+ matrix	-	Black subhedral heavy minerals, carbonized plant fragments, subrounded green glauconite, hematite	Carbonate rock fragments to calcite	Rare benthic shell fragments+ reworked radiolaria	-	Poorly	Subangular to subrounded rock fragments, very angular cherts and quartz	Calclithite	8	Pebbly fine grained sandstone
20	TL 5-2	0.2	-	99.8 (chrt:7, Crbnt:65, Siltstone, mudstone with and/ released radiolaria:27)	Mainly calcite, some clay	-	Black subhedral heavy minerals / Plant materials angular green glauconite, %7 percent bitumen fillings in pores	Carbonate rock fragments to calcite	Rare benthic shell fragments+ reworked radiolaria	Microfractures filled by calcite	Poorly	Subangular- rock fragments, very angular cherts and quartz	Calclithite	20	Pebbly fine grained sandstone
21	TL 5-3	0.4	0.1	99.5 (chrt:2,Crbnt:83, Siltstone, mudstone with and/ released radiolaria:15)	Calcite (%20)	-	Black euhedral heavy minerals 1%+ very well rounded green glauconite, carbonized plant fragments, rare tiny bitumen fillings	Carbonate rock fragments to calcite, feldspar to clay	Rare benthic shell fragments+ reworked radiolaria	Light wavy calcite filled fractures, early stage for stylolite	Poorly	Subangular- subrounded rock fragments, very angular cherts and quartz	Calclithite (greywacke)	22	Pebbly fine grained sandstone

-**Table 8.4.** Continued-

NO	Thin Section No:	%Q	%F	%RF	Cement	Matrix	Other components	Alteration/ dissolution	Fossils	Sedimentary structures	Sorting	Roundness	Modal Classification	No. Of photos	Rock name
22	TL 5-4	0.2	-	99.8 (chrt:12,Crbnt:73, Siltstone, mudstone with and/ released radiolaria:10)	Calcite	-	Black euhedral heavy minerals + rare tiny bitumen fillings, hematite	Carbonate rock fragments to calcite	Rare benthic shell fragments+ reworked radiolaria	Veins filled by calcite+ early stage for stylolite	Poorly	Subangular-subrounded rock fragments, very angular cherts and quartz	Calclithite	6	Pebbly coarse grained sandstone
23	TL 5-5	0.3	-	99.7 (chrt:9, Crbnt:67, Siltstone, mudstone with and/ released radiolaria:24)	Calcite	-	Black subhedral opaque minerals, subrounded green glauconite, micro pores filled by bitumen very rare	Carbonate rock fragments to calcite	Rare benthic shell fragments+ reworked radiolaria	Slightly grain orientation	Very poorly	Subangular-rock fragments, very angular cherts and quartz	Calclithite	14	Pebbly fine grained sandstone
24	TL 6-3	0.2	-	99.8 (chrt:6,Crbnt:67, Mudstone and released radiolaria:27)	Calcite (%20)	-	carbonized plant fragments, euhedral opaque minerals, reddish brownish hematite, bright glauconite, bitumen fillings in nano pores	Carbonate rock fragments to calcite	Globigerina+ reworked radiolaria, foram fragments with pellets	-	Well	Subangular-subrounded rock fragments, very angular cherts and quartz	Calclithite (greywacke)	8	Very fine grained sandstone
25	TL 6-4	0.7	0.1	99.2 (chrt:10,Crbnt:55, Siltstone, mudstone with and/ released radiolaria:35)	Calcite	-	Black subhedral heavy minerals + very well rounded green glauconite +plant materials	Carbonate rock fragments to calcite, feldspar to clay	Rare benthic shell fragments+ reworked radiolaria	-	Poorly	Subangular-subrounded rock fragments, very angular cherts and quartz	Calclithite	8	Pebbly medium grained sandstone

-**Table 8.4.** Continued-

NO	Thin Section No:	%Q	%F	%RF	Cement	Matrix	Other components	Alteratio n/ dissolution	Fossils	Sedimentar y structures	Sorting	Roundness	Modal Classification	No. Of photos	Rock name
Average		0.376	0.044	Lithic chert : 12.08 Carbonate rf : 64.04 Others :23.88	Calcite	-	Carbonized plant fragments, euhedral to subhedral opaque minerals, reddish brownish hematite, bright green subrounded glauconite, bitumen fillings (1-8 percentage) in nano to micro pores	Carbonate rock fragments to calcite, feldspar to clay	Globigerina, reworked radiolaria and bioclasts	Slightly grain orientation (not represent-ative for the all sections)	Poorly to moderately	Subangular-subrounded rock fragments, very angular cherts and quartz	Calclithite	15.16	Very fine to coarse grained sandstone

Note: All the quartz in the thin sections are monocrystalline, with strait extinction except two in the photo TL1-1-0007 and TL5-5-0007 are polycrystalline

8.4. Provenance

The application of the analyzed data to the tectonic provenance plots (Qm-F-Lt) by Dickinson et al. (1983) indicate that the sedimentary rocks are included within the “lithic recycled” category (Figure 8.6). In addition to the sandstone modal analysis (Table 8.4 and Figure 8.4), palaeocurrent data from the unidirectional and bidirectional sedimentary structures in the turbidites, indicating flows to SE (Figure 7.15 and Figure 7.16), are also essential to accurately establish the location of source area.

The composition of the turbidite sandstones of Tanjero Formation in the studied area shows to the occurrence sedimentary rocks in the source area. Taking together into account the petrographic and palaeocurrent data (Table 8.4, Figure 7.15and Figure 7.16) it is possible to consider only one source area as the main responsible for the composition of sandstones.

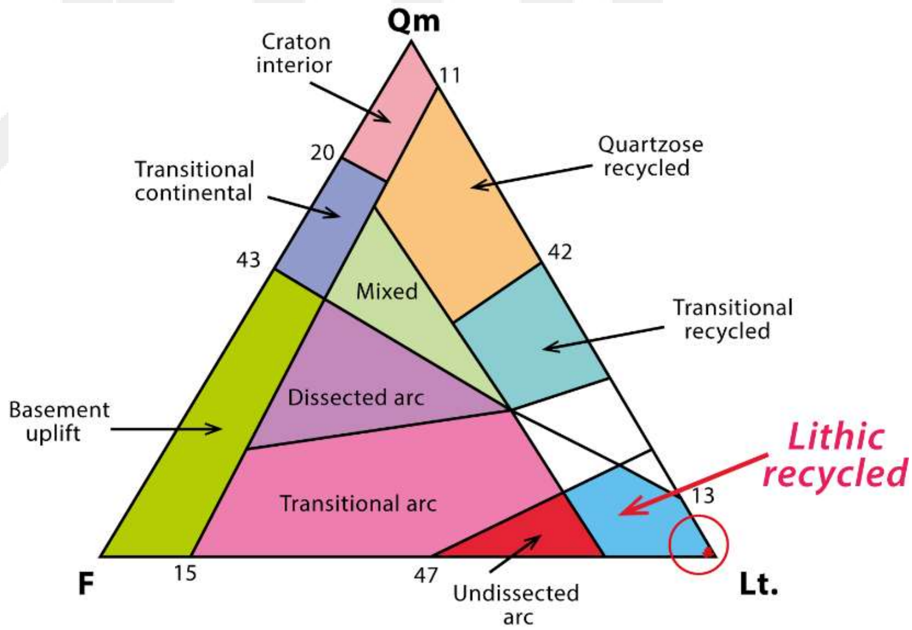

Figure 8.6. Qm-F-Lt ternary diagram illustrating tectonic provenance for the sandstone of Tanjero Formation in the studied area indicate “lithic recycled” category (after (Dickinson et al., 1983), redrawn in computer).

The only source area corresponds to the Lower Cretaceous Qulqula Formation situated in the lowermost right hand side of the stratigraphic column of the Northern Iraq region (Figure 7.1). In Early Cretaceous times, this represented a structural high to the north of the basin composed by radiolarian chert, black limestone, radiolarian mudstone and limestone rocks of variable grade (Karim et al., 2008, Karim, 2010). This provenance study is giving us the same result and in compliance with Karim's provenance interpretations in his studies in 2008 and 2010.

Petrographic characteristics of the sandstone studied indicate that provenance is not changing during deposition of the turbidite sandstones in Tanjero Formation for the studied area since the average sandstone composition is not vary among lower, middle, and upper parts of the measured sections. Sandstone was supplied to this area throughout the turbidite time and the interpreted source area Qulqula Formation to the North, remained the same during deposition. This illustrates same sequence stratigraphic position which is lowstand slope-fan deposits containing mainly rock fragments.

PETROGRAPHIC EXPLANATIONS
OF SOME IMPORTANT THIN SECTION
MICROPHOTOGRAPHS

(PLATES)

PLATE 8.1

Thin section and *photo* numbers: **TL2-3**-*0009-0010*

Bt: Solid bitumen fillings

BCrf: Black carbonate rock fragment

Crf: Carbonate rock fragment

PPL: Plain Polarised Light

R: Radiolaria fossil in the lithic chert clast

Rch: Radiolarian chert

Red arrows: Calcite cement

XPL: Cross Polarised Light

Plate 8.1

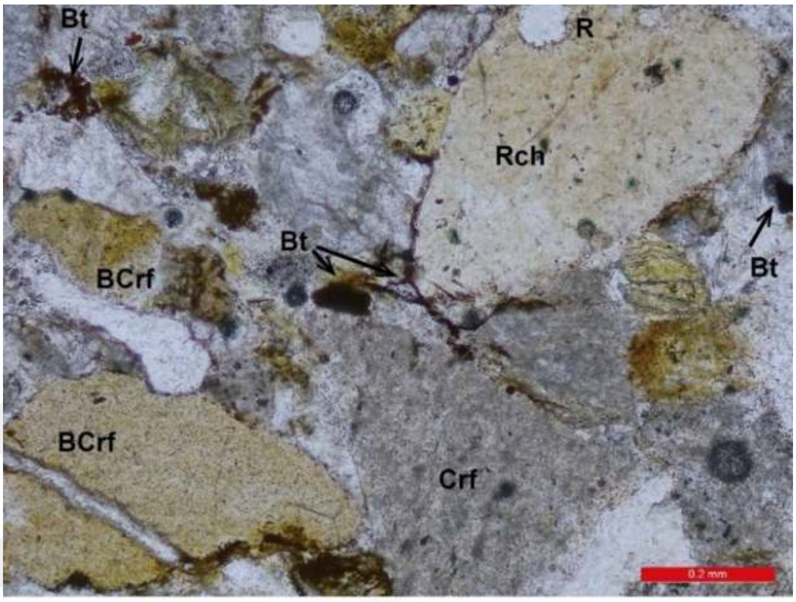

PPL

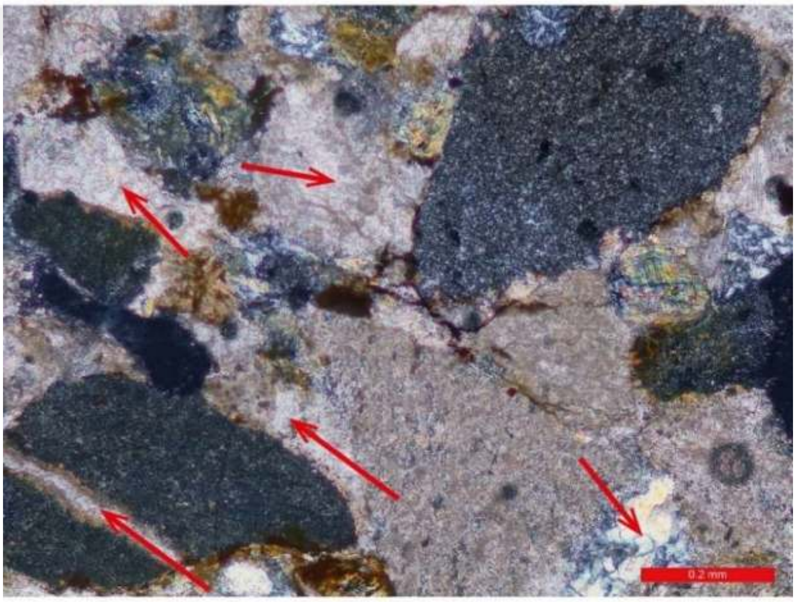

XPL

PPL and XPL images show differences between radiolarian chert (Rch) and black carbonate rock fragments (BCrf) in PPL and XPL view. BCrf is pale dirty yellowish while Rch shows colourless - white in PPL view. Under XPL cherts microcrystals are visible and lighter than BCrf in contrast as a whole clast. Red arrows represent calcite cement. Solid bitumen visible in both images causes brownish-yellowish staining on the calcite cement. A radiolaria fossil (R) on the Rch.

PLATE 8.2

Thin section and *photo* numbers: **TL2-6**-*0009-0010*

Bt: Solid bitumen fillings

BCrf: Black carbonate rock fragment

Crf: Carbonate rock fragment

G: Glauconite

PPL: Plain Polarised Light

R: Radiolaria fossil in the lithic chert clast

Rch: Radiolarian chert

Red arrows: Calcite cement

XPL: Cross Polarised Light

Plate 8.2

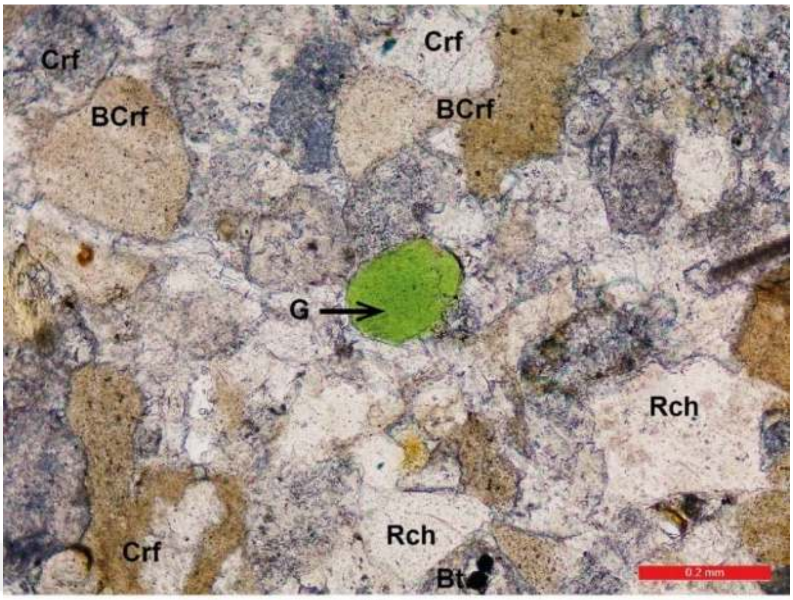

PPL

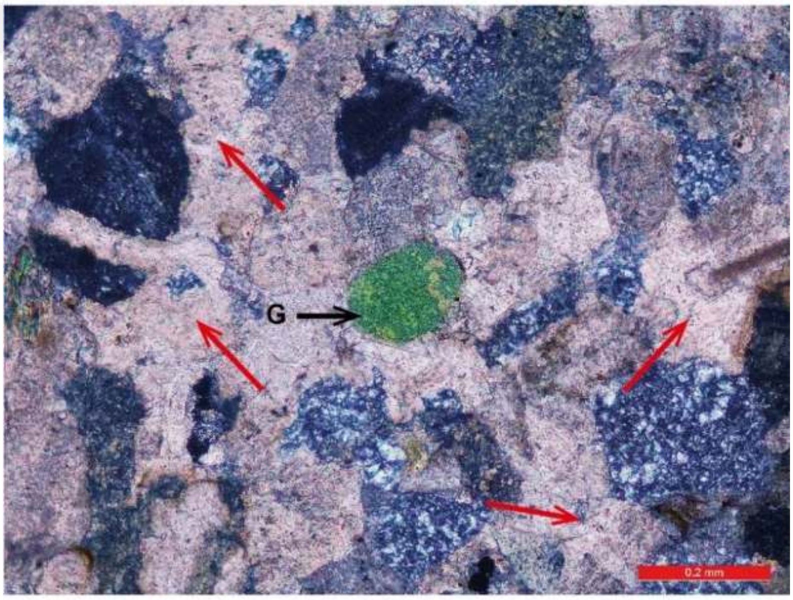

XPL

Greywacke; calcite cement ratio (red arrows) is more than 15%, including well rounded reworked bright green glauconite. Macrocrystalline lithic chert fragments are bearing radiolaria fossils infilled by chalcedony seen just above the scale bar in XPL image. Note the calcite filling in the microfracture in BCrf on the left upper part of the photo and calcite replacement on the grains in XPL image.

PLATE 8.3

<u>**Thin section** and *photo* numbers: **TL2-7**-*0013-0014*</u>

Bt: Solid bitumen fillings

BCrf: Black carbonate rock fragment

Crf: Carbonate rock fragment

MaCh: Macrocrystalline chert

CtCh: Cyrptocrystalline chert

PPL: Plain Polarised Light

R: Radiolaria

Rch: Radiolarian chert

Red arrows: Calcite cement

XPL: Cross Polarised Light

Plate 8.3

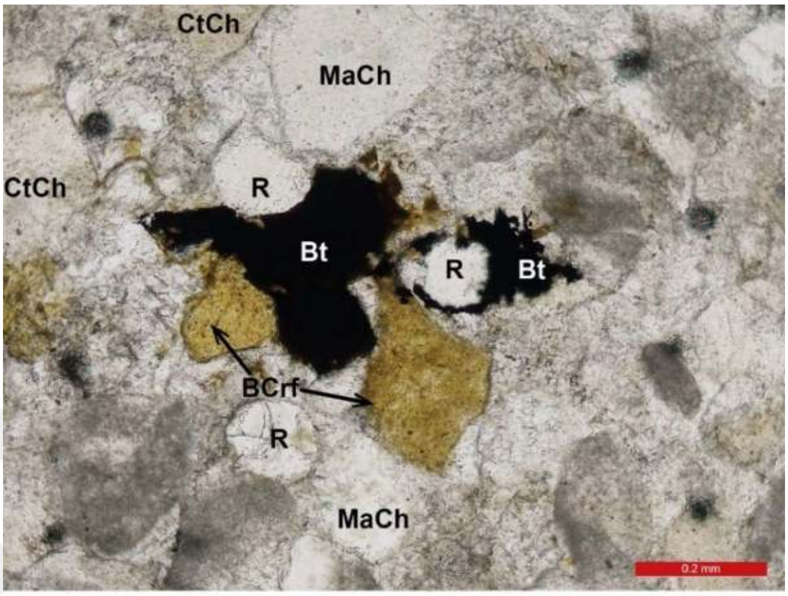

PPL

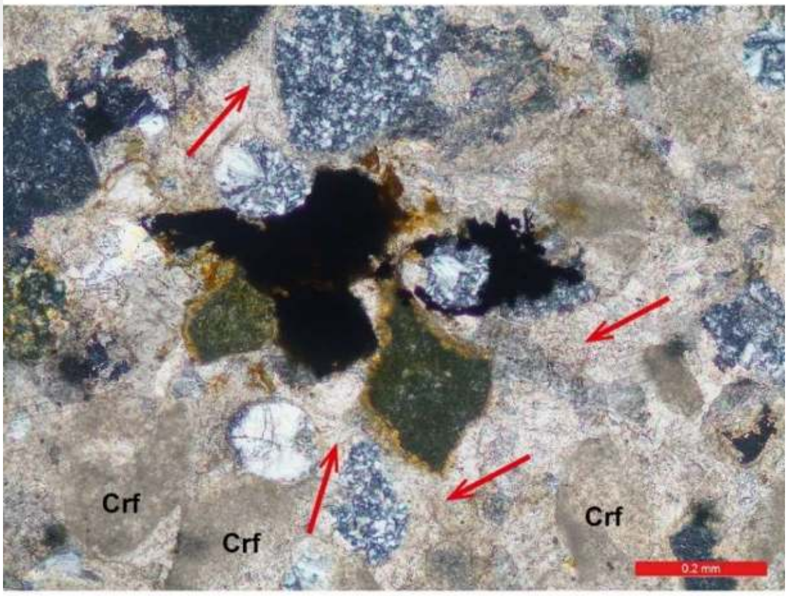

XPL

Solid bitumen (Bt) in the intergranular and moldic pores. The right side of the center bitumen filling is encircling one of the released- reworked and chalcedony filled radiolaria (R) fossil. Left one fills the pore space between a radiolaria fossil and a BCrf. Macrocrystalline and cyrptocrystalline lithic chert clasts are seen together on the right up side of the image. Note the bitumen related stained calcite rim around the angular BCrf clasts.

PLATE 8.4

Thin section and *photo* numbers: **TL2-7**-*0015-0016*

BCrf: Black carbonate rock fragment

Crf: Carbonate rock fragment

Hm: Hematite

PPL: Plain Polarised Light

R: Radiolaria

Rm: Radiolarian mudstone

Red arrows: Calcite cement

XPL: Cross Polarised Light

Plate 8.4

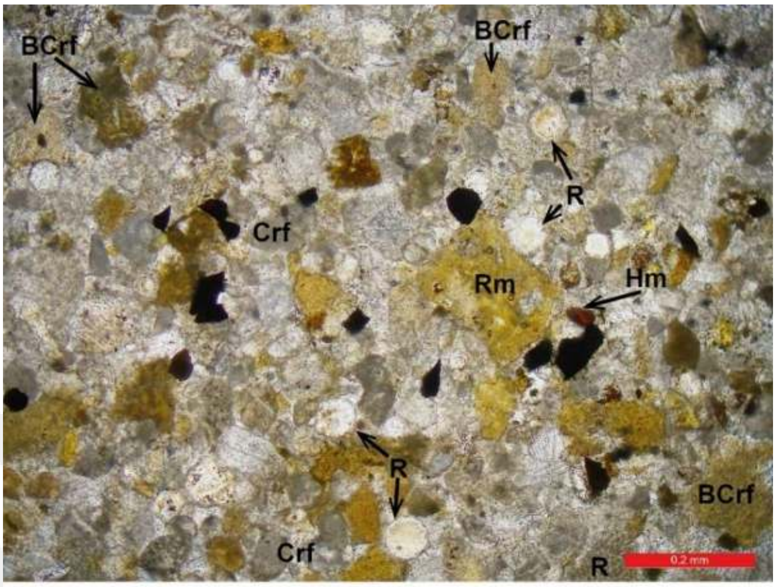

PPL

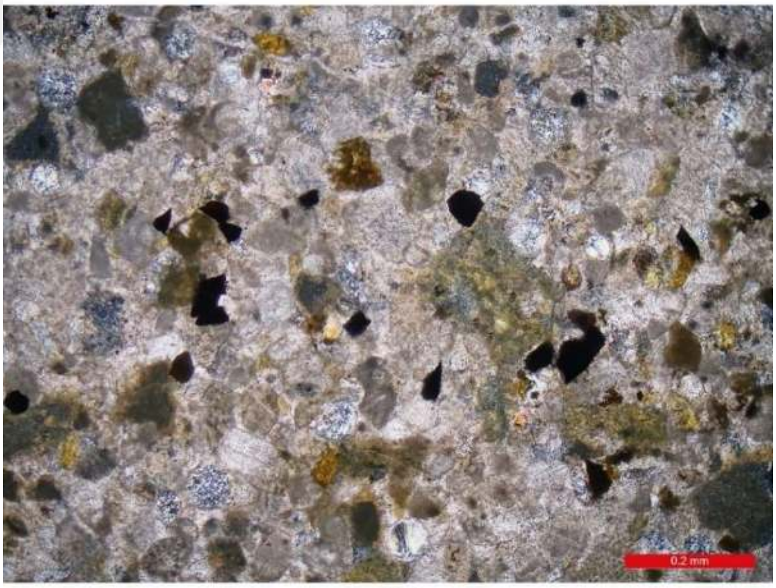

XPL

Euhedral and subhedral opaque minerals are concentrated in this part of the thin section. These are interpreted as organic matter (solid bitumen) related pyrite and hematite. One hematite (Hm) is in reddish-brownish in colour. Less in the other parts of this section and the other samples in this thesis. Pale yellowish rectangular clast is an altered/calcite replaced radiolarian mudstone (Rm) clast having radiolaria fossils. Calcite cement and calcitization is common especially visible around the BCrf.

PLATE 8.5

<u>Thin section</u> <u>and *photo* numbers:</u> **<u>TL3-5-</u>**<u>*0036-0037*</u>

Bt: Solid bitumen fillings

BCrf: Black carbonate rock fragment

C: Calcite crystal

CtCh: Cyrptocrystalline chert

MaCh: Macrocrystalline chert

MiCh: Microcrystalline chert

PPL: Plain Polarised Light

R: Radiolaria

Rch: Radiolarian chert

Red arrows: Calcite cement

Red dashed lines: Border of the Rch clasts

XPL: Cross Polarised Light

Plate 8.5

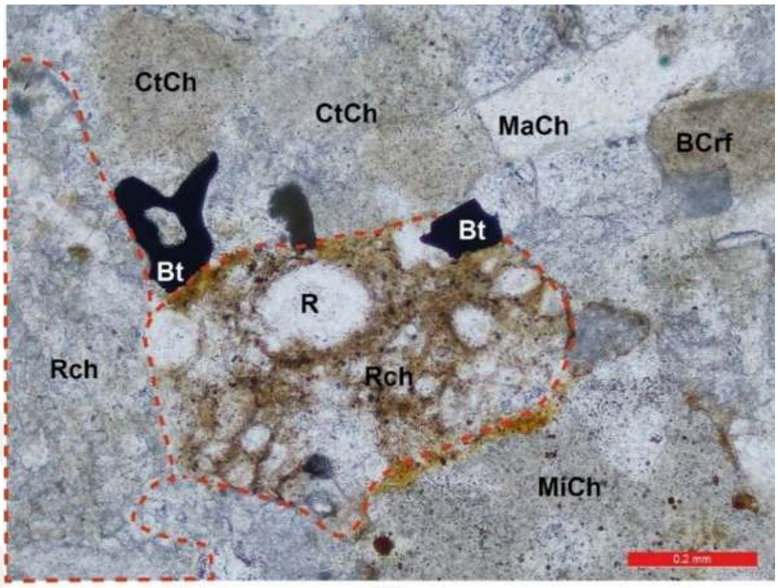

PPL

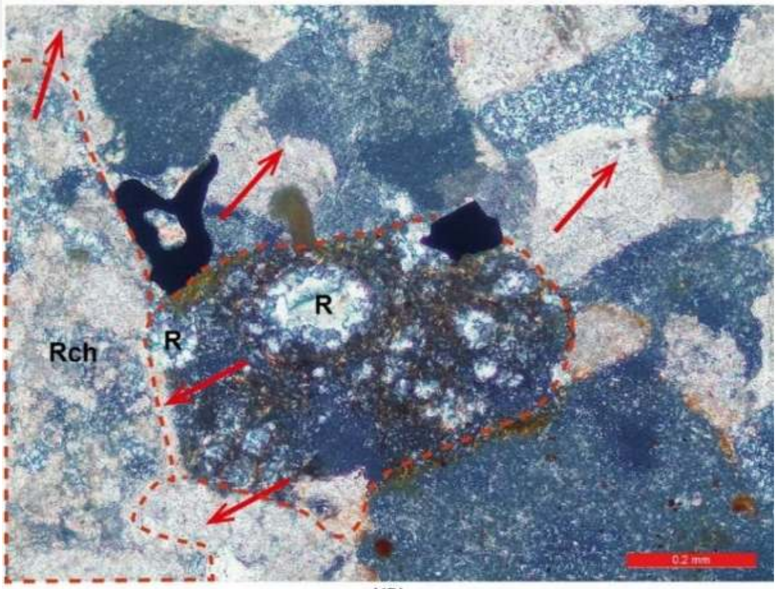

XPL

Red dashed lines are showing the grain contacts. Since the radiolarian chert (Rhc) along the left margin of the image mainly replaced by calcite it is hard to recognize contact of the grain. These kind of clast and the other stained lithic Rch clast below the bitumen fillings with full of in situ radiolaria fossils (white circulars) misinterpreted as matrix in some of the previous studies however there is a clear visible calcite cement represented by red arrows in the images here. Macro (MaCh), micro (MiCh) and cyrptocrystalline (CtCh) cherts are together in the image.

PLATE 8.6

Thin section and *photo* numbers: **TL4-4**-*0003-0004*

Bt: Solid bitumen fillings

BCrf: Black carbonate rock fragment

Crf: Carbonate rock fragment

PPL: Plain Polarised Light

Qm: Monocrystalline quartz

R: Radiolaria

Rch: Radiolarian chert

Red arrows: Calcite cement

Rm: Radiolarian mudstone

Sh: Shale clast

XPL: Cross Polarised Light

Plate 8.6

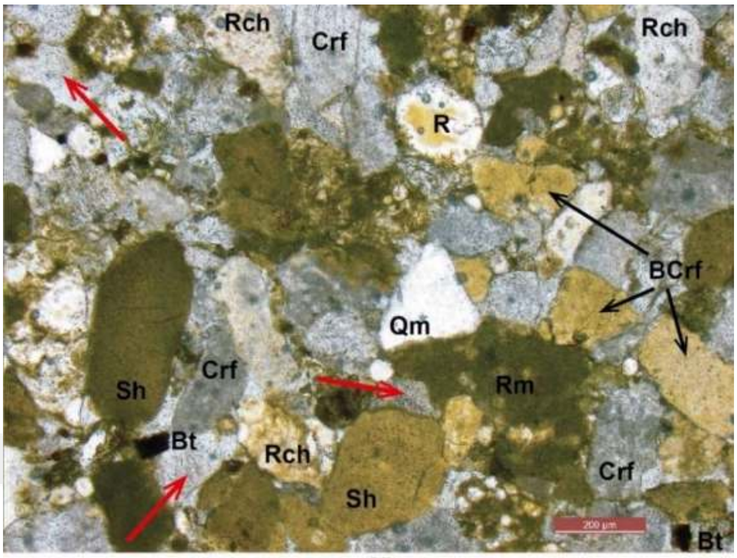

PPL

XPL

An example of angular monocrystalline quartz (Qm) having straight full extinction in the middle of the images has very low percentage in the all thin sections. Note the concavo convex contact between the quartz and Rm below and BCrf and Rm (PPL view). Long grain contact is also common in this thin section. Released and reworked radiolaria fossils (R) was accepted as lithic fragments like Rch and Rm. This photo is a good example for tightly compaction. Note the colour diversity between shale (Sh) and black carbonate rock fragments (BCrf) in both PPL and XPL images. Calcite cement was generally effected and stained by bitumen fillings possibly close area of this sample although it is not so much in this image.

PLATE 8.7

<u>**Thin section** and *photo* numbers: **TL4-4**-*0023-0024*</u>

Bt: Solid bitumen fillings

BCrf: Black carbonate rock fragment

C: Calcite crystal

Crf: Carbonate rock fragment

MaCh: Macrocrystalline chert

MiCh: Microcrystalline chert

PPL: Plain Polarised Light

R: Radiolaria

Rch: Radiolarian chert

Red arrows: Bitumen stained calcite cement

XPL: Cross Polarised Light

Plate 8.7

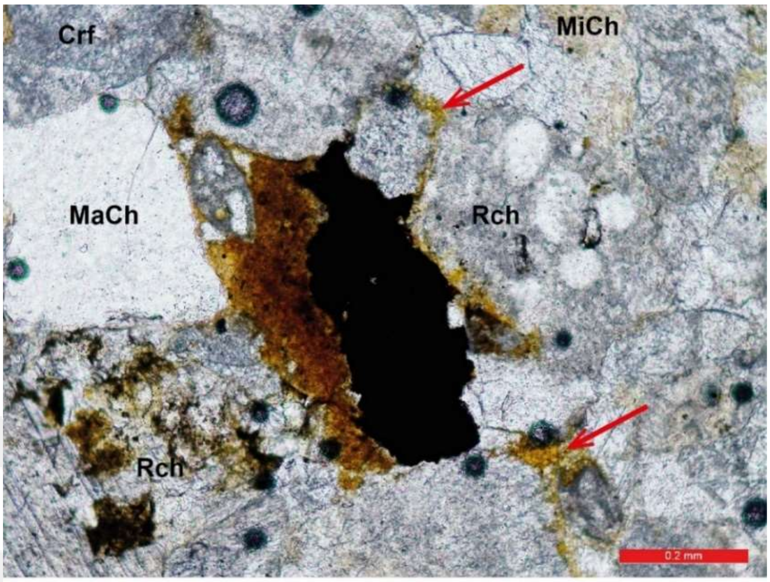

PPL

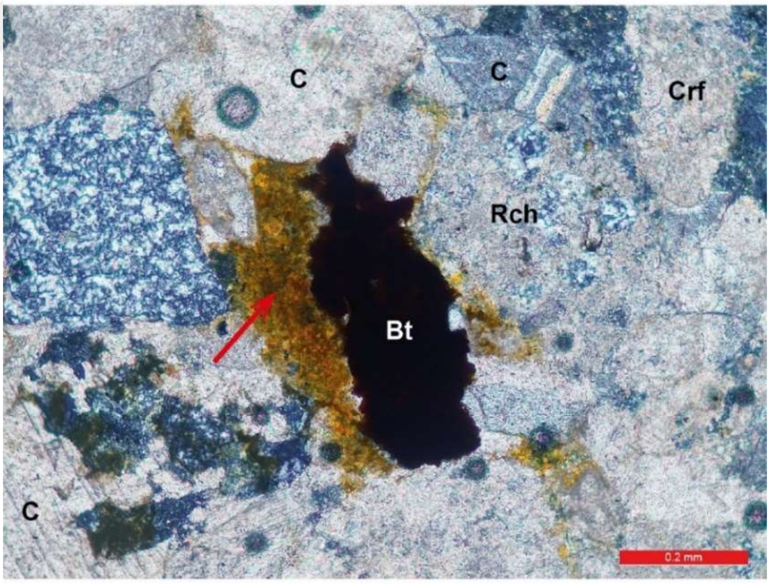

XPL

Very angular macrocrystalline chert (MaCh). Solid bitumen (Bt) filling in the intergranular pores and its brownish-yellowish stain on the calcite cement (red arrows) around the contact of Bt. Radiolaria fossils (white circular specks in Rch in PPL image) bearing cherts (Rch) are mainly replaced by calcite and bitumen fillings in the moldic pores. Calcite crystals (C) with cleavage left lower part and twins right up side of the image. Concavo convex and weak sutured contact types are present between calcite crystals, cherts and carbonate rock fragments.

PLATE 8.8

Thin section and *photo* numbers: **TL5-1**-*0001-0002*

Bt: Solid bitumen fillings

C: Calcite crystal

Crf: Carbonate rock fragment

BCrf: Black carbonate rock fragment

G: Glauconite

PPL: Plain Polarised Light

Qm: Monocrystalline quartz

R: Radiolaria

Rch: Radiolarian chert

XPL: Cross Polarised Light

Plate 8.8

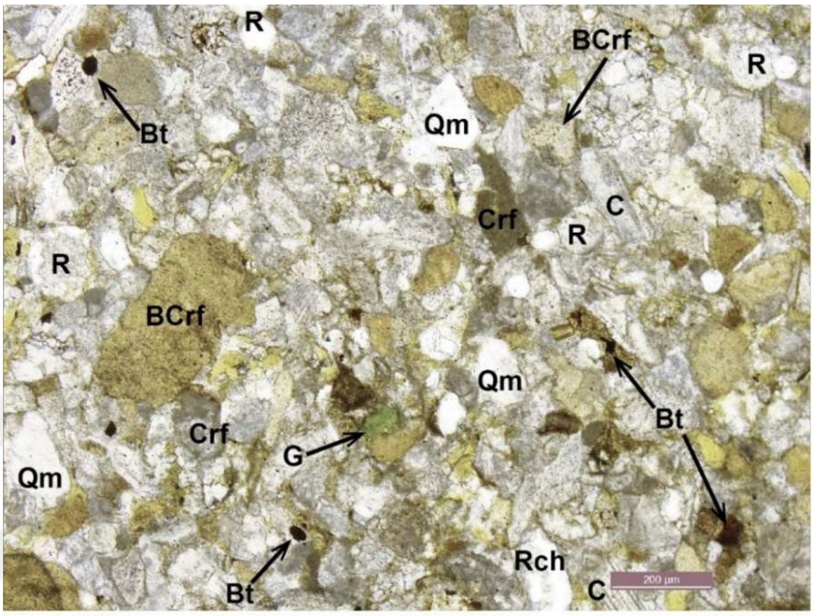

PPL

XPL

Poorly sorted, angular to subangular, tightly compacted grain composition. Green glauconite in the center of a shell reworked together. Three angular monocrystalline common quartz grains with straight fully extinction. Note that there is no any grain orientation. Bitumen fillings cause staining on the calcite cement. Released radiolaria fossils ratio as fragment (white circular specks in PPL image) is rising in this section.

PLATE 8.9

<u>**Thin section** and *photo* numbers: **TL5-3**-*0019-0020*</u>

Ab: Air bubble (thin section fault)

Bt: Solid bitumen fillings

C: Calcite crystal

Crf: Carbonate rock fragment

CtCh: Cyrptocrystalline chert

Dbt: Disseminated solid bitumen fillings

MiCh: Microcrystalline chert

PPL: Plain Polarised Light

Sf: Fossil shell fragment

Str: Sutured grain contact

XPL: Cross Polarised Light

Plate 8.9

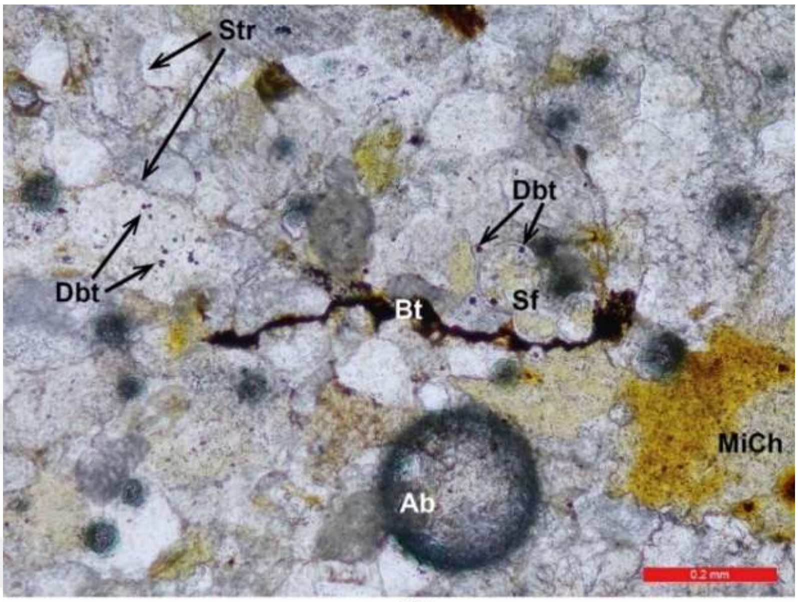

PPL

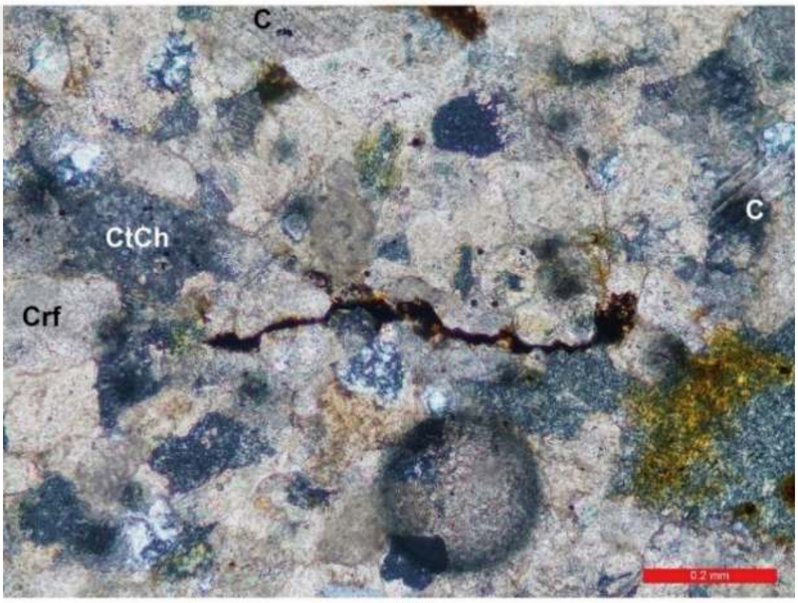

XPL

Hard to see the constituents of the thin section since intensely calcitization and calcite replacements. Two types of pore space filled by solid bitumen. Intragranular pores on the lithic clasts and reworked fossil shell fragment (Sf) were filled by disseminated bitumen (Dbt), and connected intergranular pore was filled by solid bitumen (Bt). Calcite crystals with twins and cleavage are common. Weak sutured contact type (Str) between some rock fragments.

PLATE 8.10

<u>Thin section</u> <u>and *photo* numbers:</u> **<u>TL6-4-</u>**<u>*0005-0006*</u>

Bt: Solid bitumen fillings

Crf: Carbonate rock fragment

CtCh: Cyrptocrystalline chert

F: Feldspar

PPL: Plain Polarised Light

R: Radiolaria

Red arrows: Calcite cement

Red dashed lines: Border of the Rch clasts

Rch: Radiolarian chert

Sh: Shale clast

X: Thin section glue (thin section fault)

XPL: Cross Polarised Light

Plate 8.10

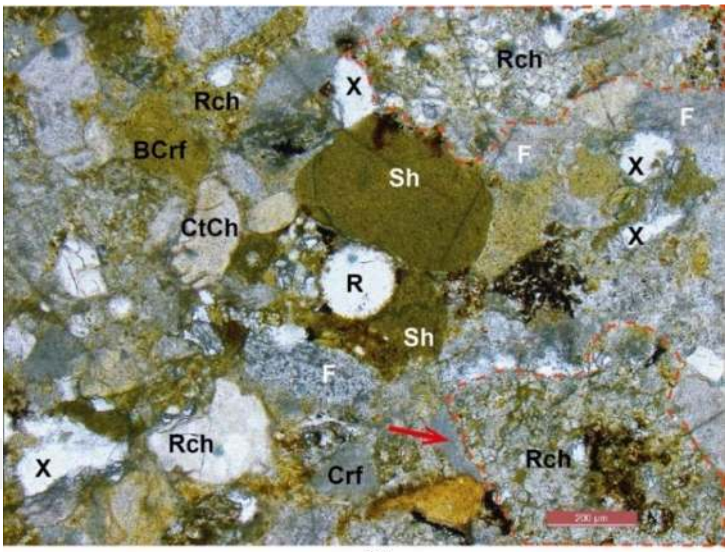

PPL

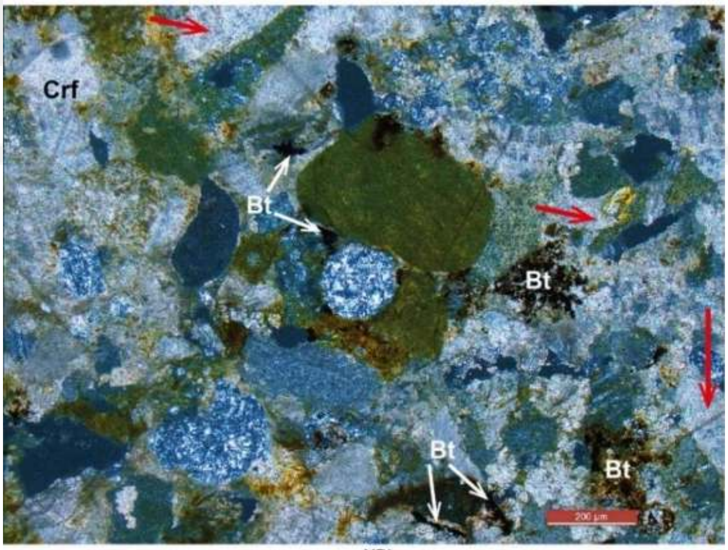

XPL

Released single radiolaria filled by chalcedony relatively bigger (0,17 mm) than the others in the thin sections with concavo convex contact with the two shale (Sh) clast around it. Red arrows show calcite cement. Intragranular (in the big Rch clast which mainly replaced by calcite at the right down corner of the image) and intergranular pores were blocked by bitumen fillings (Bt). Tangential (Point) grain contact between. Red dashed lines show single grain border. Solid bitumen stains majority of the calcite cement. Poorly sorted, very angular to subrounded grains were tightly compacted.

9. CONCLUSIONS

The current study, conducted in the close southeastern part of Sulaimaniyah city on the road to Arbat town, Northern Iraq combines, reservoir characterization including porosity and permeability, facies analysis and petrographic examination of the Tanjero Formation, a peripheral foreland unit of Upper Cretaceous basin on the north extension of the Arabian Plate.

Porosity of the studied sandstones range from 4.56% to 16.56% which is poor to beginning of fair with an average value of 9.2%. The obtained permeability varies between 36.388-623.328 md and their mean value is 426.68 md representing “very good” permeability. Poorly to moderately sorting, tightly packing and moderate compaction, high amount of calcite precipitation from fossiliferous carbonate rock fragments and the ratio of the bitumen fillings ranging from 1% to 8% are blocking the pores. Solid bitumen fillings indicate that before the fillings many sandstones had an initial “good” porosity value of (9.5% + 8 %) 17.5 % before the bitumen fillings.

Depending on the three main lithofacies 49 subfacies and the ratio of sandstone (49.8%) and shale (51.2%), it was pointed out that “lob off-axis and lobe fringe” are the depositional environments for the turbidite sandstone of Tanjero Formation depending on lobe hierarchy.

The only architectural element recognized in the section is small sandy channel fills in about ten meters length and a few meters thick representing beginning of outer fan or in lobe fringe. Also grain size, bed thicknesses and combinations of Bouma turbidite divisions show that the sandstones in the studied area are indicate a transition between middle fan and outer fan.

Palaeocurrent data evidence flow towards the SE measured from flute mark and current ripples in Bouma Tc divisions.

Petrographycally the analyzed sandstones are calclithite of litharenite division according to ternary diagrams.

The compositional characteristics show the presence of only sedimentary rocks in the source areas. The data obtained in the modal analysis illustrated to a lithic recycled orogen as the source area. Both the sandstone composition and the palaeocurrent analysis suggest that the source area was the structural highs of the North of the Upper Cretaceous basin consisting of Qulqula Formation.

Less than 5 percentage clay, angular to subangular grains, poorly sorting, show “submature” maturity stage indicating a short transportation and a close source area for the sandstones.

Contact types are tangential, mainly long grain, concavo convex and sutured (rare) types. Contac types and high contact index (3.6) represent moderate to tightly packing, moderate compaction which are negatively effecting the reservoir quality.

10. REFERENCES

ABDEL-KIREEM, M. R. 1986a. Contribution to the Stratigraphy of the Upper Cretaceous and Lower Tertiary of the Sulaimaniya - Dokan Region, Northeastern Iraq. *N. JB. Geol. Paleont.,* Abh. 172 (1), 121-139.

ABDEL-KIREEM, M. R. 1986b. Planctonic Foraminifera and stratigraphy of the Tanjero Formation (Maastrichtian), northeastern Iraq. *Micropaleontology,* 32, 215-231.

AHMED, S. H. 2013. Tectonostratigraphic Evolution of the Northeastern Arabian Plate in Kurdistan since the Jurassic. PhD Thesis.

AL-MEHAIDI, H. M. 1975. Tertiary nappe in Mawat range, NE Iraq. *Geological Society of Iraq,* 8, 31 - 44.

AL-RAWI, I. 1981. Sedimentology and Petrology of Tanjero Clastic Formation in north and northeastern Iraq. *Unpublished Ph. D. Thesis, University of Baghdad,* 295.

AL-RAWI, Y. & AL-RAWI, I. Tanjero Formation from northeast and north Iraq. A turbidite example of flysch type. Proceeding of 15th Iraqi Geological Conference, 2002. 15-18.

AWDAL, A., BRAATHEN, A., WENNBERG, O. & SHERWANI, G. 2013. The characteristics of fracture networks in the Shiranish formation of the Bina Bawi Anticline; comparison with the Taq Taq field, zagros, Kurdistan, NE Iraq. *Petroleum Geoscience,* 19, 139-155.

BAZIANY, M. M. Q. 2014. *Depositional Systems and Sedimentary Basin Analysis of the Qulqula Radiolarian Formation of the Zagros Suture Zone, Sulaimani Area, Iraqi Kurdistan Region.* PhD, University of Sulaimani.

BEARD, D. C. & WEYL, P. K. 1973. Influence of Texture on Porosity and Permeability of Unconsolidated Sand. *American Association of Petroleum Geologists Bull,* 57, 349-369.

BELLEN, R. C. V., DUNNINGTON, H. V., WETZEL, R. & MORTON, D. M. 1959. *Lexique. Stratigraphique international,* Asie paris.

BUDAY, T. 1980. *The Regional Geology of Iraq,* Baghdad.

BUDAY, T. & JASSIM, S. Z. 1987. *The Regional geology of Iraq: Tectonism Magmatism, and Metamorphism,* Baghdad.

DICKINSON, W. R., BEARD, L. S., BRAKENRIDGE, G. R., ERJAVEC, J. L., FERGUSON, R. C., INMAN, K. F., KNEPP, R. A., LINDBERG, F. A. & RYBERG, P. T. 1983. Provenance of North American Phanerozoic sandstones in relation to tectonic setting. *Geological Society of America Bulletin,* 94, 222-235.

DZULINSKI, S. & WALTON, E. K. 1965. *Sedimentary features of flysch and graywackes* Amsterdam, Elsevier.

FOLK, R. L. 1951. Stages of textural maturity in sedimentary rocks. *Journal of Sedimentary Research,* 21.

JASSIM, S. Z. & GOFF, J. C. 2006. *Geology of Iraq,* Brno, Dolin, Hlavin 2732, Prague and Moravian Museum Zelny trh 6.

JAZA, I. 1992. *Sedimentary facies analysis of the Tanjero Clastic Formation in Sulaimaniya District, northeast Iraq. Unpl.* M. Sc. Thesis, Salahaddin University, 121p.

KARIM, K. 2006b. Environment of Tanjero Formation as inferred from sedimentary structures, Sulaimanyia area, NE-Iraq. *Kurdistan Academician Journal (KAJ),* 4**,** 1-18.
KARIM, K. Modification of the time-expanded stratigraphic column of North East Iraq during Cretaceous and Tertiary. Published in: Petroleum Geology of Iraq (First Symposium, 21-22april, Baghdad, Abstract book, p4, 2010.
KARIM, K. & SURDASHY, A. 2005a. Paleocurrent analysis of Upper Cretaceous Foreland basin: a case study for Tanjero Formation in Sulaimanyia area, NE-Iraq. *Iraqi Journal of Earth Science,* 5**,** 30-44.
KARIM, K. H. 2004. Basin Analysis of Tanjero Formation in Sulaimaniyah Area, NE-Iraq. PhD. Thesis.
KARIM, K. H. 2005c. Origin of Ball and Pillow-like Structures in Tanjero and Kolosh Formations in Sulaimaniya area, NE-Iraq. *Kurdistan Academics Journal,* 4.
KARIM, K. H. 2006c. Comparison study between the Khabour and Tanjero formations from North Iraq. *Iraqi Journal of Earth Sciences,* 6**,** 1-12.
KARIM, K. H. 2007. Possible effect of storm on sediments of Upper Cretaceous Foreland Basin: a case study for tempestite in Tanjero Formation, Sulaimanyia Area, NE-Iraq. *Iraqi Journal of Earth Science,* 7**,** 1-10.
KARIM, K. H., AL-HAMADANI, R. K. & AHMAD, S. H. 2012. Relations between Deep and Shallow Stratigraphic Units of Northern Iraq during Cretaceous. *Iranian Journal of Earth Sciences,* 4**,** 95-103.
KARIM, K. H., ISMAIL, K. M. & AMEEN, B. M. 2008. Lithostratigraphic Study of The Contact Between Kometan And Shiranish Formations (Cretaceous) From Sulaimaniyah Governorate, Kurdistan Region, NE-Iraq. *Iraqi Bulletin of Geology and Mining,* 4**,** 16-27.
KARIM, K. H., ISMAIL, K. M. & BZIANY, M. M. 2014. Origin of Fossiliferous Limestone Beds inside the Upper Part of Tanjero Formation at the Northwest of Sulaimani Area, Kurdistan Region, NEIraq. *Journal of Zankoy Sulaimani,* 17**,** 155-165.
KARIM, K. H. & KHANAQA, P. A. 2016. CENOMANIAN/ TURONIN BOUNDARY IN ZAGROS OROGENIC BELT EXAMPLES FROM KURDISTAN REGION, NORTHEASTERN IRAQ. *Iraqi Geological Journal,* 39-49.
KARIM, K. H. & SURDASHY, A. M. 2005b. Tectonic and depositional history of Upper Cretaceous Tanjero Formation in Sulaimaniya area NE-Iraq. *Journal of Sulaimaniya University (JZS),* 8**,** 1-20.
KARIM, K. H. & SURDASHY, A. M. 2006a. Sequence stratigraphy of Upper Cretaceous Tanjero Formation in Sulanmaniya area, NE-Iraq. *KAJ,* 4**,** 19-43.
KASSAB, I. I. M. 1975. Planktonic Foraminifera Range in the type Tanjero Formation Upper Campanian-Maastrichtian) of N. Iraq. *Geological Society of Iraq,* 8**,** 73 - 86.
LAWA, F. A., AL-KARADAKHI, A. I. & ISMAIL, K. M. 1998. An interfingering of the Upper Cretaceous rocks from Chwarta-Mawat Region (NE-Iraq). *Iraqi Geology,* 31.

MATTERN, F. 2002. Amalgamation surfaces, bed thicknesses, and dish structures in sand-rich submarine fans: numeric differences in channelized and unchannelized deposits and their diagnostic value. *Sedimentary Geology,* 150**,** 203-228.

MEYER, L. & ROSS, G. 2007. Channelized lobe and sheet sandstones of the Upper Kaza Group basin-floor turbidite system (Windermere Supergroup), British Columbia, Canada. *American Association of Petroleum Geologists, Studies in Geology,* 56.

MINAS, H. 1997. *Sequence stratigraphic analysis of the Upper Cretaceous succession of Central and Northern Iraq. Unpubl.* Ph. D. Thesis, Univ. Baghdad. 188p.

MUTTI, E. & RICCI LUCCHI, F. 1972. Le torbiditi dell' Appenino settentrionale: introduzione all' analisi di facies. *Memoir of the Geological Society of Italy***,** 11, 161–199.

MUTTI, E. & RICCI LUCCHI, F. 1975. Turbidite facies and facies associations. Field Trip Guidbook. *9th International Association of Sedimentologists Congress***,** 21–36.

MUTTI, E. & RICCI LUCCHI, F. 1978. Turbidites of the northern Apennines: introduction to facies analysis. *International geology review,* 20**,** 125-166.

NORTH, F. 1985. *Petroleum geology*, Springer.

PETTIJOHN, F., POTTER, P. & SIEVER, R. 1987. Sand and Sandstone.—553 pp. Springer) Berlin, Heidelberg, New York.

POTTER, P. E. & PETTI JOHN, F. J. 1977. *Paleocurrents and Basin Analysis,* Berlin, Spinger –Verlag.

PRELAT, A., HODGSON, D. & FLINT, S. 2009. Evolution, architecture and hierarchy of distributary deep-water deposits: a high-resolution outcrop investigation from the Permian Karoo Basin, South Africa. *Sedimentology,* 56**,** 2132-2154.

PRÉLAT, A. & HODGSON, D. M. 2013. The full range of turbidite bed thickness patterns in submarine lobes: controls and implications. *Journal of the Geological Society,* 170**,** 209-214.

QADIR, F. M. 2008. FORMATION EVALUATION OF UPPER QAMCHUQA RESERVOIR, KHABBAZ OIL FIELD, KIRKUK AREA, NORTHEASTERN IRAQ. *PhD Theses***,** 183.

SAADALLAH, A. & HASSAN, A. H. 1987. Sedimentological study of selected section of Tanjero Formation. *Iraqi Journal of Science,* 28**,** 483-506.

SHANMUGAM, G. & MOIOLA, R. 1988. Submarine fans: characteristics, models, classification, and reservoir potential. *Earth-Science Reviews,* 24**,** 383-428.

SHARBAZHERI, H. G. 2008. Sequence Stratigraphy of Cretaceous Successions from Selected Sections in Kurdistan Region, NE Iraq. Sulaymaniyah: Unpublished MSc thesis, University of Sulaimani.

SHARBAZHERI, K. 2007. Aging of unconformity within Tanjero Formation in Chwarta Area Northeast of Iraq (Kurdistan Region). *Iraqi Journal of Earth Science,* 7**,** 37-54.

SHARBAZHERI, K., GHAFOR, I. & MUHAMMED, Q. 2009. Biostratigraphy of the Cretaceous/Tertiary boundary in the Sirwan Valley (Sulaimani Region, Kurdistan, NE Iraq). *Geologica Carpathica,* 60.

SHARBAZHERI, K. M. 2010. Planktonic foraminiferal biostratigraphy of the upper Cretaceous reddish to pale brown transitional succession in Smaquli area, northeast Iraq (Kurdistan region). *Iraqi Bulletin of Geology and Mining,* 6**,** 1-20.

SO, Y. S., RHEE, C. W., CHOI, P.-Y., KEE, W.-S., SEO, J. Y. & LEE, E.-J. 2013. Distal turbidite fan/lobe succession of the Late Paleozoic Taean Formation, western Korea. *Geosciences Journal,* 17**,** 9.

TUCKER, M. E. 1988. *Techniques Sedimentology*, Blackwell Science Publication Co.

11. CURRICULUM VITAE

I- Personal data:

Name: Tavan Muhammad Hama Salih

Gender: Female

Marital Status: Single

Address: Iraq/ Sulaimani / Shorsh (Aqari)

Nationality: Iraqi

Tel. No.: 00964 (0) 751 1902015

Email: tavan.hamasalih@gmail.com

Current work: Geologist at institution for strategic studies and scientific research (KISSR).

II- Description duties and work:

- Governorate projects of Sulaimani, April 2009 until Sept. 2009.
- Kurdistan intitute for strategic studies and scientific research (KISSR), from sep.2009 untill now.

III- Education qualification:

- MSc. Student in Reservoir and Sedimentology,in Firat University,Turkey.
- BSc. In Geology- University of Sulaimani, Sulaimani, Iraq, 2004 - 2008.

IV- Training course:

- **Human Resources Management** course, from June, 07 2009 to June, 11 2009, organized and sponsored by the USAID Tatweer project, Sulaimani governorate and KRG ministry of planning.
- **Procurement** course, from June 21, 2009 to Jul. 2, 2009 organized and sponsored by the USAID Tatweer project, Sulaimani governorate and KRG ministry of planning.
- Training course in **Basic Life Support According to Sulaimani Medical Operation Standards** at KRG ministry of health.
- Participating in a workshop about **Organic Petrology**, April, 16-17, 2013 in (KISSR).
- Participating in a workshop about **Higher Education and Needs of the Labors Market in Kurdistan Region - Iraq**, Oct., 26, 2013 held by (KISSR).
- Training course (25 hrs. theoretical and practical training) about **Introduction to Organic Petrology I – Basic** Jan. 2014 held by (KISSR).

- Training course (two weeks theoretical and practical training) about **Gas Chromatography–Mass Spectrometry (GC-MS)** Jul. **2011** held by (KISSR).
- Training course (two weeks theoretical and practical training) about **Gas Chromatography–Mass Spectrometry (GC-MS)** Jul. **2013** held by (KISSR).
- Training course about **Carbon and Sulfur Analyzer** held by (KISSR).
- Training course about **Accelerated Solvent Extraction** device held by (KISSR).
- Training course about **Lead Analyzer** device held by (KISSR).
- Training course about **(Ion Chromatography IC)** device held by (KISSR).
- Training course about **Grapher Program** at (KISSR).
- Training course about well site Geologist (10 days) December, 2011 held by Kurdistan Geology Society.
- Participating in workshop about health and safety 9th and 10th May 2012 held by (KISSR).

V- Publications:

Tow abstracts published in International Conferences on Advances and Innovations in Engineering (ICAIE), Firat University, Engineering Faculty, Elazig, Turkey:

1. Lithofacies And Architectural Elements Of The Deep Marine Calciclastic Low Density Turbidites Of Upper Cretaceous Tanjero Formation, Around Arbat, Northern Iraq
2. Provenance Investigation From Sedimentary Petrography Of The Upper Cretaceous Deep Marine Low Density Turbidites Of Tanjero Formation Around Arbat, Northern Iraq

VI- Computer skills:

- Microsoft Word, Excel (Good).
- Surfer V.7, V.8 (Intermediate).
- Grapher (Intermediate).
- Power point (v. good).
- Adobe Illustrator (V.good).

VII- Language knowledge:

- Kurdish (mother tongue).
- English (Good in Reading and Writing, Intermediate in Listening and Speaking).
- Arabic (Good in Listening, Reading, Writing, Fair in Speaking).
- Turkish (little).